Alma Mater Studiorum – Università di Bologna

DOTTORATO DI RICERCA IN

Chimica

Ciclo XXIX

Settore Concorsuale di afferenza: 03/C2

Settore Scientifico disciplinare: CHIM/04

Innovative processes for the catalytic

liquid-phase oxidation of C6-based substrates

Candidato: Stefania Solmi

Coordinatore Dottorato   Relatore

Prof. Aldo Roda   Prof. Fabrizio Cavani

Esame finale anno 2017

Do. Or do not. There is no try.

Yoda

Ai miei nonni,

Bruna e Celestino

Summary

CHAPTER 1. GENERAL INTRODUCTION

1.1 Sustainable catalytic liquid-phase oxidations

Catalytic oxidations are extremely important from the scientific, technological and commercial point of view since they allow to obtain essential intermediates for the chemical industry. More than half of the products synthesized using catalytic processes are obtained by selective oxidation, and nearly all the monomers used in the production of fibers and plastics are prepared in this way[1].

These oxidation processes involve amounts of products in the order of million tons per year[2], therefore their industrial sustainability , which comprises economic, social and environmental aspects, is of paramount importance. The industrial sustainability involves continuous innovation, improvement and use of clean and safer technologies to reduce pollution levels and consumption of resources. At the same time, it has to improve both safety and quality of work, while maintaining industrial competiveness and responding to social and legislation questions[1].

Catalysis is the key for the development of a more sustainable chemistry, since over 90% of chemical industrial processes make use of a catalyst. A catalyst is a substance that can help a reaction to proceed faster or under different conditions than otherwise possible, using less resources and generating less waste. In complex reactions with several possible products, it can favor a reaction pathway and improve selectivity [1,3]. In this perspective, oxidation catalysis is playing a primary role for the development of sustainable processes by pursuing the following targets[1]:

- develop of "greener" catalytic systems and processes by means of new heterogeneous, rather than homogeneous, catalysts;
- replace traditional petrochemical building-blocks with alternative raw materials, such as renewable bio-platform molecules;
- replace stoichiometric oxidants with greener ones such as hydrogen peroxide, air or oxygen, so reducing waste and solvents;

- apply the concept of process intensification, by using smaller reactors, often with continuous instead of discontinuous feed, and under less severe reaction conditions, thus decreasing energy consumption;
- maximize selectivity and yield to the desired product, reducing costs and environmental impacts associated to its separation and purification.

Oxidation of organic substrates can be carried out either in vapor or in liquid phase[4]. Liquid phase oxidations may involve problems with catalysts recovery, if homogeneous, because they could be difficult to separate; on the other hand, if heterogeneous, they could lose the active phase which may be released into the reaction mixture. For these reasons, a multiphase system that might allow avoiding difficulties in catalyst separation and recycle, while maintaining the advantages of homogeneous over heterogeneous catalysis (typically higher specific activity relative to metal content, higher selectivity, possibility of fine tuning and better understanding at a molecular level) is a subject of great relevance for a more sustainable industrial chemistry[1]. Despite this, liquid phase oxidations are more selective than vapor-phase ones and are sometimes used in large-scale productions when products can be easily separated from the reaction medium (terephtalic acid), or they are thermally unstable (hydroperoxides), or very reactive at high temperature (epoxides, aldehydes, ketones). Moreover, the liquid phase has an higher density compared to the liquid phase, that typically may improve productivity, and make easier the control of the reaction with lower possibility of thermal runaways[4].

The cheapest and more easily available oxidant is air, since all others, for example, HNO_3, H_2SO_4, Cl_2, MnO_2, CrO_3, $KMnO_4$, as well as H_2O_2 and the organic hydroperoxides, have to be produced using oxygen or electric current. Moreover, often their use co-produces molecules that have to be separated from the desired product in the downstream effluents. The use of oxygen instead of air allow to have the same partial pressure with a much lower total pressure, decreasing the amount of polluting emissions released[1]. On the other hand, oxidation with molecular oxygen usually needs much more complex catalysts and process development to reach the high selectivity shown by those processes where, for instance, Cl_2 or HNO_3 are used[5].

Considering the several problems associated to the development of more sustainable industrial processes, someone could argue that it makes no sense to replace old and

well-known technologies, carried out in plants that are now completely depreciated, and reactions that have been fully optimized in terms of resource utilization, energy consumption and emissions abatement. Nevertheless, a more rational use of raw materials, with environmentally friendlier oxidants, would not only meet the sustainability criteria, but also bring economic advantages[6].

1.1.1 Content of this thesis

This Thesis deals with the results of different research topics aimed at the development of innovative, catalytic liquid-phase oxidation processes. All of them are characterized by the use of C6-based substrate and by targets which may fit the aim of a more sustainable industrial chemistry.

First, the oxidative cleavage of 1,2-cyclohexanediol to adipic acid was studied. This is an alternative synthesis of an important chemical intermediate which is produced by means of a process which holds serious drawbacks from the economic and environmental point of view. The reaction was carried out in water, with heterogeneous catalysts and using molecular oxygen as oxidant, obtaining high selectivity with Au-based catalysts.

The same supported active phase was used for the oxidation of D-glucose to glucaric acid (also an intermediate for the synthsis of adipic acid) with molecular oxygen. This is an important example of a reaction starting from a substrate which is obtained from renewable resources, and that can be transformed into high added-value bio-based chemicals.

Thereafter, the epoxidation of cyclohexene with Nb-based catalysts and hydrogen peroxide was studied. This study is an interesting case of catalyst design, aimed at the investigation of the molecular mechanism for the development of a more selective catalysts.

Finally, the oxidation of maltodextrins and starch was studied. The goal was to investigate on a a process with hydrogen peroxide or molecular oxygen as the oxidants, testing both homogeneous and heterogeneous catalysts, with the aim to produce molecules able to replace those which are currently synthesized with less "green" processes.

1.2 References

(1)   *Sustainable industrial processes*; Cavani, F., Ed.; Wiley-VCH: Weinheim, 2009.

(2)   Cavani, F.; Teles, J. H. *ChemSusChem* **2009**, *2* (6), 508–534.

(3)   Rothenberg, G. *Kirk-Othmer Encycl. Chem. Technol.* **2010**.

(4)   Suresh, A. K.; Sharma, M. M.; Sridhar, T. *Ind. Eng. Chem. Res.* **2000**, *39* (11), 3958–3997.

(5)   Teles, J. H.; Hermans, I.; Franz, G.; Sheldon, R. A. In *Ullmann's Encyclopedia of Industrial Chemistry*; Wiley-VCH Verlag GmbH & Co. KGaA, Ed.; Wiley-VCH Verlag GmbH & Co. KGaA: Weinheim, Germany, 2015; pp 1–103.

(6)   Cavani, F. *J. Chem. Technol. Biotechnol.* **2010**, *85* (9), 1175–1183.

CHAPTER 2. STUDY OF A NEW PROCESS FOR THE SYNTHESIS OF ADIPIC

ACID: THE OXIDATIVE CLEAVAGE OF *TRANS*-1,2-CYCLOHEXANEDIOL

2.1 Introduction

2.1.1 Adipic Acid

Adipic Acid (AA, hexanedioic acid, $C_6H_{10}O_4$) is a commercially important chemical intermediate which production amounts to $3x10^6$ t/Year[1]. AA can be used as it is or converted into adiponitrile, 1,6-hexanediamine, esters, anhydrides and amides. The main uses of this acid include the production of Nylon-6,6, plasticizers, lubricants, polyurethane and polyesters, additive for foods as acidulant, buffering or neutralizing agent, fabrication of adhesives, insecticide, tanning and dying, and for textile industries[2]. The beginning of the production of AA is associated to the discovered of Nylon in the early 1930's by W. H. Carothers' research team of Du Pont Company[1]. Despite many variations and improvements of the industrial process, the basic AA synthesis is essentially similar to that one of the first patents. The commercial production is done by means of a two-step route: the first stage is the synthesis of the intermediates cyclohexanol and cyclohexanone (the so called KA-Oil), and the second is the final oxidation to AA (Figure 2.1).
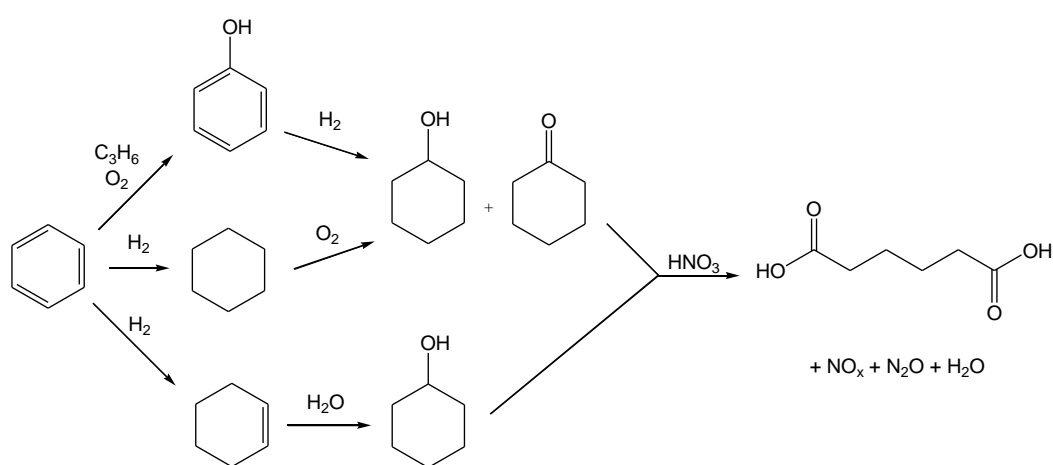
Figure 2.1. Current industrial processes for adipic acid production

KA-Oil can be obtained in different ways: oxidation of cyclohexane, phenol reduction and cyclohexene hydration. All these processes involve benzene derivatives, thus the cost of AA is influenced by hydrocarbon pricing[1]. The final oxidation of AA precursors is carry out with concentrated nitric acid in large stoichiometric excess as oxidant, Cu/V homogenous catalyst, at 60-80 °C and pressure between 1-4 bar, in a plant similar to that one reported in Figure 2.2.
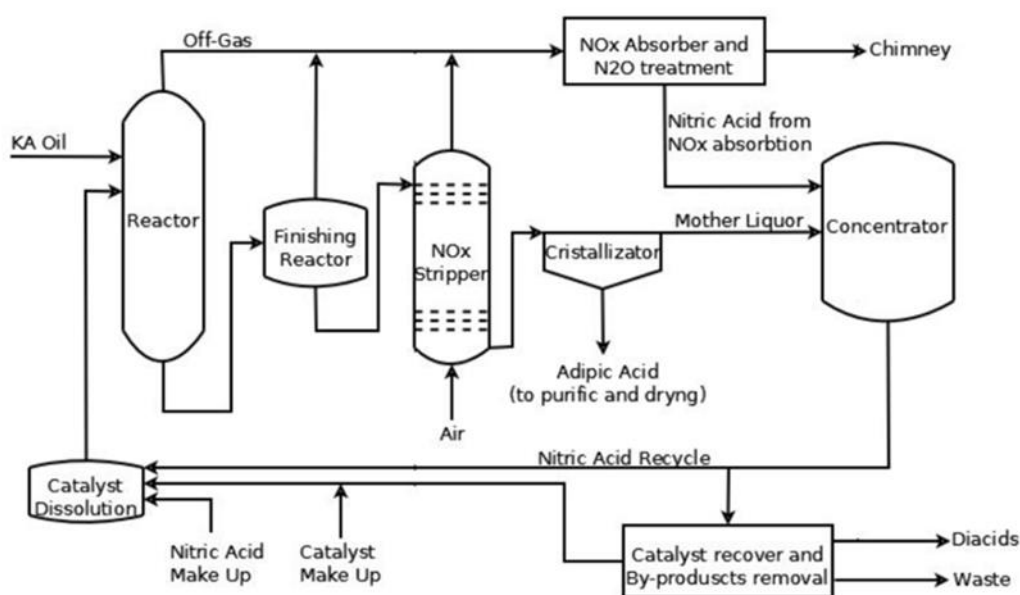
Figure 2.2. The KA-Oil oxidation plant

AA yield is 92-96 %, H_2O, NOx and N_2O are coproducts, while lighter dicarboxylic acids (glutaric and succinic acids) are reaction by-products. The process needs byproducts removal system, nitric acid and catalyst recovery, gas effluents abatement apparatus and efficient heat removal system because of the speed and exothermicity of the oxidation reaction. Because nitric acid is both a strong acid and an oxidant, plants are constructed with stainless steel or titanium able to operate under most severe exposure[2]. Because of problems from the safety, environmental and economic point of view, the research of more sustainable processes is of great interest nowadays.

In the literature it is possible to find many examples dealing with alternative ways for AA synthesis[3–5], such as the direct oxidation of cyclohexane or n-hexane with oxygen, the

direct cyclohexene oxidation with hydrogen peroxide, butadiene carboxylation or the chemical or biochemical conversion of glucose (Figure 2.3).
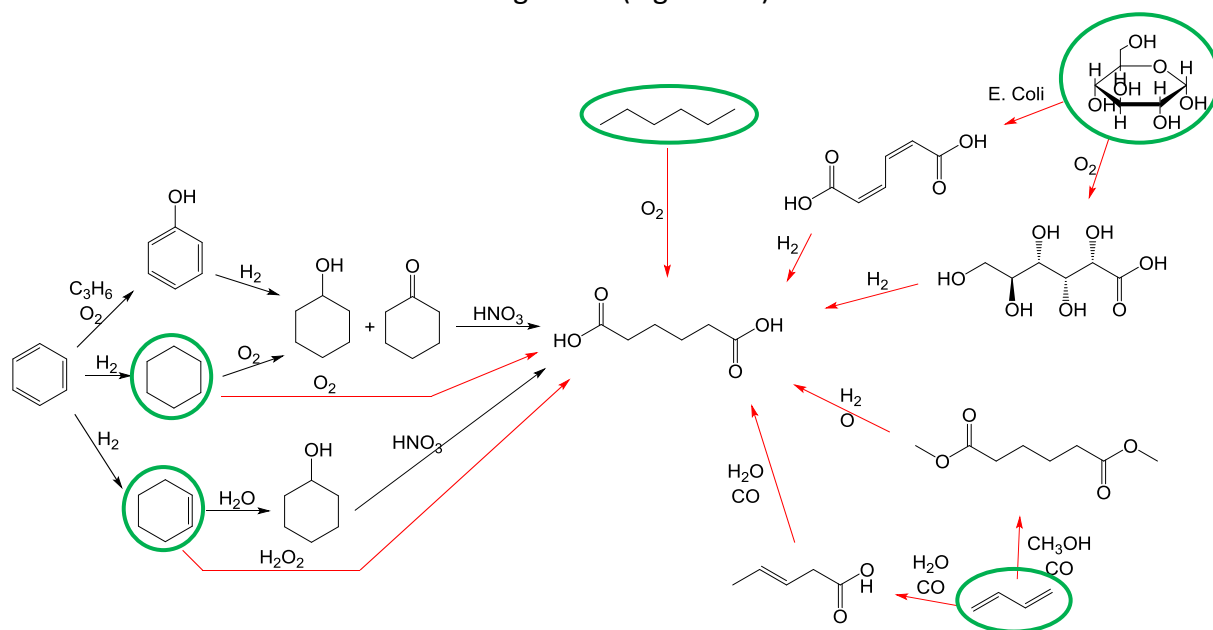
Figure 2.3. Alternative processes for adipic acid production (green circles and red arrows)

Despite these many attempts, none of these examples has been developed to the industrial scale and only few of them can be considered sustainable from both the environmental and economic point of view. For example, the biochemical process suffers from difficulties during the scale up that worsen the final result. The direct cyclohexene oxidation with hydrogen peroxide follow the rules of green chemistry, but the cost and high amount of oxidant required make the process economically disadvantageous. Other examples require acetic acid as solvent, with an increase of the cost of the plant, or long reaction time and hard recoverable catalysts, or AA yield and selectivity uncompetitive with the actual industrial process.

For these reasons, the research of alternative routes for AA synthesis is still very active and of great importance. The most sustainable process will be the one which combines cheap raw materials, low-cost green oxidant such as oxygen, green solvent like water or solvent-free reaction and simple heterogeneous reusable catalysts.

2.1.2 Catalysts for the oxidative cleavage of vicinal diols

The oxidative cleavage of vicinal diols is an important reaction for the synthesis of ketones, aldehydes and carboxylic acids (Figure 2.4). It can be performed using stoichiometric oxidants which, however, cause the formation of large amount of inorganic waste; therefore the research on this reaction with greener oxidants, such as hydrogen peroxide (HP) and oxygen, is studied in depth[3].
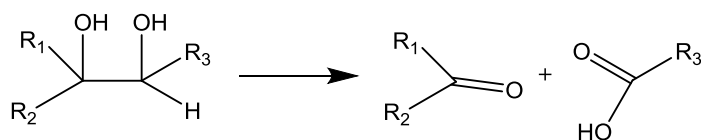
Figure 2.4. Possible products of oxidative cleavage of vicinal diols

One interesting vicinal diol is 1,2-cyclohexanediol (CHD) which, after oxidative cleavage, generates AA[3–6] (Figure 2.5).
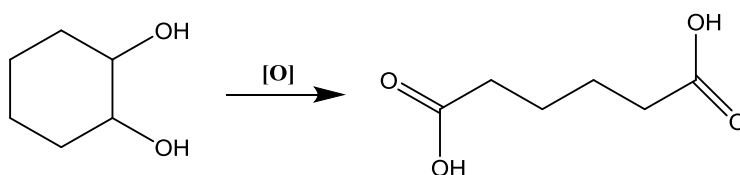
Figure 2.5. The oxidative cleavage of 1,2-cyclohexanediol to AA

The oxidation can be performed with HP and from the literature it is possible to find several examples of catalysts: heterogeneous Ti-Y, Ti-MMM-2, Ce-SBA-15, TAPO-5 and Ti-AlSBA-15[7–10], homogenous tungstate anion (suitable also for the direct cyclohexene oxidation to AA)[11,12], several type of polyoxometalates (surfactant-type, quaternary ammonium salts, Ti-containing sandwich-type)[13–17].

Also oxygen has been investigated as the oxidant: Brégeault and co-workers studied the aerobic oxidative cleavage of vicinal diols with transition metal ions as V, Cu, Fe ad Mn[18–20], and very efficient P/Mo/V polyoxometalates[21,22]. Other catalysts active for the oxidative cleavage of diols are based on ruthenium[6], such as homogeneous Ru^{2+}/Ru^{3+} complexes[23] and heterogeneous $RuCl_3$ and pyrochlore oxides[24–27].

From the literature it is well-known that gold based catalysts can oxidize alcohols, diols and polyols[28]. For instance, gold nanoparticles supported on ceria and titania have been employed in the oxidation of 5-hydroxymethyl-2-furfural into 2,5-furandicarboxylic acid

in basic aqueous medium with oxygen and air[29,30]. This type of catalyst is also active in the oxidative cleavage of unsatured hydrocarbons and aliphatic cyclic vicinal diols. Supported gold catalysts with molecular oxygen in an aqueous basic medium are active in the oxidative cleavage of 9,10-dihydroxystearic acid to azelaic acid and pelargonic acid[31]. A peculiarity of gold catalysts is that they are able to coordinate only one hydroxyl group in vicinal glycols, for example, depending on the conditions, Au nanoparticles can oxidize the primary OH group of 1,2-propandiol to lactic acid or oxidize them in sequence starting from the secondary hydroxyl group giving pyruvic acid, which is then oxidized to acetic acid and CO_2 [32] (Figure 2.6).
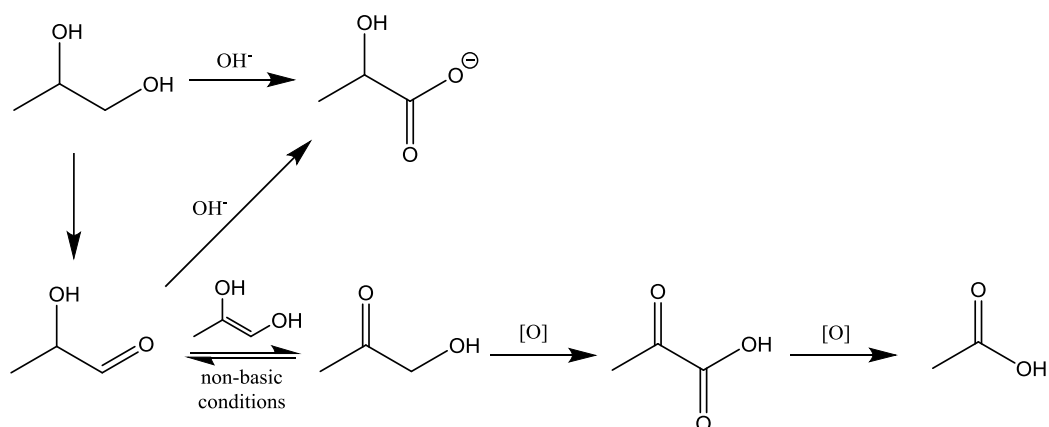
Figure 2.6.Oxidation of 1,2-propandiol with gold-based catalysts (adapted from ref [32])

2.1.3 Previous work and aim of the work

In previous works, the research group at the Department of Industrial Chemistry, University of Bologna, investigated the dihydroxylation of cyclohexene to trans-1,2-cyclohexanediol with HP[33], and the oxidative cleavage of the diol to AA with oxygen catalyzed by Ru(OH)$_3$ supported on alumina and Keggin type P/Mo/V polyoxometalates (POMs)[6,34]. Ruthenium catalysts were active in basic aqueous medium in order to activate the substrate, but the reaction network was very complex with many side reactions and low selectivity to AA. Under these conditions, the oxidehydrogenation of CHD generates 1,2-cyclohexanedione (CHDO) which is then transformed into 1-hydroxycyclopentanecarboxylic acid (HCPA) (Figure 2.7). The dione is the key intermediate under basic conditions and its formation is due to the ability of Ru(IV) oxo

complexes to coordinate both hydroxyls groups of CHD transforming both of them into carbonyl groups [35,36].
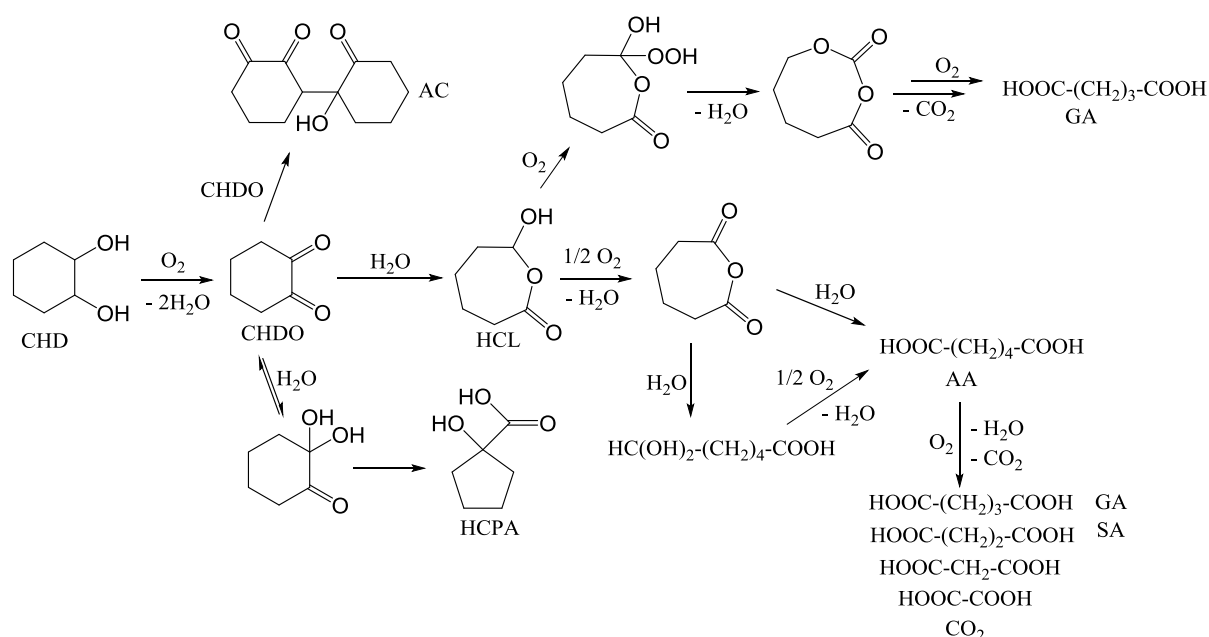
Figure 2.7. Reaction pathway with Ru-based catalysts

Homogeneous POMs were more selective in CHD oxidation to AA: the by-products formed with Ru catalyst was not observed, but under the acidic conditions at which POMs were active, AA reacted with unconverted CHD giving the corresponding ester. Therefore an additional hydrolysis step was necessary to produce AA. Moreover POMs were soluble in the reaction medium and they could be separated from the reaction mixture by precipitation. Differently from what observed with Ru-based catalysts, with POMs the key intermediate is 2-hydroxycyclohexanone (HCHN), which can be oxidized to AA with high selectivity in basic aqueous medium even in the absence of the catalyst (Figure 2.8).

Figure 2.8. Reaction pathway with POMs catalysts

Hence, a catalyst which is able to oxidise the two vicinal C-OH groups in sequence, and not at the same time, is desirable to obtain better selectivity to AA in basic medium (Figure 2.9). Therefore, it was decided to investigate the reactivity of Au NPs supporting them on different supports.

Figure 2.9. Desired reaction pathway

In this chapter, results obtained with catalysts based on Au nanoparticles supported on TiO_2 and MgO are reported.

2.2 Experimental

2.2.1 Catalysts synthesis

The catalysts have been prepared by incipient wetness impregnation of a suspension of gold nanoparticles on the supports. The suspension was prepared according to the procedure described in literature[37]. The synthesis is conducted in water as solvent and it consists in the reduction of Au(III) by glucose in a basic medium of NaOH using PVP (polyvinylpyrrolidone) as stabilizer (Figure 2.10). The molar ratio used for the synthesis is the following: Au : glucose : NaOH : PVP = 1 : 2 : 8 : 2.75.
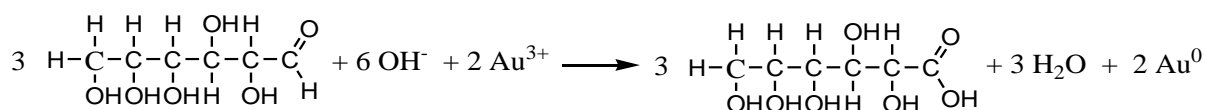
Figure 2.10. Synthesis of Au nanoparticles with glucose, NaOH and PVP

The concentration of the final suspension has to be $5 \cdot 10^{-3}$ M with a volume of 100 ml. The synthesis starts with the dissolution of the right amount of $HAuCl_4$ in 10 ml of distilled water. PVP and sodium hydroxide have to be dissolved in 90 ml of distilled water in a three necked round bottom flask provided with magnetic stirrer (600 rpm), thermometer and vapour condenser and heated to 95 °C in a glycol bath. When the desired temperature is reached, glucose is added to the solution and the mixture is warmed up for no more than 30 seconds to avoid excessive sugar degradation. Then the gold solution is added and after 2.5 minutes, the reaction is stopped by fast cooling of the flask in ice and water. The final gold suspension shows a dark red colour. To check the quality of gold nanoparticles, it is necessary to measure the hydrodynamic diameter by DLS. Based on the required weight percentage of gold on the desired amount of support, the precise amount of suspension has to be weighted and concentrated by centrifugation in tubes fitted with filters of cellulose (50 kDa Amicon Ultra Filters, Millipore) at 1700 rpm for no more than 25 minutes. After the incipient wetness impregnation of the concentrated suspension, the catalyst is dried for a night at 120 °C, then it is washed with boiling water for 30 minutes, dried ad night at 120 °C and finally

calcined in static air at 300 °C for 3 hours. Following this method, Au/TiO$_2$, Au/MgO and Au/NiO-TiO$_2$ (all with Au loading 1.5 wt%) were prepared.

2.2.2 Catalysts characterization

2.2.2.1 Dynamic Light Scattering (DLS)

The measurement of the hydrodynamic diameter of the particles in the suspension, was performed with the DLS analysis (Dynamic Light Scattering), using the Zetasizer Nanoseries (Malvern Instruments) to check the quality of the suspension synthesis. The hydrodynamic diameter is the diameter of the particles in motion in a solution that includes the coordination sphere and any adsorbed species on its surface (e.g. the stabilizer).

Before the analysis, 10 drops of samples were diluted in 10 ml of water to avoid the interactions between the particles that may change the rate of diffusion and therefore the estimation of the size.

2.2.2.2 Transmission Electron Microscopy

TEM analyses were performed with a TEM/STEM FEI TECNAI F20 microscope equipped with a Schottky emitter and operating at 200 KeV. The instrument is fitted with a Fischione High Angle Annular Dark Field Detector (HAADF) for STEM analysis and an Energy Dispersive X-Ray Spectrometer (EDX). Samples were suspended in ethanol and treated with ultrasounds for 15 minutes. A drop of the suspension was deposited on a multifoil holey-carbon film supported by a copper grid. The sample was dried at 100°C. TEM images were used to calculate the particle size; values were averaged over ca 100 particles.

2.2.3 Catalytic measurements

Reactions were conducted in a glass semi-continuous reactor (volume 100 ml, model Büchi Miniclave) supported on a rigid metal grid, closed with a steel cap and equipped with gas lines (Figure 2.11).
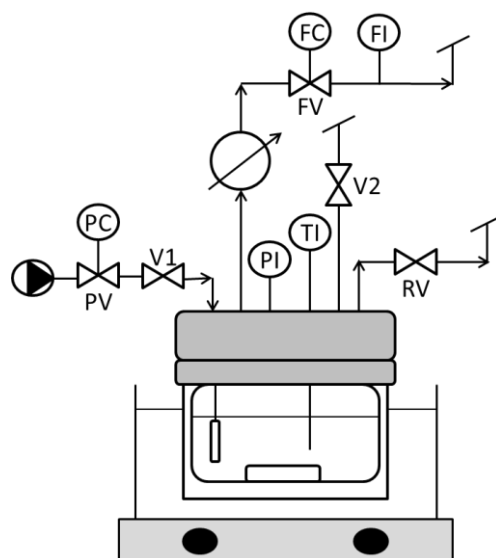
Figure 2.11. Reactor used for the oxidative cleavage of CHD. Legends: PV pressure reducer, PC manual pressure controller, V1 shut-off valve of the oxygen line, PI pressure indicator (manometer), TI temperature indicator (internal thermocouple), V2 valve for sampling, RV rupture disk calibrated at a pressure of 7 bar (connected with a security tank), FV micrometric valve for flow regulation, FC manual flow controller, FI flow indicator (bubble flow meter).

CHD (0.5 g), the catalyst, the base and the solvent (water, 25 ml) were loaded into the reactor and heated. When the desired temperature was reached, the oxygen valve was open and the reaction started (oxygen flow 100 ml/min, pressure 4 bar). At the end of the reaction, oxygen was closed and the reactor was cooled down. The catalyst was separated by centrifugation, the supernatant was acidified with 85 % H_3PO_4 to pH between 2 and 3 and the final volume was measured. Quantitative and qualitative analysis were done by means of a HPLC Agilent 1260 Infinity Series Quaternary LC provided with Agilent Technologies Poroshell 120 EC-C18 4.0 μm (4.6 x 250 mm) operating at 25 °c, a manual injector (loop 20 μl) and a Diode-Array Detector set at 254, 210 and 192 nm. Elution was done in isocratic conditions with a mobile phase composed of H_3PO_4 0,01 M : CH_3CN 95:5 v/v ratio, flow rate 0,800 ml/min. In some cases qualitative analysis were done also by means of ESI-MS spectroscopy.

2.3 Results and discussion

2.3.1 Au/TiO$_2$ catalyst

The catalyst was characterized with TEM microscopy in order to determine nanoparticles size distribution and dispersion (Figure 2.12 and 2.13).
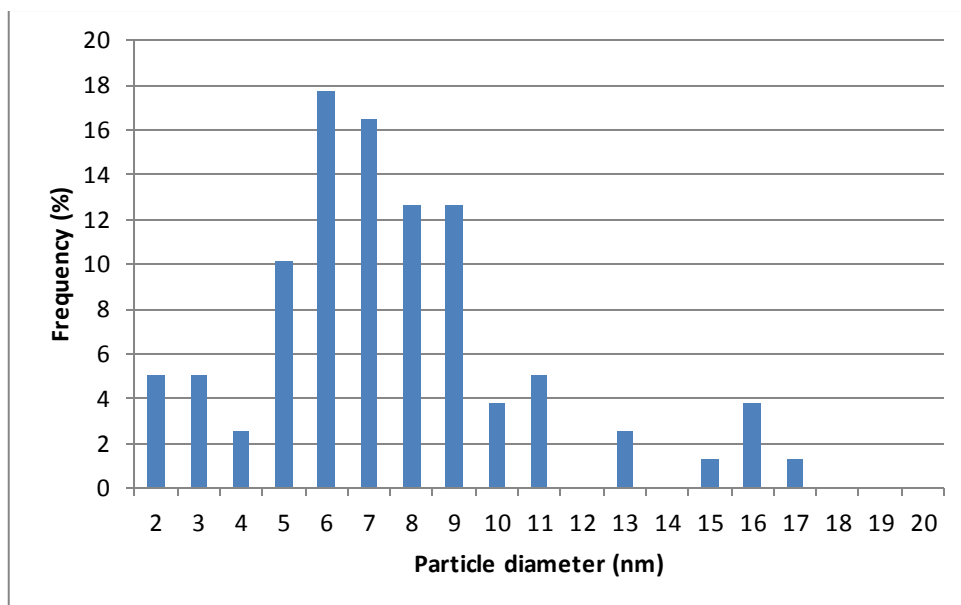
Figure 2.12. Size distribution calculated from TEM analysis
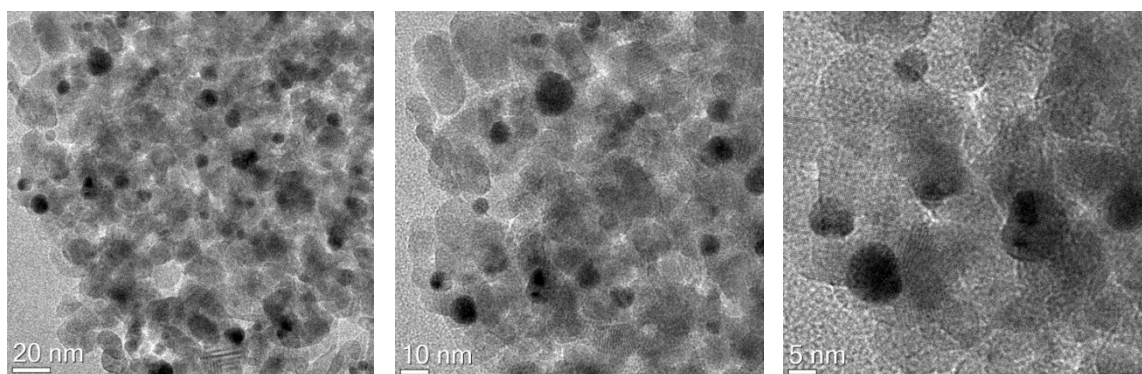
Figure 2.13. TEM pictures of Au/TiO$_2$ catalyst

Average nanoparticles size was 7.4 nm and dispersion was 15.7 %.

Figure 2.14 shows the effect of reaction time on the catalytic behavior of the Au/TiO$_2$ catalyst; the conditions chosen were: CHD : Au : NaOH = 1000 : 1 : 1000 (molar ratios); temperature 90 °C, oxygen pressure 4 bar, oxygen flow 100 ml/min (these conditions

were chosen after results obtained by variation of reaction parameters, see discussion below). In fact, direct oxidation of alcohols into acids is usually performed under basic conditions[39–48].
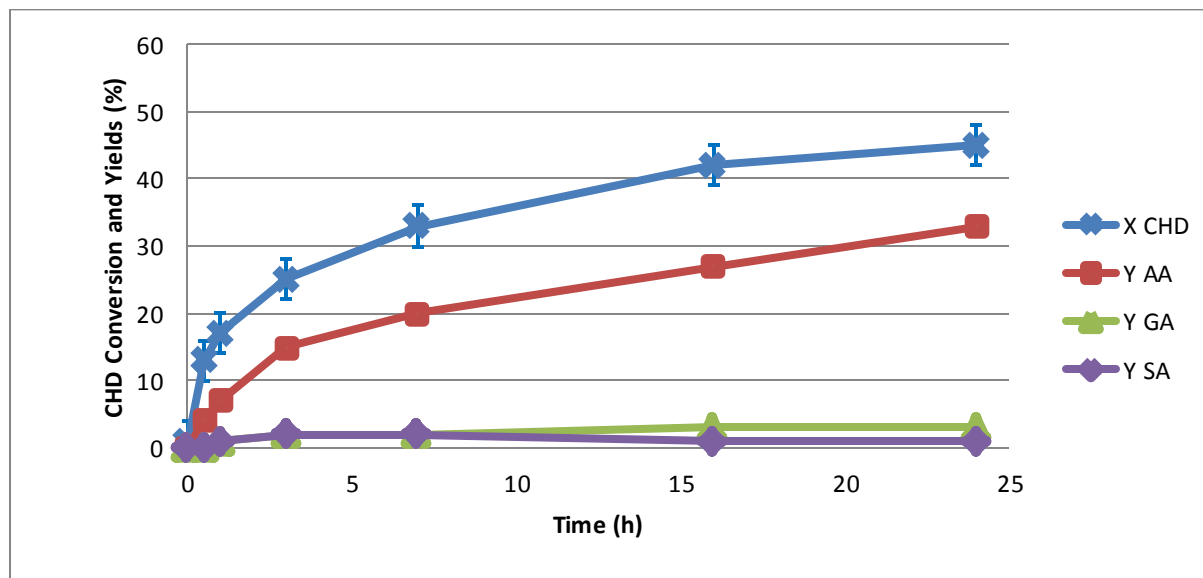
Figure 2.14. CHD conversion (x) and yields to AA (■), GA (▲), SA (♦) based on reaction time with Au/TiO₂. Conditions: CHD : Au : NaOH = 1000 : 1 : 1000 (molar ratios); temperature 90℃, oxygen pressure 4 bar, oxygen flow 100 ml/min. Starting pH was 12.5.

The products of reaction were adipic acid (AA), glutaric acid (GA) and succinic acid (SA). The formation of 2-hydroxycylohexanone (HCHN) and 1,2-cyclohexanedione (CHDO) was observed too, with yields lower than 1% in both cases; these two latter compounds were found to be the key reaction intermediates in CHD oxidation with $Ru(OH)_x/Al_2O_3$ catalysts (under similar reaction conditions as those used with supported Au NPs), and P/Mo polyoxometalates[6]. Other by-products were shown from the HPLC plot, falling in the region of lighter dicarboxylic acids (propanedioic acid, oxalic acid and carbonic acid), but were not individually quantified; taking into account the good C balance registered, and the error in conversion calculation, it possible to assume that the overall yield to these lighter compounds was slightly increasing during time, but was always lower than 5 %.

CHD conversion and AA yield increased with increasing reaction time, but then they slowed down after 3 hours. This could be due to some deactivation phenomena of the

catalyst, but recyclability tests proved that the catalyst did not suffer from deactivation (see results below). It is likely that during the reaction, some products were adsorbed on the surface blocking the active sites, while during recyclability experiments catalysts were washed before each reloading so setting Au NPs free from any weakly interacting adsorbed species.

HCHN and CHDO were the only products identified at the lowest reaction time (0.1 h); this confirms a possible role of these compounds as reaction intermediates. On the other hand, the formation of 1-hydroxycyclopentanecarboxylic acid (HCPA) was not detected, which was one of the prevailing products in CHD oxidation with Ru(OH)x-based catalysts[6]. This compound is very quickly formed under basic conditions by rearrangement of CHDO, which is the main intermediate with supported Ru(OH)x catalysts; this suggests that with Au/TiO$_2$ indeed the oxidative cleavage occurs directly on HCHN, leading to the formation of dicarboxylic acids, and that the side oxidation leading to CHDO, which also may undergo oxidative cleavage, gives a marginal contribution to the formation of the final products. Dedicated experiments carried out by reacting directly HCHN and CHDO will confirm this hypothesis (see below).

Yields of GA and SA were very low; even though their formation was not detected at the lowest reaction time examined (0.5 h), the trend of yields was not that one expected if based on a consecutive reaction network; in fact, GA yield initially increased but then reached a stable value close to 3 %, and SA yield reached the 2 % yield and then decreased down to 1 %. Furthermore, AA yield continuously increased and apparently did not undergo any consecutive oxidative degradation during the experiment time. This was confirmed by performing a reaction starting from AA, in the presence of catalyst under the same conditions chosen for reaction from CHD (CHD : Au : NaOH = 1000 : 1 : 1000 (molar ratios); temperature 90 °C, oxygen pressure 4 bar, oxygen flow 100 ml/min), that showed nil conversion and nil formation of GA and SA. Thus, it seems that the formation of three dicarboxylic acids followed three kinetically independent, parallel reaction pathways; the hypothesized intermediates, either HCHN or CHDO, or both, were so reactive (as it will be shown by the dedicated experiments, see below), that they quickly transformed into successive products by oxidative cleavage; therefore, dicarboxylic acids yields showed a dependence upon time which is that one typically shown by kinetically primary products (Figure 2.15).
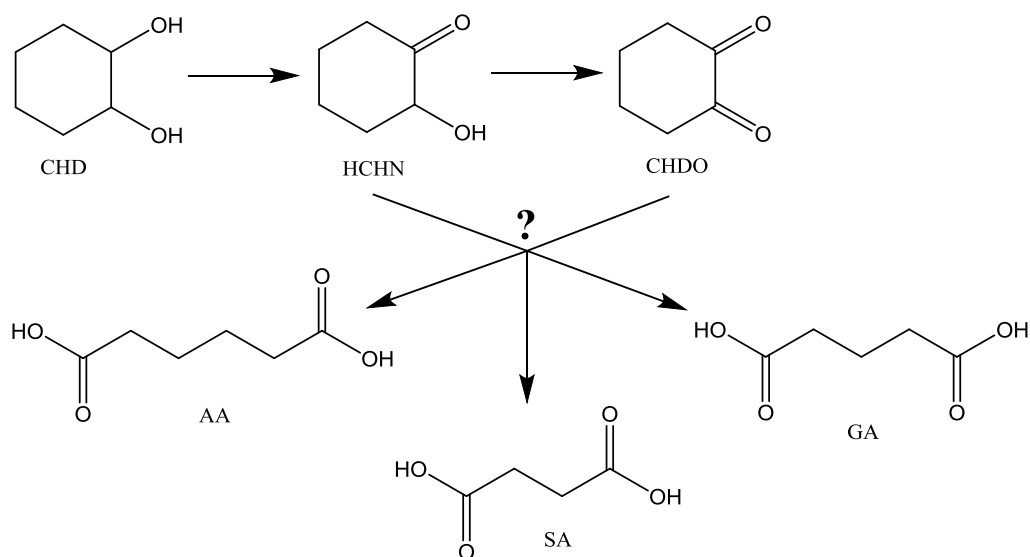
Figure 2.15. Possible reaction pathway for Au/TiO$_2$ catalyst. Sbagliata formula di CHDO.

Experiments were then carried out with the aim to verify the effective heterogeneity of the active phase, which is present in the amount of 1.5 wt%. A leaching test was performed by carrying out a 3 h reaction (molar ratio CHD : Au : NaOH = 1000 : 1 : 1000; T = 90 °C), then the catalyst was removed by filtration and the mixture was reloaded into the vessel for 3 h more of reaction in absence of the catalyst. Any relevant change in CHD conversion (from 25 ± 3 to 28 ± 3 %) and yields of AA (from 15 to 18%) and other products was seen, therefore it is possible to exclude any contribution from homogeneous Au deriving from the loss of active phase during the reaction.

Using the same operating conditions, recyclability were performed test in order to investigate if the catalyst maintained its initial activity. After 3 h of reaction, the catalyst was separated from the reaction mixture, washed with water, dry at 120 °C overnight and reloaded with fresh reagents for 3 h more. This procedure was repeated two times and results are displayed in Figure 2.16.
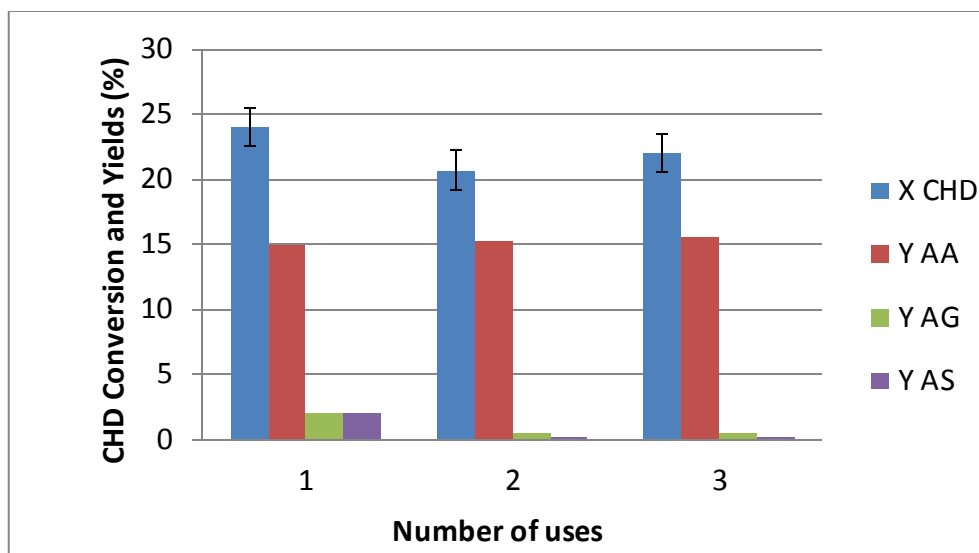
Figure 2.16. CHD conversion, yield to AA, GA and SA based on the number of uses. Conditions: CHD : Au : NaOH = 1000 : 1 : 1000 (molar ratios); temperature 90°C, oxygen pressure 4 bar, oxygen flow 100 ml/min.

It is shown that both CHD conversion and yields to AA did not vary with tests, while yields to SA decreased in the 2nd and 3rd experiment, becoming practically nil. In overall, it is possible to say that the reactivity was not affected markedly with use, and no strong deactivation phenomena occurred, at least within the 3 h reaction time tested for three repeated experiments, nevertheless a slightly increasing average dimensions of the nanoparticles was revealed by TEM (Figure 2.17):

Fresh catalyst: 7.4 nm;

After first use: 7.8 nm;

After third use: 9.1 nm.

This change might take account for the decreased yield to GA and SA, with a corresponding increase of selectivity to AA.
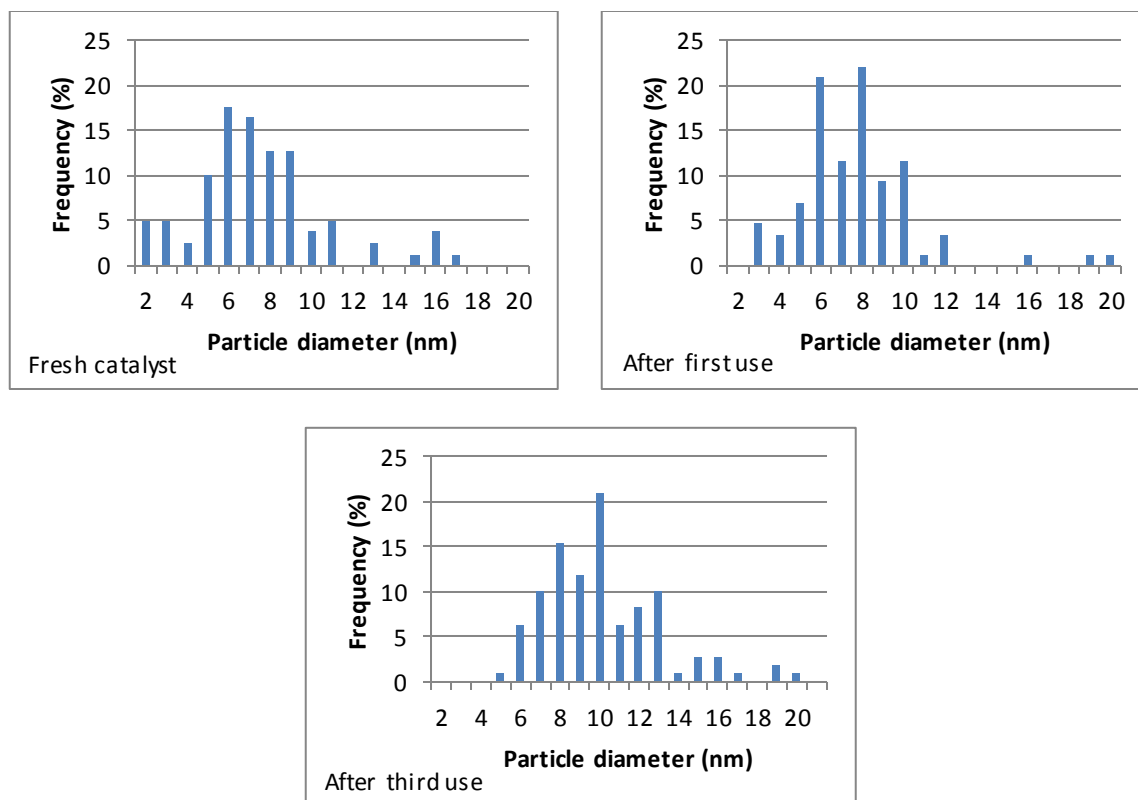
Figure 2.17. Nanoparticles size distribution of new and used catalysts.

Table 2.1 summarizes results obtained by changing some reaction parameters, such as the ratio between substrate and catalyst (entries 1-3), the ratio between substrate and NaOH (entries 4-8), and temperature (entries 9-11). It is shown that an increase of the CHD : Au ratio led to a decline of conversion and yields, as expected, but the selectivity to AA was not much affected, which further confirms that the reaction network consists of parallel reactions for the formation of the main dicarboxylic acids. The ratio CHD : Au = 1000 : 1 was chosen for further experiments (also used for experiments reported in Figure 2.14 and Figure 2.16). In regard to the effect of NaOH, it is shown that in the absence of the base CHD conversion was negligible, and no formation of dicarboxylic acids was observed; the only products were HCHN (yield 1.1 %) and CHDO (yield 0.1 %). The presence of the base led to an increase of CHD conversion until a maximum value shown for a CHD : NaOH ratio equal to 1:1; a further increase led to a decline of both conversion and AA yield, but also to an increase of GA and SA yields. The optimal ratio CHD : NaOH 1:1 (also used for experiments in Figures 2.14 and 2.16) was chosen for further experiments.

Finally, experiments carried out with variation of temperature (entries 9-11) showed the expected increase of conversion and yields along with the temperature raise.

Entry	T (°C)	CHD:Au:NaOH (molar ratios)	CHD conv. (%)	AA Y (%)	GA Y (%)	SA Y (%)
1	90	500:1:500	29±3	17	4	2
2	**90**	**1000:1:1000**	**25±3**	**15**	**3**	**1**
3	90	5000:1:5000	9±2	6	1	1
4	90	1000:1:0	3±2	0	0	0
5	90	1000:1:500	13±2	10	0.4	1
6	**90**	**1000:1:1000**	**25±3**	**15**	**3**	**1**
7	90	1000:1:1500	27±3	17	5	2
8	90	1000:1:2000	23±3	13	6	3
9	60	1000:1:1000	7±2	3	0.1	0.2
10	80	1000:1:1000	15±2	11	1	0.8
11	**90**	**1000:1:1000**	**25±3**	**15**	**3**	**1**

Table 2.1. Results of experiments carried out in function of reaction parameters. For all experiments, reaction time was 3 h.

Previous studies showed that with Ru(OH)x-based catalysts in basic environment, the key reaction intermediate was CHDO, because of the ability of Ru(IV) oxo complexes to coordinate both the hydroxyls groups of CHD[6]. However, CHDO is the precursor of several undesired side reactions, a situation which finally leads to poor selectivity to AA. A more selective oxidation route would start from HCHN, which is oxidatively cleaved even in the absence of catalyst. Therefore, the key point in order to achieve high selectivity to AA under basic conditions is to have a catalyst which performs the oxidative cleavage faster than the oxidation of the C-OH moiety to the carbonyl. In order to confirm the role of the two possible intermediates, HCHN and CHDO, experiments by using these compounds as reactants were done. Tests were carried out at 90°C for 3 h, in some cases under oxygen flow of 100 ml/min and 4 bar pressure, in other cases without oxygen, and either in the presence or absence of the Au catalyst. Moreover, since the pH of the solution is an important parameter in determining the

reactivity of these compounds, tests were also carried out by changing the amount of NaOH added. The results are reported in Table 2.2.

Reactant	pH	Catalyst	O_2	X (%)	HCPA Y (%)	AA Y (%)	GA Y (%)	SA Y (%)	Other products
CHDO	> 13	No	Yes	100	38	0	28	0	nd
CHDO	> 13	No	No	100	61	0	0	0	nd
CHDO	>13	Yes*	Yes	99	0	14	36	5	nd
CHDO	12.5	Yes	Yes	99	0	6	19	2	nd
CHDO	6.3	No	Yes	76		0	21	0	AC, HCL, AAN, light acids
CHDO	6.3	Yes	Yes	76	0	8	24	1	nd
CHDO	6.3	Yes*	Yes	64	0	9	47	1	nd
HCHN	> 13	No	Yes	100	52	20	15	11	Traces
HCHN	>13	Yes	Yes	99	0	49	5	3	nd
HCHN	>13	Yes**	Yes	99	0	73	7	3	nd
HCHN	12.5	No	Yes	100	0	71	6	3	AC, HCL, CHDO, light acids

Table 2.2. Reactivity of intermediates HCHN and CHDO. Substrate : Au 1000:1; temperature 90℃, reaction time 3 hours.* CHDO: Au 100:1; ** HCHN:Au 200:1; AC :aldol condensate; HCL: 6-hydroxycaprolactone; AAN: adipic anhydride. Nd=not determined.

First observation is that both HCHN and CHDO were much more reactive than CHD, which confirms the hypothesis about the reaction network. In the absence of the catalyst and under strongly basic pH (>13) CHDO was converted into HCPA, with 38 % yield (it also formed without catalyst); this compound was never observed under usual reactivity experiments from CHD. A considerable yield to GA was also shown (28 %), which did not form in the absence of O_2. At lower pH (pH 12.5), at conditions closer to those used for experiments with CHD, and in the presence of the catalyst, no HCPA formed, and AA was formed; however, still GA was the prevailing product. The same occurred at neutral pH; GA yield always prevailed over AA yield. This demonstrates that

CHDO cannot be the key reaction intermediate in CHD oxidation over Au-TiO$_2$ catalyst; in fact the cleavage of CHDO leads mainly to GA.

When the reaction was carried out starting from HCHN, at strongly basic pH and without catalyst, again the formation of HCPA (a compound which forms from CHDO) was shown, which indicates that the transformation of HCHN to CHDO was very rapid. However, differently from what shown from CHDO, also relevant amounts of AA, GA and SA formed. This means that even though CHDO undergoes further cleavage to GA, the direct cleavage of HCHN (which also occurs in the absence of the catalyst) leads to AA mainly. In the presence of the catalyst the cleavage of HCHN to AA (with minor formation of GA and SA) was greatly accelerated compared to the competitive reaction of HCHN oxidation to CHDO, and high yield to AA was shown; the role of the catalyst is also demonstrated by the fact that the test carried out with a higher amount of catalyst led to 73 % yield to AA. When a lower pH was used, under conditions at which the formation of CHDO and HPCA was less favoured, still a very high yield to AA was shown, even without catalyst. Results showed us that AA formation occurs selectively from HCHN also in the absence of the catalyst, but a very basic pH should be avoided in order to limit the competitive oxidation of HCHN to CHDO, precursor for GA formation. However, the presence of the Au catalyst accelerates the cleavage compared to the oxidation of HCHN to CHDO.

It is possible to conclude that HCHN is the key intermediate compound in CHD aerobic oxidation with Au-based catalyst. CHDO is a reaction intermediate which minimally contributes to AA formation, leading to several side reactions and its formation is limited because of the less basic conditions necessary for the oxidation with Au NPs compared to the Ru(OH)$_x$ based catalysts.

In regard to the mechanism through which HCHN is cleaved to AA, two different hypothesis can be formulated. One mechanism involves the hydration of the carbonyl to yield the geminal glycol, which then rearranges under oxidizing conditions by losing two H atoms with breaking of the C-C bond and formation of 6-oxohexanoic acid (precursor of AA) and H$_2$O (Figure 2.18). This mechanism, similar to that one recently proposed for oleic acid oxidative scission[31], might explain the parallel formation of AA, GA and SA by considering that the cleavage may indeed occur at different positions. If it occurs at the C(OH)-C(O) bond, it gives rise to the formation of AA. However, a concomitant cleavage

at both the latter bond and one of the two vicinal C-C bonds (either C-C(O) or C-C(OH)) might lead to the formation of GA with loss of one C atom in form of CO_2, whereas the concomitant cleavage of C-C(O) and C-C(OH) bonds would lead to the direct formation of SA with loss of two CO_2 molecules. The lower probability associated to the concomitant cleavage of two C-C bonds instead of one bond only would explain the very low selectivity to GA and SA experimentally observed. In regard to the oxidation of CHDO, which leads selectively to GA, this might be attributed to the fact that because of the high reactivity of the diketone, the concomitant cleavage of two vicinal C-C bonds (C(O)-C(O) and C-C(O)), with release of CO_2, occurs faster than the cleavage of the C(O)-C(O) bond only.
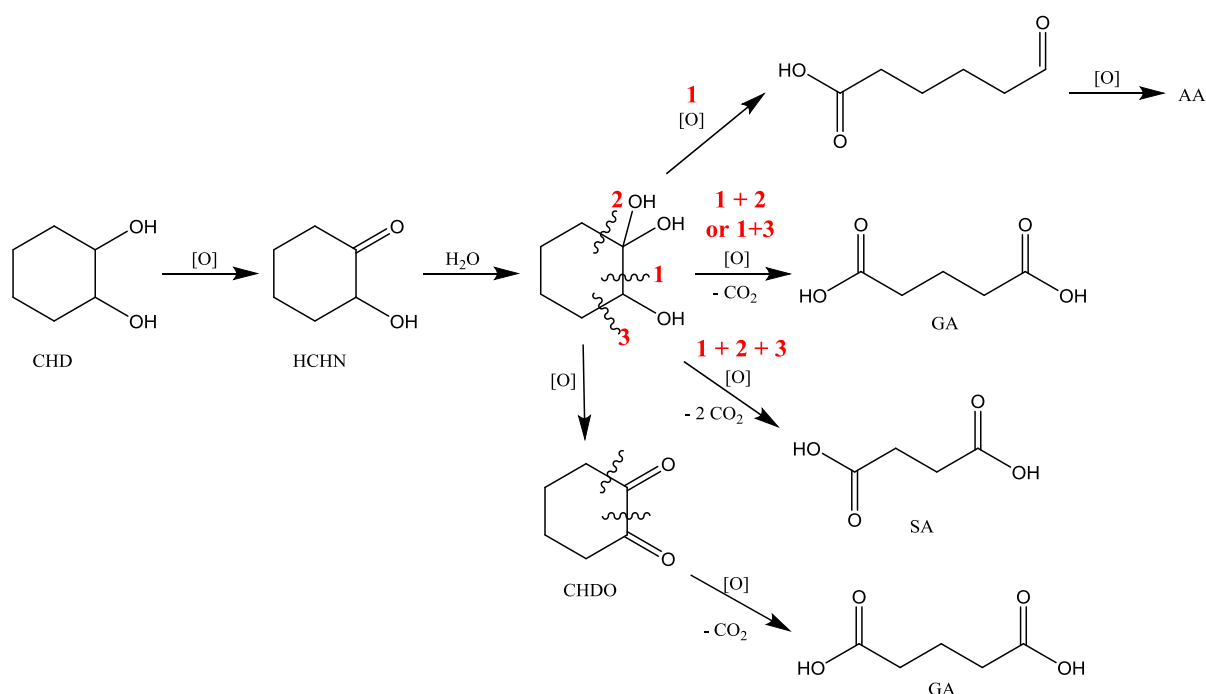
Figure 2.18. First hypothesis of HCHN oxidation to AA with Au/TiO$_2$ catalyst.

In an alternative hypothesis (Figure 2.19), the mechanism might involve the reaction of a radical at the C atom holding the -OH moiety in the intermediate HCHN (whose formation would be favoured by the delocalisation over the vicinal carbonyl) with O_2, to yield an hydroxo-peroxo species and then a hydroxo-hydroperoxo species by a H abstraction (resembling the Criegee intermediate obtained by hydroperoxidation of carbonyls), which would then rearrange into adipic anhydride; the latter would be finally hydrolysed to yield AA. The GA formation would take place starting from CHDO, since an

intramolecular rearrangement in basic conditions would lead to 6-hydroxycaprolactone. The latter might either oxidehydrogenate to adipic anhydride, or develop a radical species whose reaction with O_2 would generate again a hydroxo-hydroperoxo species. The further rearrangement of this latter compound and the subsequent hydrolysis might lead to the release of CO_2 and to the formation of 5-hydroxy-pentanoic acid, precursor of GA.

One experimental evidence in favour of the second mechanism is the finding that both 6-hydroxycaprolactone and adipic anhydride were found amongst the reaction products (but not quantified) when experiment were carried out from HCHN and CHDO.
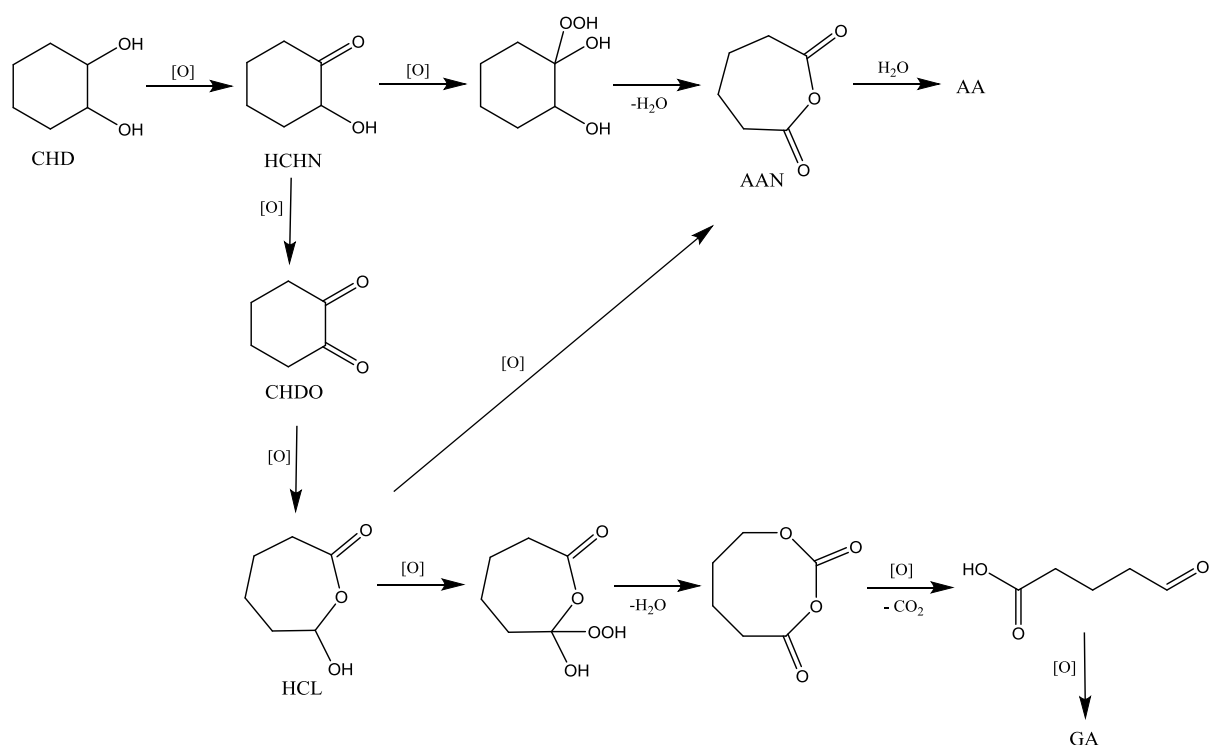
Figure 2.19. Second hypothesis for HCHN oxidation to AA with Au/TiO$_2$ catalyst.

2.3.2 Au/MgO catalyst

TEM analysis (Figure 2.20 and 2.21) gave an average nanoparticles diameter of 7.9 nm and dispersion equal to 14.7 %.
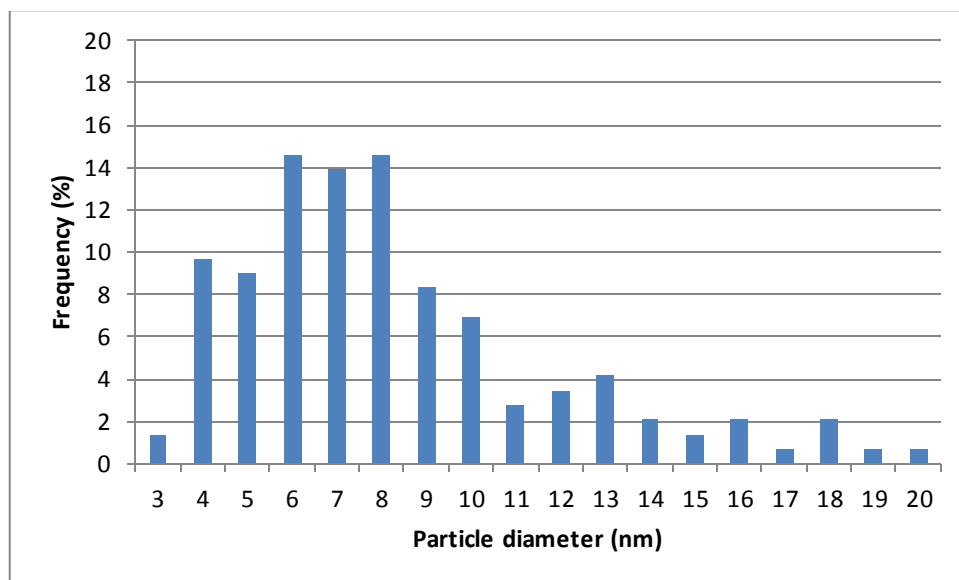
Figure 2.20. Nanoparticles size distribution of Au/MgO catalyst
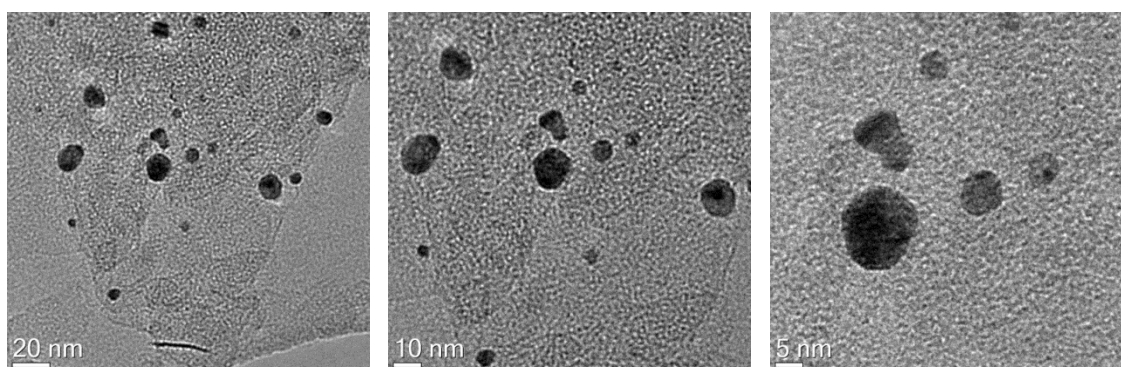
Figure 2.21. TEM pictures of Au nanoparticles of Au/MgO catalyst.

Experiments with Au/TiO$_2$ showed that a controlled basicity of the reaction media is necessary in order to activate one of the hydroxyl groups of the substrate and avoid side reactions. For this reasons, it was decided to support gold nanoparticles on magnesia in order to verify if the basicity of the oxide was sufficient for CHD activation.

Starting from the optimal reaction conditions determined with Au/TiO$_2$ catalyst, the effect of CHD : NaOH molar ratio was investigated. Without the addition of a base, no AA formation was seen, so the basicity of MgO is not strong enough to activate the

30

reaction. Adding NaOH to the reaction mixture, AA formed and its amount increased with the increasing of the basicity (CHD conversion 31 %, AA yield 18 %), so next experiments were carried out with CHD : NaOH molar ratio equal to 1:1, the same used for the titania supported catalyst.

Afterwards the activity of the catalyst was studied as a function of reaction time in the same conditions of Au/TiO$_2$: molar ratio CHD : Au : NaOH = 1000 : 1 : 1000, 90°C, oxygen pressure 4 bar, oxygen flow 100 ml/min. Results are reported in Figure 2.22. Trends for conversion of CHD and products yields are similar to those obtained with the Au/TiO$_2$ catalyst, so it is possible to hypothesize that the reaction pathway is the same for both catalysts. Gold nanoparticles supported on magnesia were slightly more active and more selective than those supported on titania: after 24 h for MgO, CHD conversion, AA yield, and AA selectivity were 45 %, 39 % and 87 % respectively, while for TiO$_2$ they were 45 %, 33 % and 74 %.
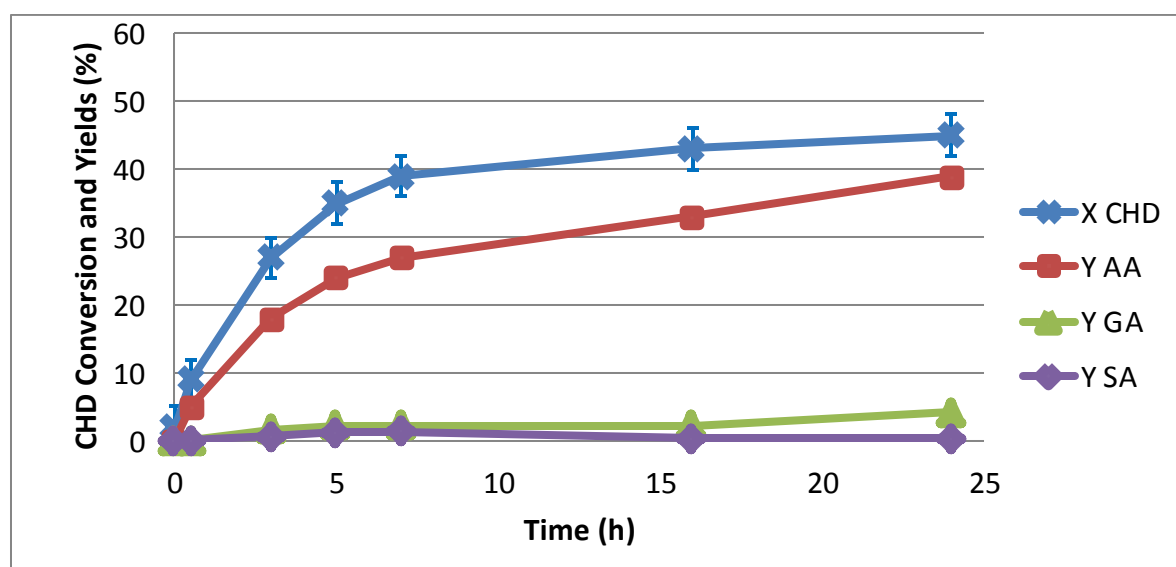
*Figure 2.22. CHD conversion (**x**) and yields to AA (■), GA (▲), SA (♦) based on reaction time for Au/MgO. Conditions: CHD : Au : NaOH = 1000 : 1 : 1000 (molar ratios); temperature 90°C, oxygen pressure 4 bar, oxygen flow 100 ml/min.*

Since the conversion and AA yield seemed to slow-down after 5 hours of reaction, a deactivation test was performed: an usual reaction was conducted for 3 hours (same reaction conditions followed for reaction of Figure 2.22), the catalyst was then

separated, washed with water, dried one night at 120 °C, and then reloaded with the same reaction mixture (the one already reacted for 3 hours) for other 3 hours. It was noticed that reaction mixture continued to react giving CHD conversion and AA yield similar to that one obtained previously after 7 hours; this means that some events takes place that affects catalysts reactivity during the reaction and slows-down the initial rate of the reaction.

Therefore, experiments in order to check the stability of the catalyst with leaching test and recyclability test were performed, in order to better understand the observed phenomenon. Dedicated experiments did not show any active phase dissolution since the conversion of CHD and AA yield did not increase during the reload of the reaction mixture without catalyst (CHD conversion constant at 27 % and AA yield from 18 to 20 %). For reuse test, the catalyst has been loaded 3 hours for three times and after every use it has been washed with cold water and dried at 120 °C for a night. CHD conversion and yields decreased after every used indicating the presence of a deactivation phenomenon (see Figure 2.23), which had not been observed with the Au/TiO$_2$ catalyst.
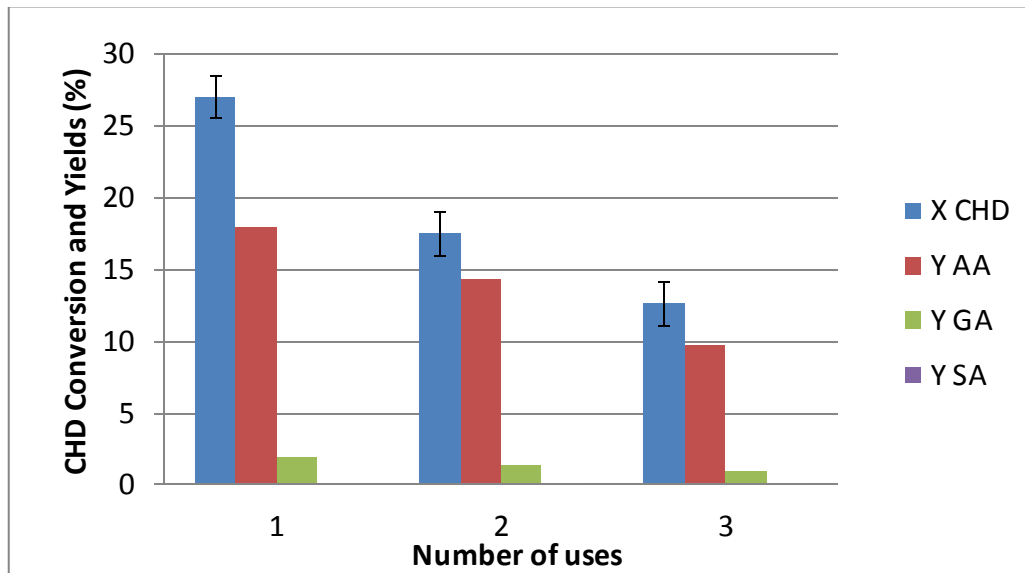
Figure 2.23. CHD conversion, yield to AA, GA and SA based on the number of uses of Au/MgO. Conditions: CHD : Au : NaOH = 1000 : 1 : 1000 (molar ratios); temperature 90℃, oxygen pressure 4 bar, oxygen flow 100 ml/min.

TEM analysis of the fresh catalyst and after use for one and three times was performed in order to see if the observed deactivation was be due to some modification of the active phase. In the case of the used catalyst (Figure 2.24), it was noticed the presence of some filaments of carbonaceous material on the surface that were not removed by simple washing with cold water, but only after calcination at 300 °C for 3h. Moreover nanoparticles size increased already after the first use, from 7.9 to 9.3 nm, an effect that can obviously affect the reactivity of the catalyst. Also after calcination at 300 °C, the catalyst did not recover its initial reactivity: after other 3 hours of reaction, CHD conversion and AA yield decreased to 10 % and 8.5 % respectively. Moreover, the thermal treatment caused an increase of nanoparticles dimensions to 10.3 nm, fact that could be the cause of this further deactivation.

Figure 2.24. TEM pictures of Au/MgO catalyst used 3 times

2.4 Conclusions

Previous studies with Ru-based catalysts and POMs for the oxidative cleavage of CHD, showed the necessity to find a catalyst able to oxidize the hydroxyl groups in sequence. The aim is to obtain HCHN which can be oxidized to AA with high selectivity also in the absence of catalyst in basic medium.

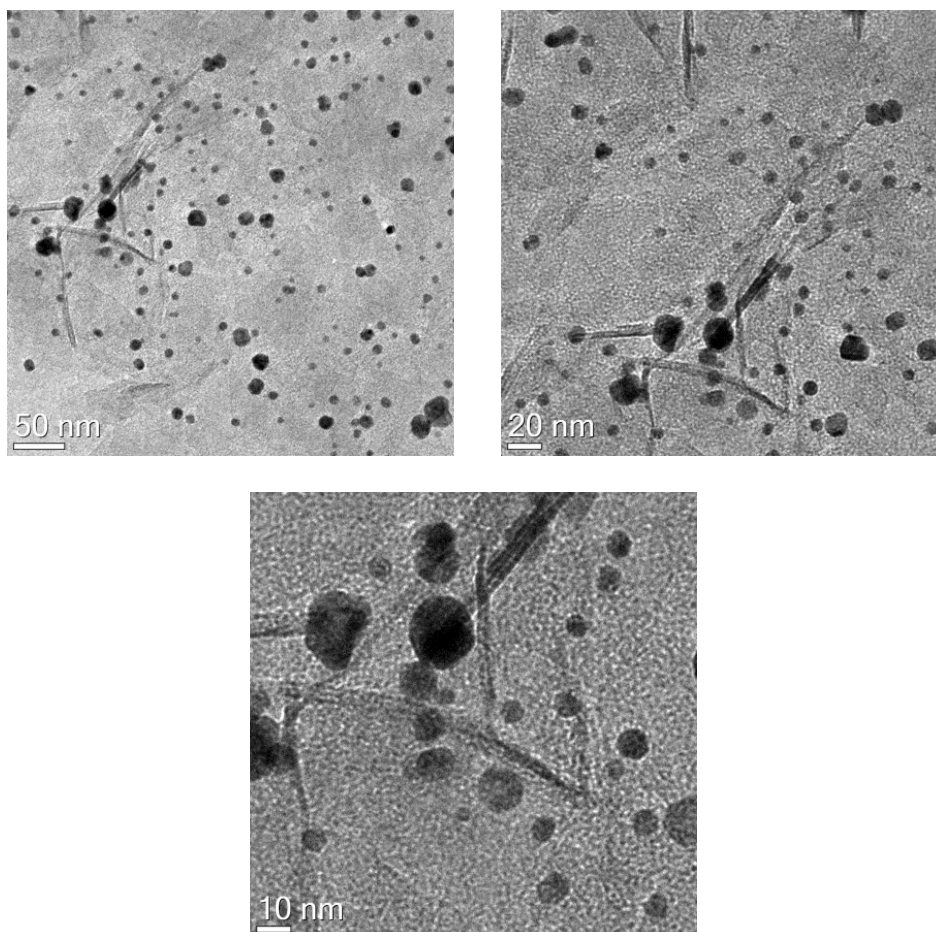Au/TiO$_2$ and Au/MgO catalysts turned out to be able to oxidize CHD to HCHN obtaining AA with high selectivity and working in less basic conditions with respect to Ru/Al$_2$O$_3$, avoiding hydrolysis of the product and catalyst separation, which is instead required with POMs. GA and SA were the minor products of the reaction formed by parallel reaction pathways and both catalysts were effectively heterogeneous. The basic character of MgO was not enough to provide the basicity needed, but with Au/MgO AA formed with a higher selectivity than Au/TiO$_2$ (87 and 74 % respectively). This characteristic could be due to a different interaction between the catalyst and CHD that allowed a better mass transfer between the substrate dissolved in the liquid phase and the supported active phase. This aspect could be an interesting object of further investigation.

Au/MgO showed deactivation during the reaction and TEM analysis revealed an increase in the nanoparticles sizes after recycle and the deposition of carbonaceous filaments that could be removed only after calcination at 300 °C. The understanding of the origin of these experimental evidences could be helpful to design a catalyst with improved activity and selectivity towards the oxidative cleavage of CHD to AA.

2.5 Acknowledgements

2.6 References

(1)   Oppenheim, J. P.; Dickerson, G. L. *Kirk-Othmer Encycl. Chem. Technol.* **2003**.

(2)   Tuttle Musser, M. In *Ullmannn's Encyclopedia of Industrial Chemistry*; 2000.

(3)   *Sustainable industrial processes*; Cavani, F., Ed.; Wiley-VCH: Weinheim, 2009.

(4)   Cavani, F. *J. Chem. Technol. Biotechnol.* **2010**, *85* (9), 1175–1183.

(5)   Cavani, F.; Teles, J. H. *ChemSusChem* **2009**, *2* (6), 508–534.

(6)   Rozhko, E.; Raabova, K.; Macchia, F.; Malmusi, A.; Righi, P.; Accorinti, P.; Alini, S.; Babini, P.; Cerrato, G.; Manzoli, M.; Cavani, F. *ChemCatChem* **2013**, *5* (7), 1998–2008.

(7)   Schindler, G.-P.; Bartl, P.; Hoelderich, W. F. *Appl. Catal. Gen.* **1998**, *166* (2), 267–279.

(8)   Timofeeva, M. N.; Kholdeeva, O. A.; Jhung, S. H.; Chang, J.-S. *Appl. Catal. Gen.* **2008**, *345* (2), 195–200.

(9)   Lee, S.-O.; Raja, R.; Harris, K. D. M.; Thomas, J. M.; Johnson, B. F. G.; Sankar, G. *Angew. Chem. Int. Ed.* **2003**, *42* (13), 1520–1523.

(10)   Lapisardi, G.; Chiker, F.; Launay, F.; Nogier, J. P.; Bonardet, J. L. *Microporous Mesoporous Mater.* **2005**, *78* (2–3), 289–295.

(11)   Sato, K.; Aoki, M.; Noyori, R. *Science* **1998**, *281* (5383), 1646–1647.

(12)   Noyori, R.; Aoki, M.; Sato, K. *Chem. Commun.* **2003**, No. 16, 1977.

(13)   Venturello, C.; Ricci, M. *J Org Chem* **1986**, *51* (9), 1599–1602.

(14)   asutaka Ishii, Y.; Yamawaki, K.; Ura, T.; Yamada, H.; Yoshida, T. *J Org Chem* **1988**, *53*, 3581–3593.

(15)   Chen, H.; Dai, W.-L.; Gao, R.; Cao, Y.; Li, H.; Fan, K. *Appl. Catal. Gen.* **2007**, *328* (2), 226–236.

(16)   Zhu, W.; Li, H.; He, X.; Zhang, Q.; Shu, H.; Yan, Y. *Catal. Commun.* **2008**, *9* (4), 551–555.

(17)   Donoeva, B. G.; Trubitsyna, T. A.; Al-Kadamany, G.; Kortz, U.; Kholdeeva, O. A. *Kinet. Catal.* **2010**, *51* (6), 816–822.

(18)   Vennat, M.; Brégeault, J.-M.; Herson, P. *Dalton Trans.* **2004**, No. 6, 908–913.

(19)   Vennat, M.; Herson, P.; Brégeault, J.-M.; Shul'Pin, G. B. *Eur. J. Inorg. Chem.* **2003**, *2003* (5), 908–917.

(20)   El Aakel, L.; Launay, F.; Brégeault, J.-M.; Atlamsani, A. *J. Mol. Catal. Chem.* **2004**, *212* (1–2), 171–182.

(21)   Brégeault, J.-M. *Dalton Trans* **2003**, No. 17, 3289–3302.

(22)   Bregeault, J. M.; F. Launay; Atlamsani, A. *C R Acad Sci Paris* **2001**, *IIc*, 11–26.

(23)   Vennat, M.; Brégeault, J.-M. *Appl. Catal. Gen.* **2010**, *386* (1–2), 9–15.

(24)   Carlsen, P. H.; Katsuki, T.; Martin, V. S.; Sharpless, K. B. *J. Org. Chem.* **1981**, *46* (19), 3936–3938.

(25)   Kumobayashi, H.; Akutagawat, S. *J Org Chem* **1993**, *58*, 2929–2930.

(26)   Felthouse, T. R. *J. Am. Chem. Soc.* **1987**, *109* (24), 7566–7568.

(27)   Zabjek, A.; Petric, A. *Tetrahedron Lett.* **1999**, *40*, 6077–6078.

(28)   Hashmi, A. S. K.; Hutchings, G. J. *Angew. Chem. Int. Ed.* **2006**, *45* (47), 7896–7936.

(29)   Gorbanev, Y. Y.; Klitgaard, S. K.; Woodley, J. M.; Christensen, C. H.; Riisager, A. *ChemSusChem* **2009**, *2* (7), 672–675.

(30)   Casanova, O.; Iborra, S.; Corma, A. *ChemSusChem* **2009**, *2* (12), 1138–1144.

(31)   Kulik, A.; Janz, A.; Pohl, M.-M.; Martin, A.; Köckritz, A. *Eur. J. Lipid Sci. Technol.* **2012**, *114* (11), 1327–1332.

(32)   Ryabenkova, Y.; Miedziak, P. J.; Dummer, N. F.; Taylor, S. H.; Dimitratos, N.; Willock, D. J.; Bethell, D.; Knight, D. W.; Hutchings, G. J. *Top. Catal.* **2012**, *55* (19–20), 1283–1288.

(33)   Antonetti, C.; Galletti, A. M. R.; Accorinti, P.; Alini, S.; Babini, P.; Raabova, K.; Rozhko, E.; Caldarelli, A.; Righi, P.; Cavani, F.; Concepcion, P. *Appl. Catal. Gen.* **2013**, *466*, 21–31.

(34)   Solmi, S.; Rozhko, E.; Malmusi, A.; Lolli, A.; Albonetti, S.; Cavani, F.; Accorinti, P.; Alini, S.; Babini, P. DGMK Tagungsbericht; Hamburg, 2014.

(35)   Hirai, Y.; Kojima, T.; Mizutani, Y.; Shiota, Y.; Yoshizawa, K.; Fukuzumi, S. *Angew. Chem. Int. Ed.* **2008**, *47* (31), 5772–5776.

(36)   Shiota, Y.; Herrera, J. M.; Juhász, G.; Abe, T.; Ohzu, S.; Ishizuka, T.; Kojima, T.; Yoshizawa, K. *Inorg. Chem.* **2011**, *50* (13), 6200–6209.

(37)   Albonetti, S.; Pasini, T.; Lolli, A.; Blosi, M.; Piccinini, M.; Dimitratos, N.; Lopez-Sanchez, J. A.; Morgan, D. J.; Carley, A. F.; Hutchings, G. J.; Cavani, F. *Catal. Today* **2012**, *195* (1), 120–126.

(38)   Bergeret, G.; Gallezot, P. In *Handbook of Heterogeneous Catalysis (G. Ertl, H. Knözinger, F. Schüth, J. Weitkamp)*; Wiley-VCH Verlag GmbH & Co. KGaA, 2008; pp 738–765.

(39)   Mallat, T.; Baiker, A. *Chem. Rev.* **2004**, *104* (6), 3037–3058.

(40)   Donze, C.; Korovchenko, P.; Gallezot, P.; Besson, M. *Appl. Catal. B Environ.* **2007**, *70* (1–4), 621–629.

(41)   Korovchenko, P.; Donze, C.; Gallezot, P.; Besson, M. *Catal. Today* **2007**, *121* (1–2), 13–21.

(42)   Besson, M.; Gallezot, P. *Catal. Today* **2000**, *57* (1), 127–141.

(43)   Garcia, R.; Besson, M.; Gallezot, P. *Appl. Catal. Gen.* **1995**, *127*, 165–176.

(44)   Carrettin, S.; McMorn, P.; Johnston, P.; Griffin, K.; Kiely, C. J.; Attard, G. A.; Hutchings, G. J. *Top. Catal.* **2004**, *27* (1–4), 131–136.

(45)   Biella, S.; Prati, L.; Rossi, M. *J. Catal.* **2002**, *206* (2), 242–247.

(46)   Pasini, T.; Piccinini, M.; Blosi, M.; Bonelli, R.; Albonetti, S.; Dimitratos, N.; Lopez-Sanchez, J. A.; Sankar, M.; He, Q.; Kiely, C. J.; Hutchings, G. J.; Cavani, F. *Green Chem.* **2011**, *13* (8), 2091.

(47)   Albonetti, S.; Lolli, A.; Morandi, V.; Migliori, A.; Lucarelli, C.; Cavani, F. *Appl. Catal. B Environ.* **2015**, *163*, 520–530.

(48)   Gallezot, P. *Catal. Today* **2007**, *121* (1–2), 76–91.

CHAPTER 3. THE OXIDATION OF D-GLUCOSE TO GLUCARIC ACID USING Au/C CATALYSTS
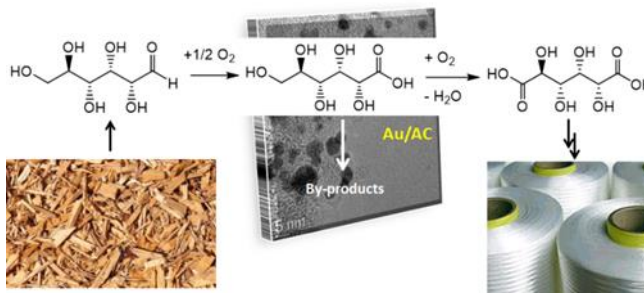
This chapter was previously published as:

Stefania Solmi, Calogero Morreale, Francesca Ospitali, Stefano Agnoli, Fabrizio Cavani, *The oxidation of D-glucose to glucaric acid using Au/C catalysts*, ChemCatChem, DOI: 10.1002/cctc.201700089R1

See Appendix A for Permission for journal article use.

3.1 Introduction

The conversion of renewable biomass into fuels and high-value chemicals is a sustainable alternative to the use of fossil resources[1–5]. In this context, carbohydrates are a widely available and inexpensive resource[6–9], while selective oxidation catalysis plays an important role in the functionalisation of these oxygenated building blocks[10–12]. In fact, sugar dicarboxylic acids (aldaric acids) are important chemicals used for the detergent, pharma, and polymer industries which are currently produced by the oxidation of saccharides with nitric acid[13–19]. For instance, glucarate builders are used in consumers' dishwashers and show a potential in functional materials and as a building block for new polymers, such as hyper-branched polyesters[15,16]. Glucarate derivatives have also been studied for therapeutic purposes. Recently Rivertop Renewables began a pilot-scale production of glucarate via oxidation of D-glucose with nitric acid[17]. Rivertop has improved the oxidation technology by turning it into a catalytic process that reduces nitric acid consumption, while increasing the glucarate yield[18,19]. In an alternative approach, the nitroxide-mediated oxidation of glucose using bleach and

NaBr produces glucaric acid (GA) in a yield of >90 %[20,21]. Electrochemical oxidation has also been reported as an efficient synthesis method[22,23].

These technologies, however, suffer from the use of corrosive and hazardous reagents, difficult separation and recyclability of homogeneous catalysts, and generation of toxic co-products. Therefore, processes that are more sustainable are desirable: processes in which heterogeneous catalysts are used with air, oxygen, or hydrogen peroxide as oxidants.

Catalysts which have been investigated for the aerobic oxidation of monosaccharides to aldaric acids are based on platinum or gold. With Pt-based systems, earlier works reported yields close to 60 %[24,25]. In a recent work, Lee et al.[26] stated that the use of a commercial Pt/C catalyst enabled the oxidation of glucose and gluconic acid (GO), the main intermediate of glucose oxidation, at a neutral pH and mild conditions, with a glucose/Pt molar ratio of 54, and an optimized GA yield of 74 %. Chaudhari and co-workers described the catalytic performance of supported PtPd and PtCu NP alloys for glucose oxidation with O_2[27,28]. For example, PtPd-TiO_2 catalysts showed a significantly enhanced catalytic activity and improved selectivity to GA (44 %) in the oxidation of aqueous glucose solution, compared to monometallic catalysts. The best performance was achieved at 10 bar O_2 pressure, at a temperature of 45 °C, in the presence of NaOH. Derrien et al.[29] recently reported a maximum glucarate yield of 54 % with a Pt/C catalyst. Besson et al.[30] reported that in a two-step process, gluconate was first formed with an 80 % yield in the catalytic oxidation of glucose over Pt/C in alkaline medium (pH 9), whereas in a second step gluconate was further oxidized to glucarate, with a final selectivity of 57 % at 97 % conversion.

Recent patents by Rennovia Inc. claim the oxidation of glucose to GA over Pt and Pt-Au NP catalysts in non-neutralised conditions[31–36]; GA is an intermediate for the synthesis of adipic acid[34]. Rennovia and Johnson Matthey Process Technologies recently claimed to have successfully started up a fully integrated mini-plant for the production of GA from glucose and catalytic hydrogenolysis of GA to adipic acid[35]. The GA yield reported is 66 % in the presence of Pt/SiO_2 and 71 % using a Au–Pt/TiO_2 catalyst. Boussie et al.[33] reported yields to GA as high as 50-60 % with an overall selectivity to GA + on-path intermediates (GO, gururonic acid, d-gluco-hexodialdose and glucuronic acid) of 85-90 %, while operating at native pH, 5 bar O_2 pressure, and T between 80 and 120 °C. The

process is claimed to operate at approximately 50 % per-pass glucose conversion, with the separation and recycling of intermediates, to achieve an overall process yield to GA higher than 90 %. The same authors patented a method for the separation of GA, which involves contacting the reaction mixture with an ion exchange medium and eluting with an eluent which comprises an organic acid[36].

Gold NPs have been used as efficient catalysts for the aerobic oxidation of monosaccharides to aldonic acids (i.e. glucose to GO, arabinose to arabinonic acid, galactose to galactonic acid), and of uronic acids (e.g. glucuronic, mannuronic, and galacturonic acids) to corresponding aldaric acids[37–43]. Typically, both high selectivity and stability are shown by supported Au NPs. For example, the aldehyde group of D-glucose is efficiently oxidized to GO either in mildly alkaline conditions (pH range 8–10), which are required to neutralize the produced acid and keep the catalyst surface clean, or even in the absence of a base.

A variety of Au-based catalysts have been reported in literature, with yields to GO which can be higher than 80 %[44–55]. Au/MgO, Au/CeO$_2$, Au/Al$_2$O$_3$ and Au/TiO$_2$ show optimal performance, the yield to GO being a function of both reaction conditions (pH, temperature, O$_2$ pressure) and the method used for NP preparation and deposition.

Conversely, there are very few reports dealing with the direct oxidation of glucose to GA using Au-based heterogeneous catalysts, because of the difficult consecutive oxidation of GO to GA (Scheme 3.1). In fact, the oxidation of the primary alcohol requires more severe conditions than the aldehyde. The oxidation of secondary alcohols to internal keto products may also occur, and this is known to give rise to C-C fragmentation, thus resulting in poor selectivity to GA.
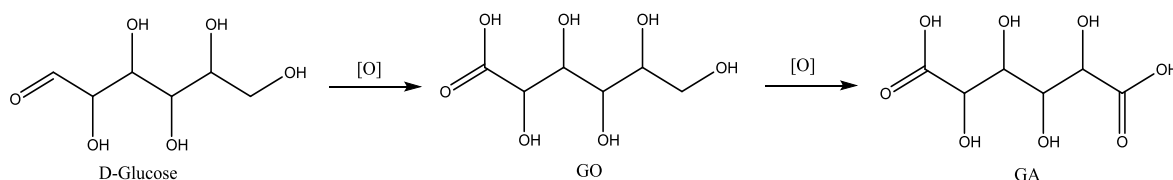
Scheme 3.1. The oxidation of D-glucose to glucaric acid (GA) via the intermediate formation of gluconic acid (GO).

In this chapter are reported the results of a study aimed at investigating the catalytic performance of activated carbon (AC)-supported Au NPs and bimetallic AuM NPs, for the direct oxidation of glucose to GA. Major investigations were done on AuBi/AC catalyst because bismuth is a promoter of selectivity for selective oxidation in catalysts based on supported Au NPs[53,54].

3.2 Experimental

3.2.1 Chemicals

D-Glucose >99 % (Fluka) and sodium hydroxide pellets (Sigma) were used as reagents for catalytic tests. Tetrachloroauric (III) acid 99.99 % (Sigma), bismuth (III) nitrate pentahydrate 99.99 % (Sigma), polyvinylalcohol (PVA, MW 13.000 – 23.000 g/mol, hydrolyzed 87-89 %, Sigma), granular sodium borohydride 98 % (Aldrich) and activated carbon SX1G (AC, Norit) were used for catalyst preparation. Gluconic acid sodium salt 97 % (Aldrich), glucaric acid potassium salt monohydrate ≥ 98 % (Sigma), glyceric acid hemicalcium salt monohydrate ≥ 97 % (Aldrich), sodium mesoxalate monohydrate ≥ 98 % (Sigma), oxalic acid dihydrate ≥ 98 % (Aldrich), tartronic acid ≥ 97 % (Sigma), glycolic acid 98 % (Sigma), arabinose ≥ 98 % (Sigma), formic acid > 95 % (Fluka), lactic acid 85% (Fluka), and D-Glucose were used as reference compounds for HPLC analysis. The commercial Pt/C catalysts were purchased from Sigma-Aldrich (3 and 5 wt% Pt).

3.2.2 Preparation of catalysts

3.2.2.1 Method 1

The Au/AC monometallic catalyst was prepared by dissolving 0.06 g of hydrate tetrachloroauric (III) acid (0.18 mmol) in 15 mL DI water. A suspension of 3.5 g of activated carbon (AC) in 60 mL DI water was prepared. The amount of AC used was calculated in order to have a final 1 % wt metal loading. The Au solution was added to the AC suspension and the resulting mixture was stirred for 2 h. A freshly prepared solution containing an excess of $NaBH_4$ (0.01 g in 5 mL DI water) was added to the solution, which was stirred for an additional 16-20 hours. Then the catalyst was separated by filtration, washed with water, and dried overnight at 120 °C. For the preparation of bimetallic catalysts (AuM/AC), 0.06 g of tetrachloroauric (III) acid (0.18 mmol) was dissolved in 15 mL of DI water. A calculated amount of the second metal precursor (bismuth nitrate pentahydrate, ruthenium chloride trihydrate, copper(II) chloride dihydrate, ammonium iron(II) sulfate hexahydrate, silver nitrate, chloroplatinic acid hydrate, palladium(II) chloride) was dissolved in 15 mL DI water, in order to have

the molar ratio Au:M=3:1. A suspension with the desired amount of activated carbon in 60 mL DI water was prepared, to achieve a final total metal loading of 1 wt%. Solutions containing metal precursors were added to the activated carbon suspension and the resulting mixture was treated with the same procedure as used for the monometallic catalyst.

The AuPtBi/AC catalyst was prepared using three solutions each one containing one metal precursors: 0.06 g tetrachlooauric (III) acid (0.18 mmol) in 15 ml DI water, 0.02 g tetrachloroplatinic (IV) acid (0.06 mmol) in 15 ml DI water, 0.03 g bismuth nitrate (0.06 mmol) in 15 ml DI water. Then the same procedure as for the monometallic and bimetallic catalysts was followed, in order to obtain 1 wt% as the final overall metal loading.

3.2.2.2 Method 2

Polyvinyl alcohol (PVA)-protected Au nanoparticles (catalyst AuPVA/AC, with 1 wt% Au) was prepared by dissolving 0.06 g tetrachloroauric (III) acid (0.18 mmol) in 15 mL of DI water. A solution containing 0.0039 g of PVA in 15 mL of DI water (PVA : Au = 0.5 : 1 wt/wt) was added to the first solution. After some minutes, the resulting solution was added to a suspension containing 3.5 g of activated carbon in 60 mL of DI water and the resulting mixture was stirred for 2 hours. A freshly prepared solution of sodium borohydride (0.01 g in 5 ml of DI water) was added to the suspension, which was stirred for an additional 16-20 hours. After that, the catalyst was filtered, washed with water, and dried overnight at 120 °C.

3.2.2.3 Method 3

Another type of PVA-protected Au NP catalyst (AuW/AC, with 1 wt% Au), was prepared following a procedure adapted from ref[56,57]. Tetrachloroauric (III) acid (0.051 mmol) and PVA (Au : PVA = 1 : 0.5 wt/wt, PVA solution 1 wt%) were added to 100 mL of DI water. After 3 minutes, a freshly prepared 0.1 M solution of sodium borohydride was added (NaBH$_4$:Au = 1:1 mol/mol). The pH was adjusted to 2 with H$_2$SO$_4$ and, after 3 minutes, 1 g of AC was introduced; the suspension was then stirred for 2 hours. Finally,

the catalyst was suspended in water at 60 °C for 2 hours and then filtered, and dried at 80 °C for 4 hours.

3.2.3 Characterization of catalysts

3.2.3.1 Transmission Electron Microscopy

TEM analyses were performed with a TEM/STEM FEI TECNAI F20 microscope equipped with a Schottky emitter and operating at 200 KeV. The instrument is fitted with a Fischione High Angle Annular Dark Field Detector (HAADF) for STEM analysis and an Energy Dispersive X-Ray Spectrometer (EDX). Samples were suspended in ethanol and treated with ultrasounds for 15 minutes. A drop of the suspension was deposited on a multifoil holey-carbon film supported by a copper grid. The sample was dried at 100 °C. TEM images were used to calculate the particle size; values were averaged over ca 150 particles for Au/AC, AuPVA/AC and AuW/AC, and ca 100 particles for AuBi/AC.

3.2.3.2 BET analysis and porosimetry

Porosimetry analysis was performed with an ASAP 2020 Micromeritics apparatus measuring N_2 adsorption/desorption isotherms at -196 °C.

3.2.3.3 X-Ray Powder Diffraction

XRD analysis were carried out with a Bragg-Brentano X'PertProPANanalytical diffractometer equipped with a fast X'Celerator detector and a Cu anode as X-Ray source (Kα, λ = 1.5418 Å), from 10 to 80 °2θ, counting for 20 s at each 0.05 °2θ step. The nanoparticle sizes were calculated with the Scherrer equation based on acquisitions from 41 to 47 °2θ, counting for 1500 s at each 0.08 °2θ step.

Metal dispersion was calculated using the average particle size, as measured by means of XRD and TEM, and the equation reported at pages 738 and 739 of ref[58].

3.2.3.4 Thermal Gravimetric Analysis

TGA analyses were performed with a RA SDT 600 analyzer heating from 25 to 1000 °C (heating rate 10 °C/min) with air (flow 100 ml/min).

3.2.3.5 Atomic Absorption Spectroscopy

AAS measurements were done with Thermo Scientific iCE 3000 Series, AA Spectrometer. Samples were prepared by AC calcination at 1000 °C for 8 hours, the recovery of Au and Bi with aqua regia and dilution with water. Analyses were performed by measuring absorbance at 242.8 nm for Au and 223.1 nm for Bi, with an air-acetylene flame.

3.2.4 Catalytic Tests

All catalytic tests were performed in an autoclave Parr reactor equipped with a pressure gauge and a thermocouple. A solution of D-Glucose (2.5 - 20 wt%) and sodium hydroxide (molar ratio Glu : NaOH = 1:0 – 1:3) in 15 mL of DI water was used as the starting reaction mixture. After loading the catalyst, the autoclave was pressurized with pure oxygen (5-20 bar) and heated to the desired temperature (40-90 °C). Reactions were conducted in a range of time between 1 h and 24 h, during which the mixture was continuously stirred at 400 rpm using a magnetic stirrer. The stirring rate was chosen after preliminary experiments aimed at determining the effect of this parameter (Figure 3.1). After cooling, the catalyst was separated from the reaction mixture by centrifuging at 4300 rpm for 15 min.
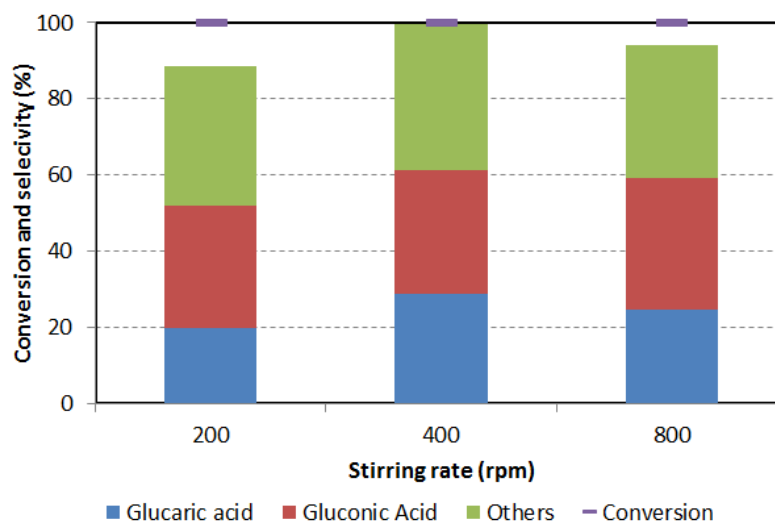
Figure 3.1. Effect of stirring rate. Reaction conditions: glucose : metal$_{tot}$: NaOH = 4.4 : 0.0088 : 13.2 mmol, T 60 °C, O$_2$ pressure 10 bar, reaction time 3 h. Catalyst AuBi/AC.

3.2.5 Products analysis

Qualitative analyses were performed with ESI-MS and HPLC, by comparing the elution time of reaction products and reference compounds. Quantitative analyses were carried out using an Agilent 1260 Infinity Quaternary HPLC system. Analyses were performed in isocratic conditions using 0.0025 M sulfuric acid in ultra-pure water as the eluent (flow 0.5 ml/min). The injection system consisted of a six-way valve with a sampling volume of 20 µl. Two Rezex ROA-H+ (8 %) 300x7.8 mm ion exclusion columns were used for the analytical separation of products. Columns were thermostated at 80 °C for an optimal separation. A diode array detector (DAD) set to 202 nm was used to detect organic acids and a refractive index detector (RID) thermostated at 40 °C was used to detect monosaccharides. GO and glucose peaks overlapped in the HPLC chromatogram obtained using DAD, but the glucose signal obtained with DAD is irrelevant. For this reason, it was possible to perform a quantitative analysis of glucose, when present, by subtracting the GO concentration obtained with DAD from the total GO and glucose concentrations obtained with RID. This method was validated by injecting solutions with different known amounts of glucose and GO and by verifying the existence of a correlation between the areas in the chromatogram and the theoretical ones. Glyceric acid and arabinose peaks also overlapped in RID chromatograms: the acid gave signals with both DAD and RID, while sugar did so only

with RID, but in this case it was not possible to subtract the concentrations as in the case of Glucose-GO mixtures, because there was no proportion between the theoretical sum of single areas and the area of GC peaks. Since these two compounds had a response factor similar to that of the RID detector, it was decided to quantify them together by using an average response factor.

Glucose conversion was calculated by dividing the difference between the initial and the final number of glucose moles by the initial number of glucose moles. The yield to a specific product was calculated by dividing the number of moles generated of that compound by the initial number of glucose moles, normalized with respect to the number of C atoms. The selectivity to a specific compound was calculated by dividing the yield to that compound by glucose conversion. C balance was calculated by summing the selectivity to all quantified products.

3.3 Results and Discussion

3.3.1 Catalyst characterization

Table 3.1 summarizes the main features of the catalysts prepared (see details on the method of preparation used in Experimental), while Figure 3.2 shows TEM pictures and the distribution of particle size for monometallic samples Au/AC, AuPVA/AC, and AuW/AC.

Catalyst[a]	Method of preparation	Average particle size, nm	Metal dispersion, %[b]	Metal content, wt%[c]
Au/AC	1	9.1 (XRD) 12.9 (TEM	13 (XRD), 9 (TEM)	1.00 (AA)
Au$_{PVA}$/AC	2	nd (XRD),[a] 7.3 (TEM)	nd (XRD),[a] 16 (TEM)	0.94 (AA) 0.85 (XRF)
Au$_W$/AC	3	nd (XRD),[a] 4.1 (TEM)	nd (XRD),[a] 28 (TEM)	1,02 (AA) 0.93 (XRF)
AuBi/AC	1	9.2 (XRD), 15.8 (TEM)	13 (XRD), 7 (TEM)	Au 0.69 (AA) Au 0.71 (XRF) Bi 0.20 (XRF)
Bi/AC	1			Bi 1.02 (XRF)
AuCu/AC	1	13.6 (XRD)	8 (XRD)	
AuRu/AC	1	10.4 (XRD)	11 (XRD)	
AuFe/AC	1	12.8 (XRD)	9 (XRD)	
AuAg/AC	1	10.5 (XRD)	11 (XRD)	
AuPt/AC	1	7.6 (XRD)	15 (XRD)	
AuPd/AC	1	9.2 (XRD)	13 (XRD)	
AuPtBi/AC	1	6.4 (XRD)	18 (XRD)	

Table 3.1. Main characteristics of catalysts prepared. Legend: [a] due to the small intensity and broadness of XRD reflection, it was not possible to calculate particle size and metal dispersion. XRD: X-Ray Diffraction; TEM: Transmission Electron Microscopy. [b] see text for details on the method used to calculate metal dispersion. [c] AA: Atomic Absorption; XRF: X-Ray Fluorescence.
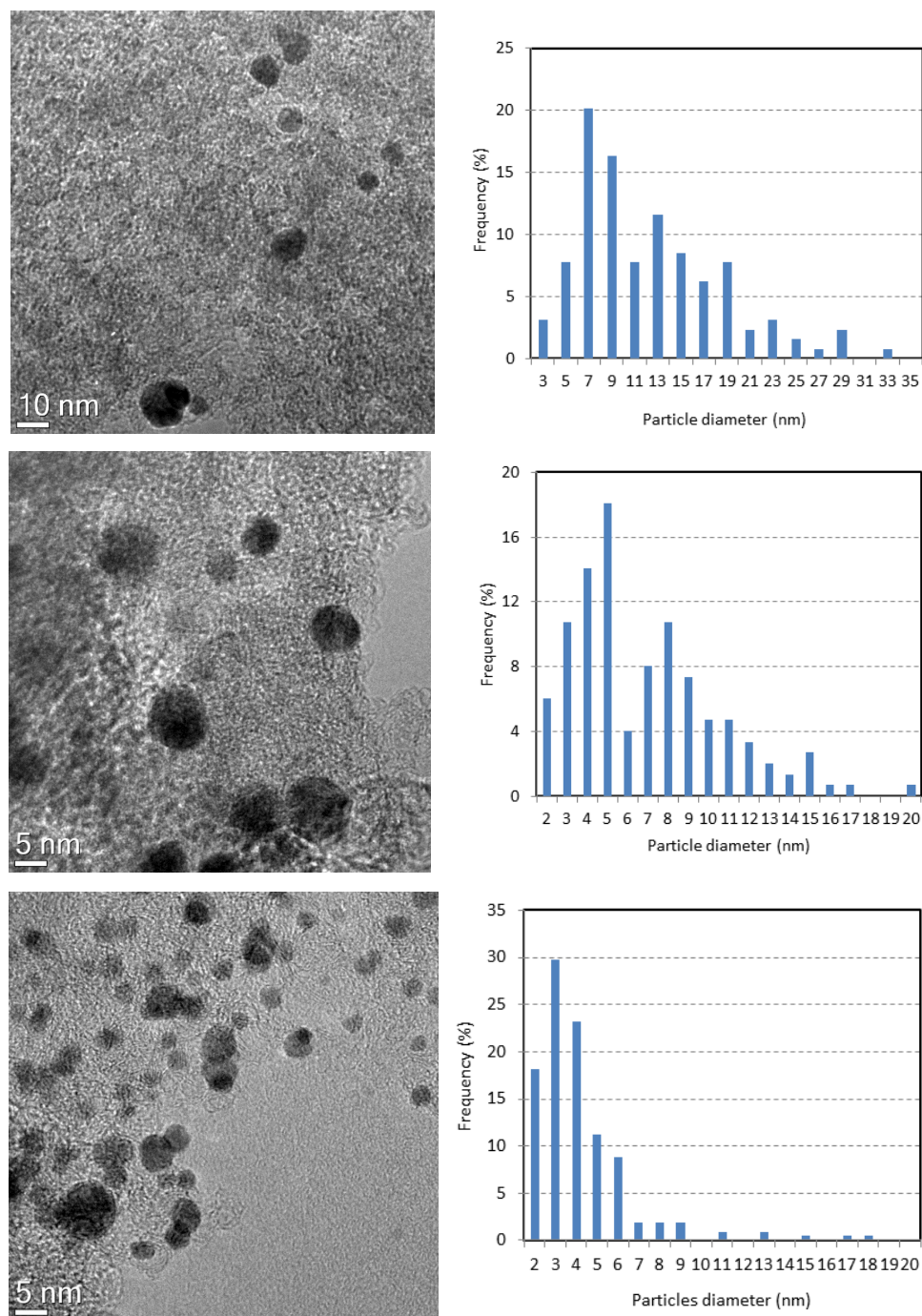
Figure 3.2. TEM pictures and particle distribution for catalysts Au/AC (top), Au$_{PVA}$/AC (middle), and Au$_W$/AC (bottom).

In general, samples had low metal dispersion, in agreement with literature reports that deposition on AC typically leads to relatively large NPs[52]. However, the preparation method used had an important effect on particle size distribution; the smallest NPs were obtained by method 3, the largest ones by method 1.

Sample AuBi/AC was characterized too, which was then used for most reactivity experiments. The particle size distribution, the mapping of Au and Bi measured along the particle section and X-Ray Photoelectron spectra are reported in Figures 3.3-3.6. From XPS, the catalyst showed an homogeneous composition, with no metal segregation. Au was mainly in the metallic form, whereas Bi was present mainly as Bi^{3+}. EDX measurements on nanoparticles with different size confirmed a constant Au:Bi atomic ratio along the profile and no metal segregation. However smaller particles were richer in Bi while bigger ones were richer in Au. It should be considered that due to the partial overlap of Au and Bi signals of EDX, it is not possible to use the experimental value for a quantitative assessment of the Au/Bi atomic ratio.

Details on porosity of samples are reported in Table 3.2.

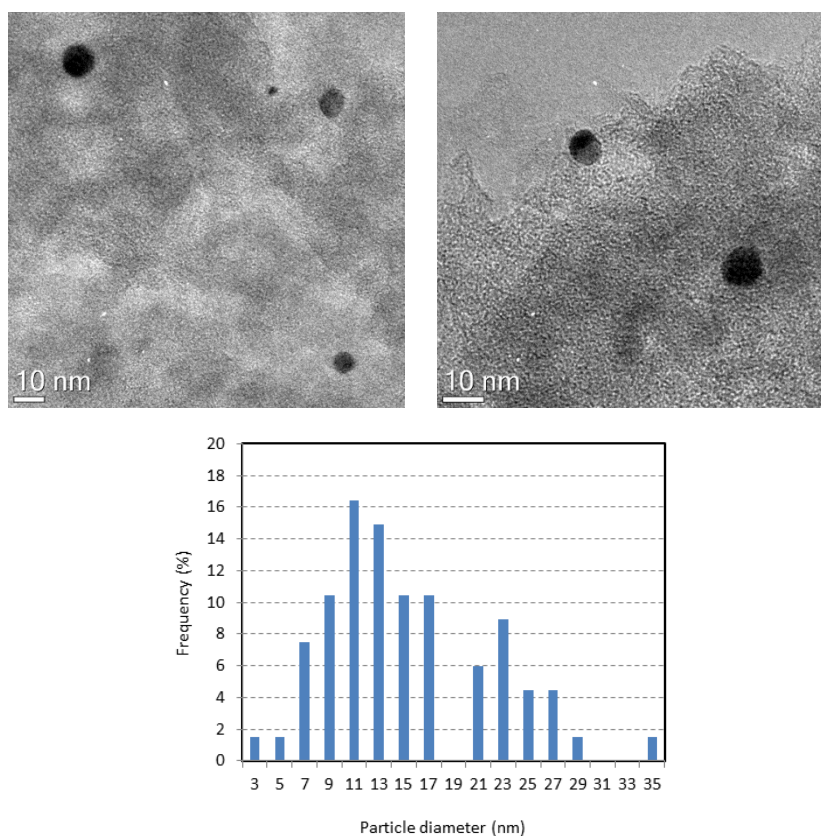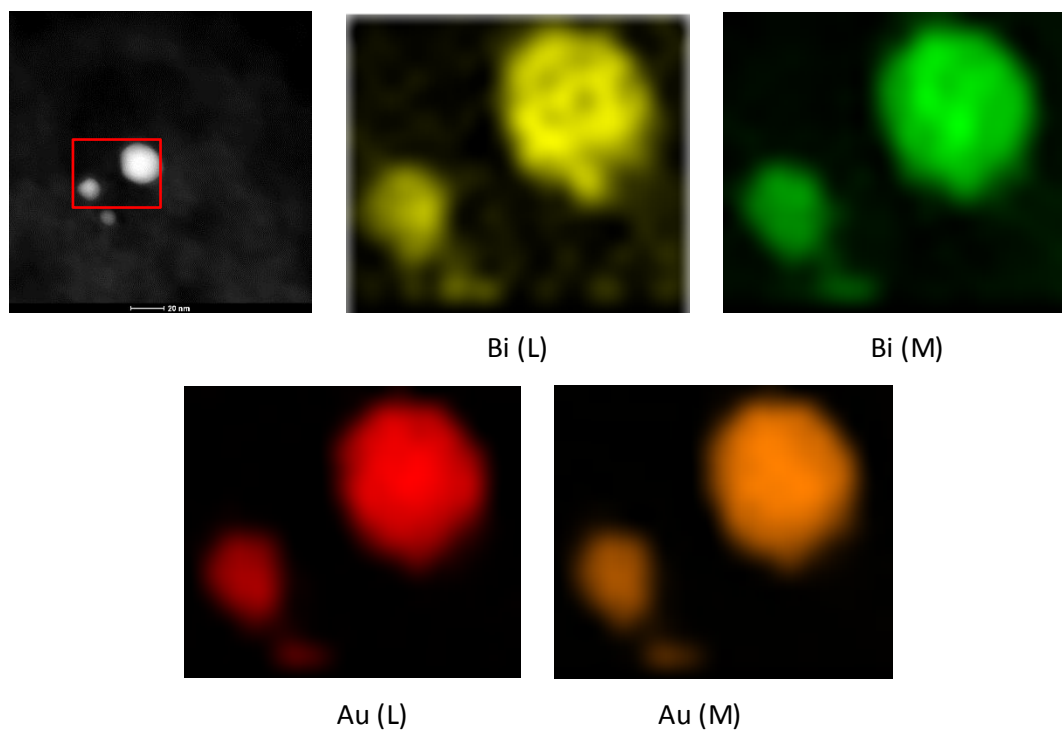*Figure 3.3. TEM image and particle size distribution for AuBi/AC catalyst.*

51

Figure 3.4. STEM-EDX mapping of AuBi/AC catalyst.

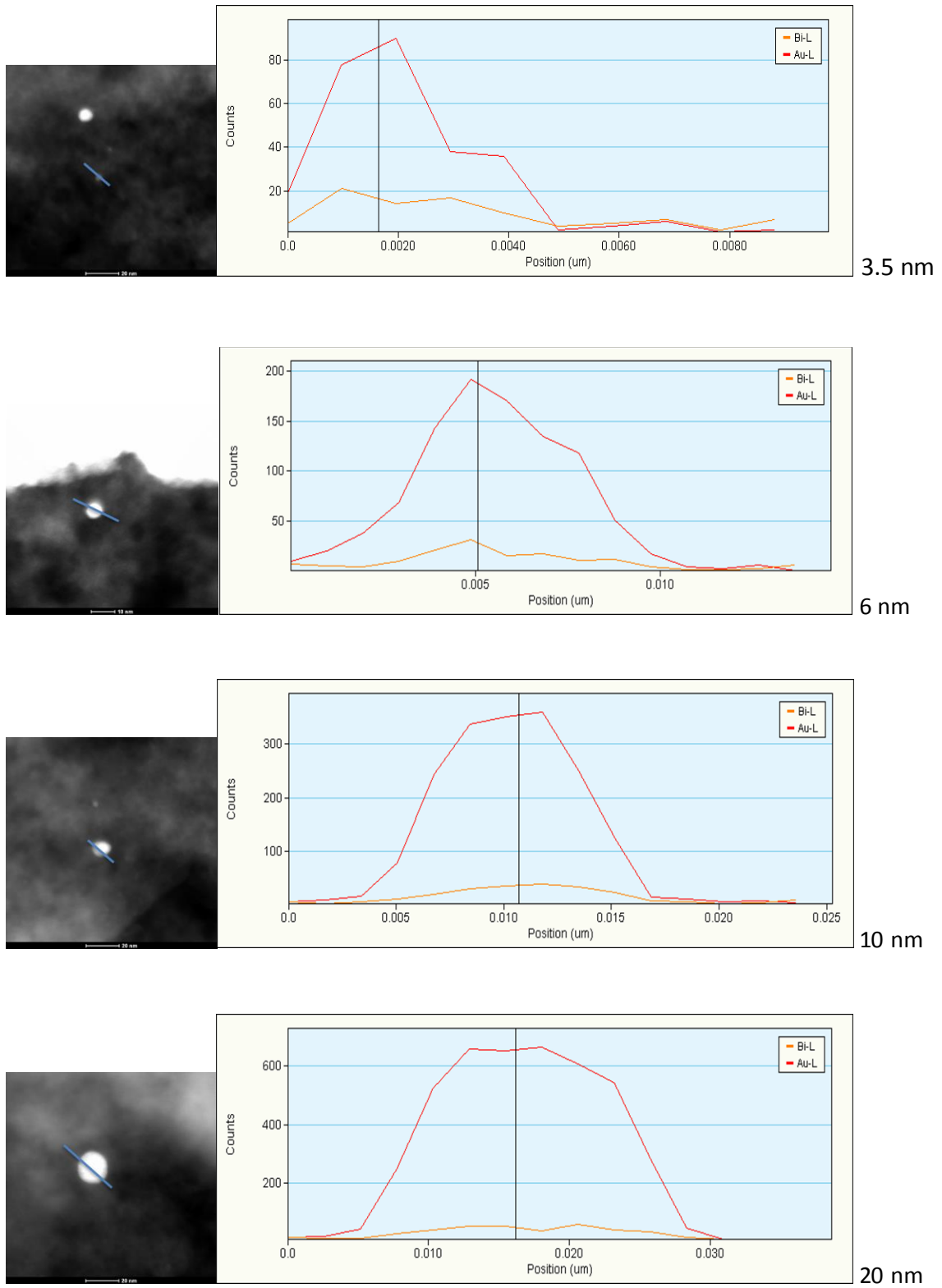3.5 nm

6 nm

10 nm

20 nm

Figure 3.5. STEM-EDX composition profiles of AuBi/AC NPs with different particle diameter .
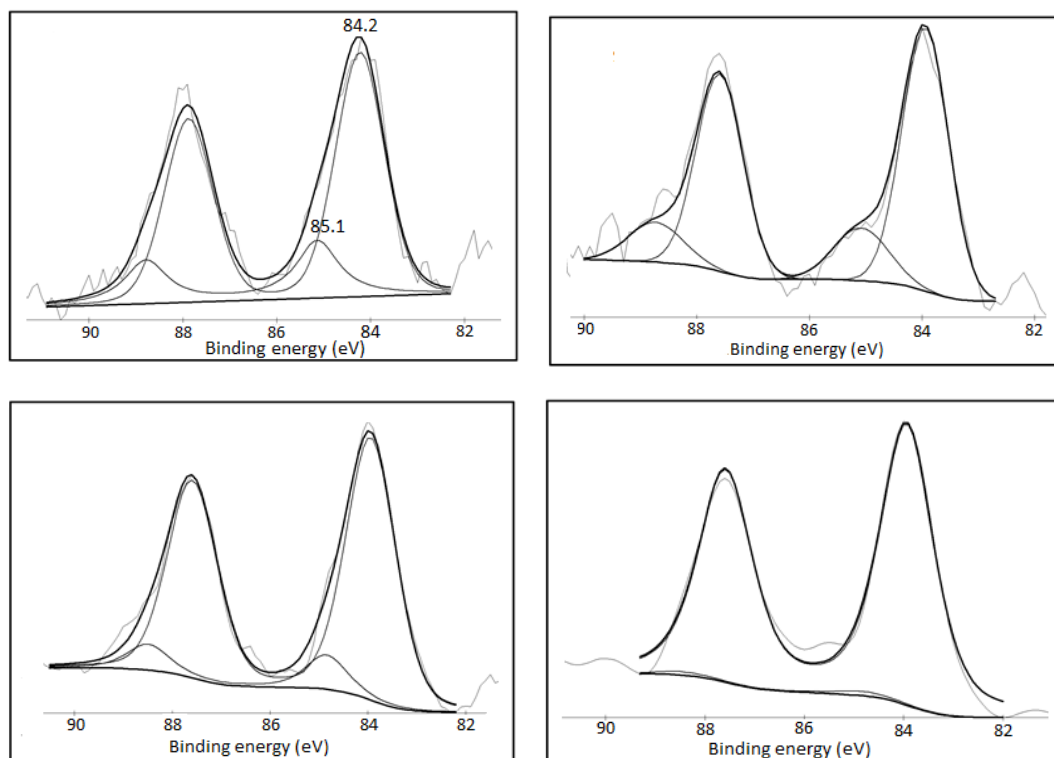
Figure 3.6. X-Ray Photoelectron Spectra of fresh AuBi/AC (top, left), AuBi/AC used after reaction at glucose-rich conditions (20 wt% glucose, 10 bar O_2 pressure) (top, right), AuBi/AC used after reaction at optimised conditions (5 wt% glucose, 10 bar O_2 pressure) (bottom, left), and AuBi/AC used after reaction at O_2-lean conditions (5 wt% glucose, 3 bar O_2 pressure) (bottom, right). Signal at 84.2 eV : Au; 85.1 eV: $Au^{\delta+}$.

Sample	Surface area (m^2/g)	Micropores area (m^2/g)	Mesoporous area (m^2/g)	Mesoporous volume (cm^3/g)	Micropores Volume (cm^3/g)	Total pores volume (cm^3/g)
AC	1270	1021	249	0.64	0.42	1.06
Au/AC	1245	1005	240	0.75	0.41	1.16
Au$_{PVA}$/AC	1270	1031	239	0.85	0.42	1.27
Au$_W$/AC	1335	1066	269	0.70	0.41	1.11
AuBi/AC	1200	996	204	0.73	0.37	1.10

Table 3.2. Porosity of samples.

3.3.2 Reactivity experiments

Preliminary experiments were carried out in the absence of a catalyst, in order to verify the stability of glucose, GO, and GA in reaction conditions. Experiments were conducted with different glucose : NaOH molar ratios, at 60 °C for 3 h, in the presence of 10 bar O_2 pressure (Figure 3.7). These conditions were chosen based on literature reports for Au-based catalysts in alcohol oxidation, which state that a moderate reaction temperature and a basic aqueous medium are necessary. Indeed, later on, the study was conducted on the most selective catalyst, aiming for the optimization of the reaction parameters, and it was found that the chosen conditions were the optimal ones (vide infra).
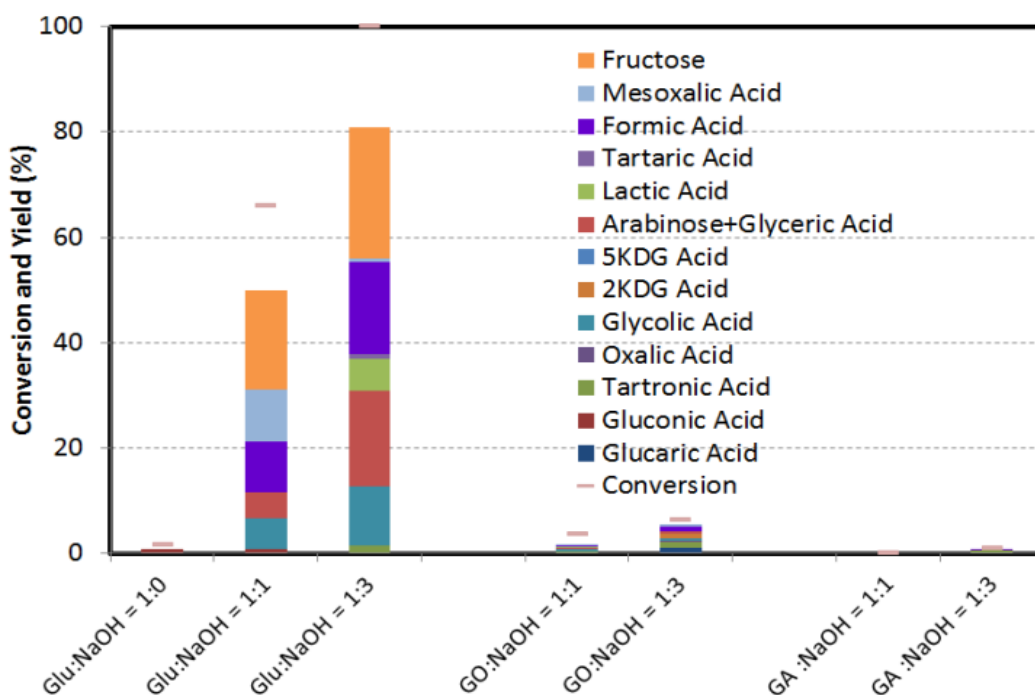
Figure 3.7. Influence of Glucose(GO,GA):NaOH molar ratio on glucose, GO and GA conversion, without catalyst. Reaction conditions: Glucose 5 wt% in water (GO and GA in equivalent molar amount), T 60°C, O_2 pressure 10 bar, reaction time 3 h.

In the absence of the base, glucose conversion was negligible, but when the NaOH amount was increased (up to a Glucose : NaOH molar ratio equal to 1:3), the sugar was converted into a variety of products, such as fructose, arabinose, 2-keto-d-gluconic acid (2KDG), 5-keto-d-gluconic acid (5KDG), tartronic acid, mesoxalic acid, oxalic acid,

glyceric acid, glycolic acid, and formic acid, with traces of GO (which was the predominant product in the absence of the base), and no formation of GA at all. GO showed a negligible conversion to GA and other by-products in the presence of the base, whereas GA proved to be fully stable. Clearly, in the presence of the base, all carboxylic acids were present in the form of corresponding Na salts. These experiments demonstrate that the non-catalyzed (thermal) oxidative degradation of glucose may greatly contribute to catalytic performance in the presence of the base.

Then a comparison of the performance of catalysts made of supported monometallic Au NPs, prepared using three different methods was done (i.e. Au/AC, AuPVA/AC and AuW/AC). The three samples differed in the average NP size and dispersion degree (see Table 3.1); therefore, these experiments were aimed at checking the importance of NP morphology on catalytic performance as well as the possible presence of structure-sensitivity effects[50,59,60]. Figure 8 compares catalytic results; reactions were performed with glucose : metal tot : NaOH quantities equal to 4.4 : 0.0088 : 13.2 mmol (molar ratio: 500:1:1500).

With all catalysts, glucose conversion was complete. The products identified were the same as those already found in non-catalytic experiments: GO, GA, fructose, arabinose, 2KDG, 5KDG, tartronic acid, mesoxalic acid, oxalic acid, glyceric acid, glycolic acid, and formic acid. In this case, however, the major products were GO and GA. There were only minor differences in the distribution of products between Au/AC and AuPVA/AC; in the latter case, however, the C balance was only 92 %, a result that can be attributed to the formation of other unidentified compounds (the analysis of the gas-phase revealed that no CO or CO_2 were formed). Conversely, the catalyst AuW/AC showed the greatest selectivity to by-products, and the lowest selectivity to GO. For comparison purpose, Figure 3.8 also shows the performance of the support alone (AC) and the results of the experiment carried out with no catalyst at all (No Cat).

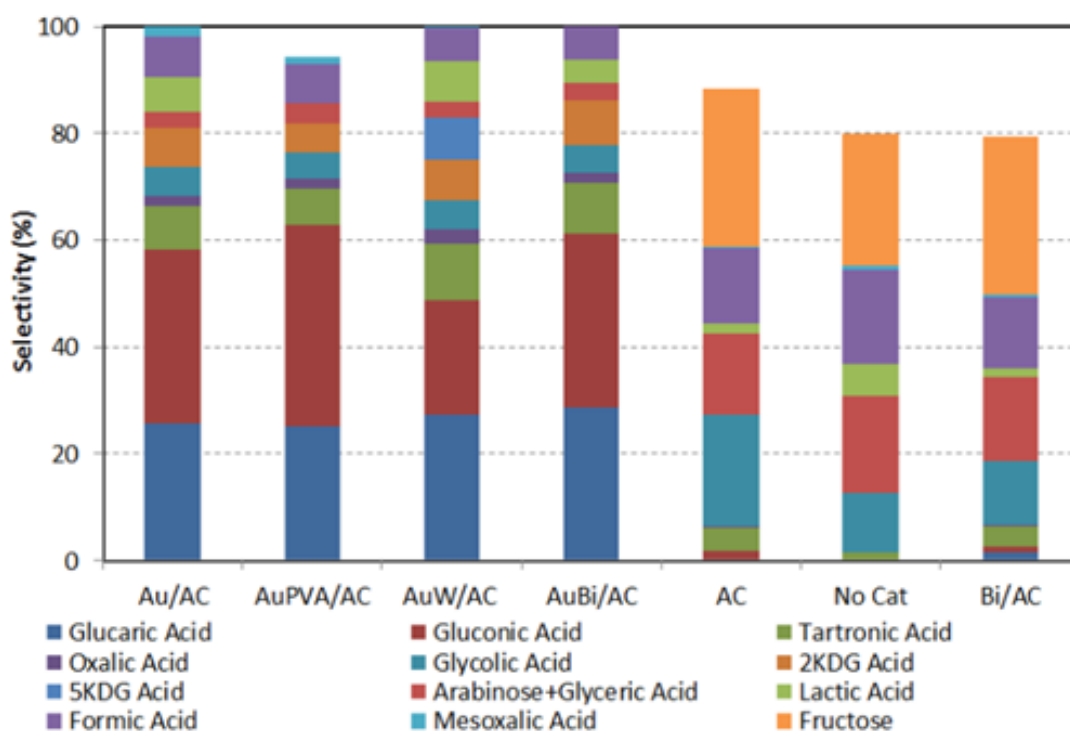*Figure 3.8. Reactivity in glucose oxidation with and without catalysts. Reaction conditions: Glucose 5 wt%*
in water, glucose : metal$_{tot}$: NaOH= 4.4 : 0.0088 : 13.2 mmol, T 60 °C, pressure 10 bar, reaction time 3 h.
Glucose conversion was complete in all cases.

It is worth noting that in the absence of a catalyst glucose was exclusively converted to others products (Figure 3.7 and Figure 3.8). Therefore, results indicate that the homogeneous thermal reactions which are responsible for the oxidative degradation of glucose into lighter acids are suppressed in the presence of the catalyst, whose activity predominates and fully controls the reaction pattern.

It should also be mentioned that even though the catalysts were compared at complete glucose conversion, a detailed analysis of the reaction scheme (vide infra) will reveal that the only kinetically primary product of the reaction is GO, and that the consecutive transformation of GO into either GA or other by-products occurs by means of kinetically parallel routes. The relative importance of these routes is substantially unaffected by GO conversion, but is a function of both catalyst composition and reaction conditions. Therefore, for a specific catalyst, glucose conversion only affects the GO/(GA+by-products) selectivity ratio, but has no influence on the GA/by-products selectivity ratio. In other words, in order to achieve the highest possible selectivity to GA, it is necessary to push glucose conversion in order to promote the transformation of the intermediate

GO, but this inevitably leads to the concurrent formation of other by-products. Overall, catalysts have to be compared at complete glucose conversion, in order to obtain information on performance in terms of selectivity and maximum yield achievable to GA.

The three catalysts were compared under milder conditions (see Figures 3.9-3.13), in order to obtain information on TOF at moderate glucose conversion. However, in the presence of the base the conversion was always higher than 95 %. With a glucose : NaOH ratio of 1:1, no trace of GA was observed, GO was the prevailing product, and there were no relevant differences between catalysts. This means that Au particle size plays its major role in affecting the ratio between the two parallel reactions of GO transformation into either GA or by-products. In fact, the results shown in Figure 3.8 demonstrate that the smallest Au particles, those present in AuW/AC (prepared with method 3), were inductive to the preferred formation of lighter acids by GO oxidative degradation. Catalysts Au/AC and AuPVA/AC, characterised by greater particle size, behaved similarly.

Figure 3.9. Effect of catalyst type on the catalytic performance. Reaction conditions: Glucose 5 wt% in water, glucose : metal$_{tot}$: NaOH = 4.4 : 0.0044 : 13.2 mmol, T 40 ℃, O$_2$ pressure 10 bar, reaction time 20 min.

Figure 3.10. Effect of catalyst type on the catalytic performance. Reaction conditions: Glucose 5 wt% in water, glucose : metal$_{tot}$: NaOH = 4.4 : 0.0088 :4.4 mmol, T 60 ℃, O$_2$ pressure 10 bar, reaction time 1 h.

Figure 3.11. Effect of catalyst type on the catalytic performance. Reaction conditions: Glucose 5 wt% in water, glucose : metal$_{tot}$: NaOH = 4.4 : 0.0088 : 4.4 mmol, T 60 ℃, O$_2$ pressure 10 bar, reaction time 3 h.
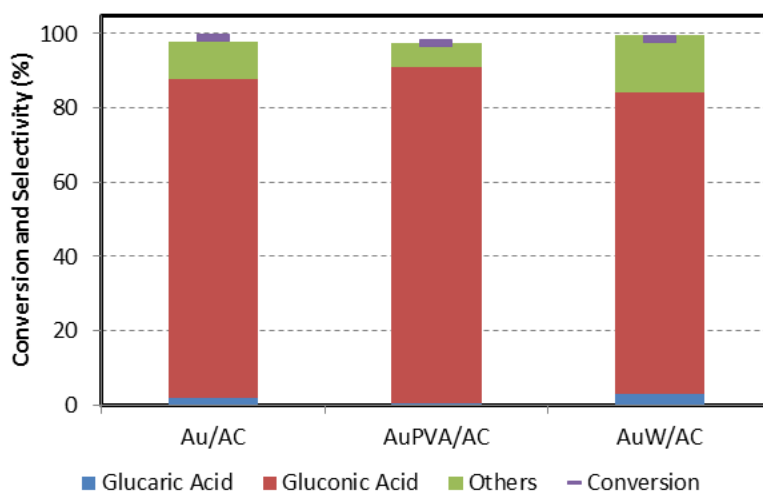
Figure 3.12. Effect of catalyst type on the catalytic performance. Reaction conditions: Glucose 5 wt% in water, glucose : metal$_{tot}$: NaOH= 4.4 : 0.0088 : 4.4 mmol, T 60 °C, O$_2$ pressure 10 bar, reaction time 20 min.
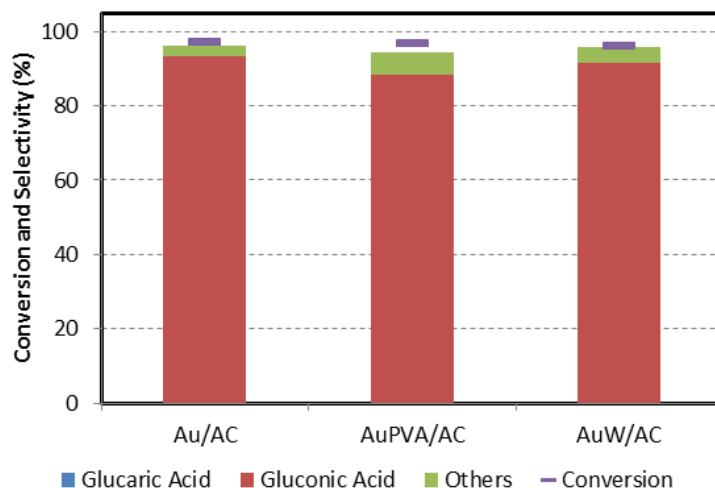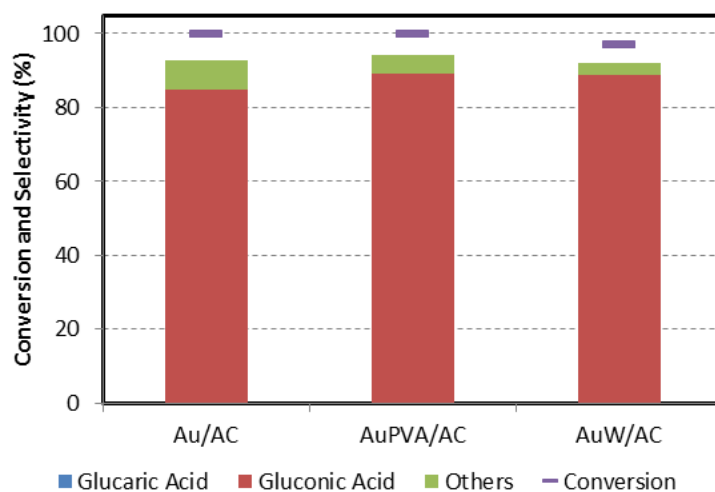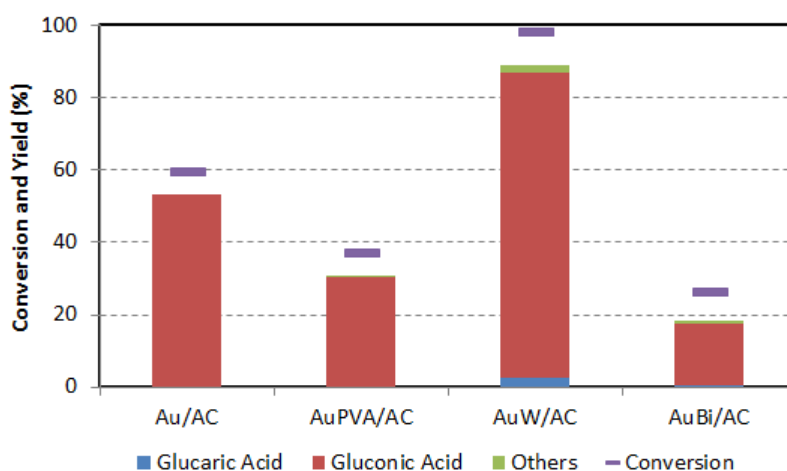

Figure 3.13. Effect of catalyst type on the catalytic performance. Reaction conditions: Glucose 5 wt% in water, glucose : metal$_{tot}$: NaOH= 4.4 : 0.0088 : 0 mmol, T 120 °C, O$_2$ pressure 10 bar, reaction time 60 min.

Only in the absence of the base, it was possible to achieve moderate glucose conversion (Figure 3.13); in this case, the rank of activity was AuW/AC (TOF 480 h^{-1}) > Au/AC (TOF 300 h^{-1}) > AuPVA/AC (TOF 190 h^{-1}). The low activity of AuPVA/AC can be explained by taking into account the presence of the PVA, which may cover Au NPs. For the other two catalysts, the order corresponds to the particle size, with AuW/AC showing the highest TOF and the smallest particle size.

60

Experiments starting from GO were also carried out (Figure 3.14); again, catalyst AuW/AC turned out to be slightly more active than Au/AC and AuPVA/AC, but less selective to GA (selectivity to GA 46 % for AuPVA/AC, 44 % for Au/AC and 40% for AuW/AC), because of the greater yield to Others (especially 2KDG). For all catalysts, conversion of GO was less than 100 %, a clear indication of the lower reactivity of GO compared to glucose. Moreover, data also confirmed that GO is rapidly converted to both GA and several by-products.
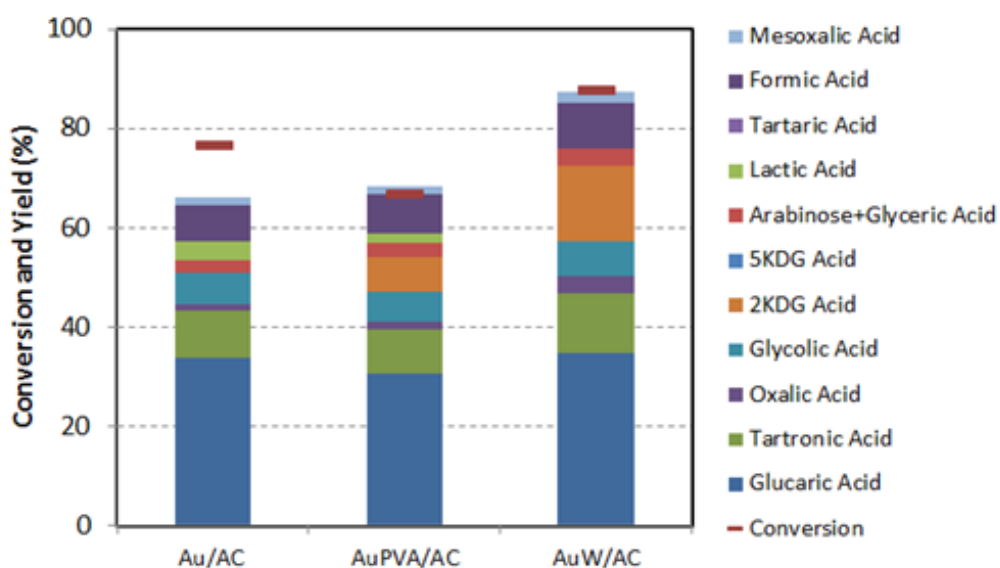
Figure 3.14. Reactivity in GO oxidation. Reaction conditions: GO 4.6 wt% in water, GO : metal : NaOH = 4.4 : 0.0088 : 13.2 mmol, T 60 °C, O_2 pressure 10 bar, reaction time 3 h.
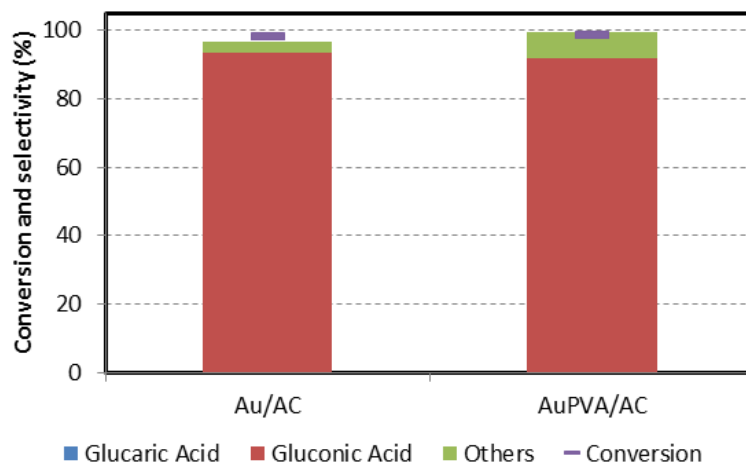
Finally, it was decided to adopt method 1 for the preparation of AuBi/AC (Table 3.1 and Figure 3.8); a catalyst containing only Bi (Bi/AC) was also prepared, for comparison purpose. The AuBi/AC catalyst gave the highest yield to GA (29 % at 60 °C, Figure 3.8), and 100 % C balance. Therefore, it was decided to continue this study with the AuBi/AC catalyst.

Figure 3.15 shows the effect of the glucose : NaOH molar ratio. In the absence of NaOH (non-neutralized conditions), glucose conversion was very low, with the formation of trace amounts of GO. With an equimolar amount of glucose and NaOH, glucose conversion was total, with the almost exclusive formation of GO and a very small yield to Others. On the other hand, no formation of GA was observed under these

conditions. Conversely, GO was converted to both GA and Others when a Glucose : NaOH ratio equal to 1:3 was used. These experiments confirm the need for the base in the oxidation of glucose to GO, and for an excess of NaOH in the consecutive oxidation of GO to GA.
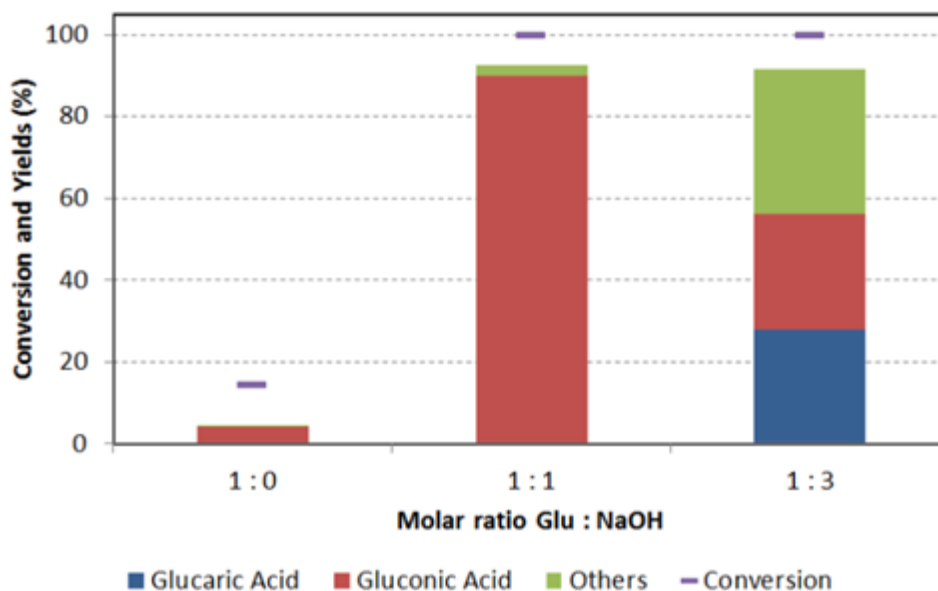
Figure 3.15. Effect of Glucose:NaOH molar ratio on the catalytic performance. Reaction conditions: Glucose 5 wt% in water, glucose : metal$_{tot}$: NaOH = 4.4 : 0.0088 : x mmol, T 60 ℃, O$_2$ pressure 10 bar, reaction time 3 h. Catalyst AuBi/AC.

The effect of the temperature (at two different reaction times) and O$_2$ pressure are shown in Figure 3.16 and 3.17, respectively.
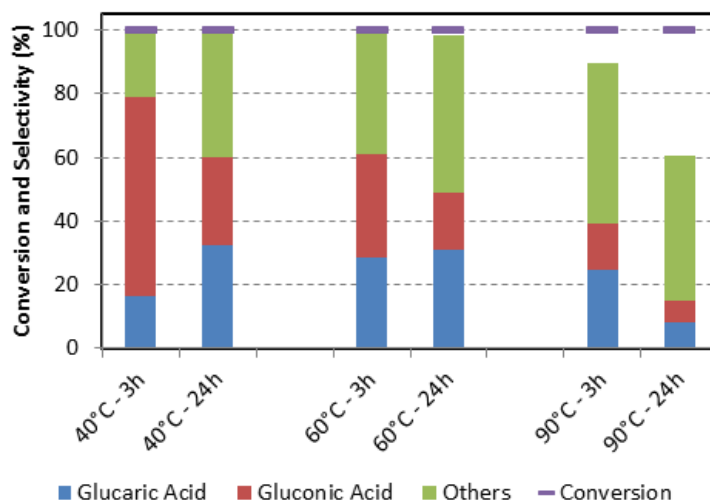
Figure 3.16. Effect of reaction temperature on catalytic performance. Reaction conditions: Glucose 5 wt% in water, glucose : metal$_{tot}$: NaOH = 4.4 : 0.0088 : 13.2 mmol, oxygen pressure 10 bar, reaction time 3 h or 24 h.
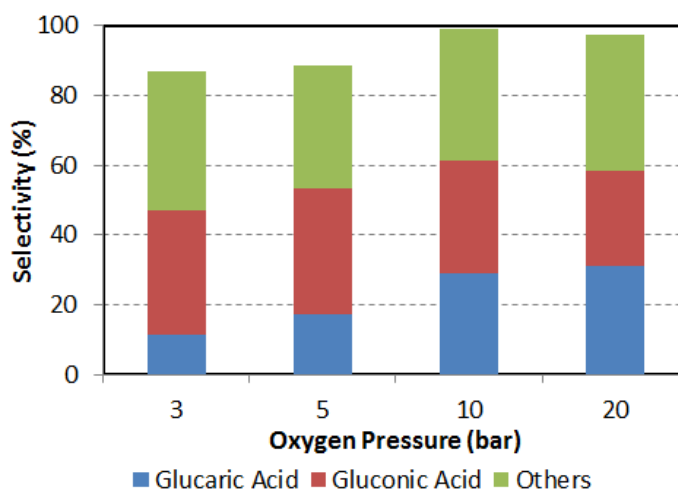
Figure 3.17. Effect of O$_2$ pressure on catalytic performance. Reaction conditions: Glucose 5 wt% in water, glucose : metal$_{tot}$: NaOH= 4.4 : 0.0088 : 13.2 mmol, T 60 °C, reaction time 3 h. Glucose conversion is always complete.

The experiment conducted at 40 °C again produced a complete glucose conversion after 3 h reaction time, with 78 % selectivity to GO+GA, the highest value recorded, although with a selectivity to GA of only 15 %. This result led to hope that by prolonging the reaction time it would be possible to further selectively convert GO to GA while limiting the formation of Others. However, the selectivity to GA registered after 24 h reaction time at 40 °C was 32 %, i.e. very similar to that observed at 60 °C (31 % after 24

h reaction time), again because of the significant formation of Others (selectivity 41 %). As expected, the experiment conducted at 90 °C led to the predominant formation of Others and a poor C balance.

At 5 bar O_2 pressure (Figure 3.17), glucose conversion was again 100 %, but C balance was only 87 %, and selectivity to GO+GA was 53 % (selectivity to GA 17 %); the poor C balance suggests the occurrence of side reactions with the formation of undetected by-products, similarly to what has been observed in experiments conducted without catalysts (Figure 3.7). This indicates that a relatively high O_2 pressure is needed in order to accelerate reactions occurring on the catalyst surface and to overcome the contribution of homogeneous reactions. A similar effect was shown at 3 bar O_2 pressure. Conversely, at 20 bar O_2 pressure, the performance was very similar to that observed at 10 bar.

The last parameters investigated were glucose concentration in the starting reactant mixture (Figure 3.18), and glucose : metal ratio (Figure 3.19).

Glucose concentration had a dramatic effect on the catalytic performance. In all experiments, the total conversion of glucose was achieved, but at low (2.5 wt%) and high (10 and 20 wt%) glucose concentration in water, a poor C resulted. Moreover, high glucose concentration afforded very low selectivity to both GO and GA, whereas the formation of Others was practically unaffected. A comparison of performances at 2.5 and 5 wt% glucose shows that the overall GO+GA selectivity was similar in the two cases, but with a lower glucose concentration, the selectivity to GA was clearly lower. These experiments demonstrate that an optimal O_2 : glucose ratio in the liquid phase is needed (e.g. with 5 % glucose and 10 bar O_2 pressure), in order to achieve both the minimal formation of by-products (responsible for the poor C balance) and the highest GA/GO selectivity ratio.

Figure 3.18. Effect of glucose concentration on catalytic performance. Reaction conditions: glucose : metal$_{tot}$: NaOH = x : 0.002x : 3x mmol, T 60 ℃, O$_2$ pressure 10 bar, reaction time 3 h. Catalyst AuBi/AC.
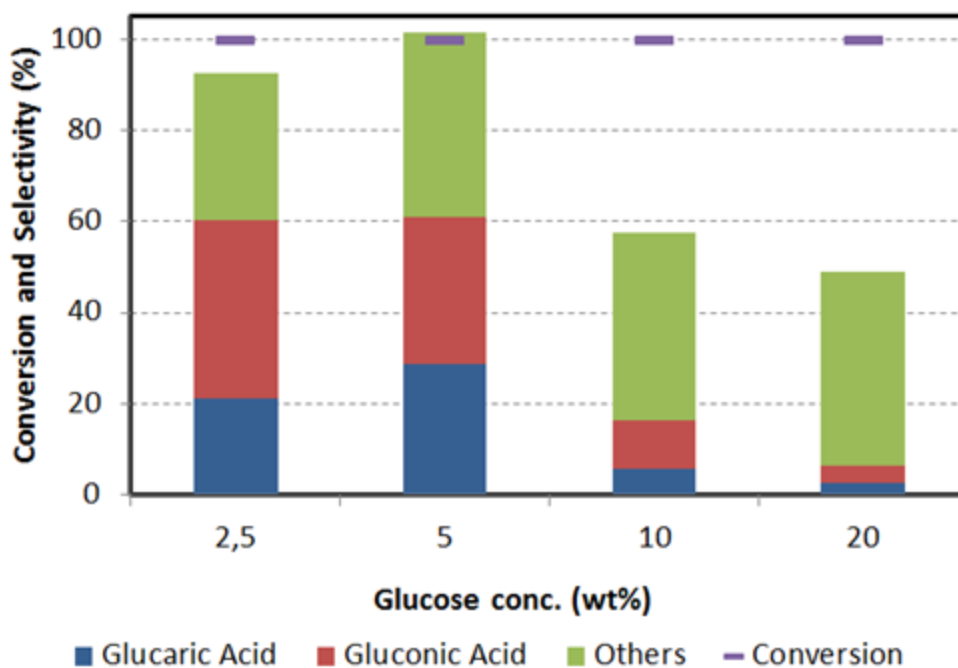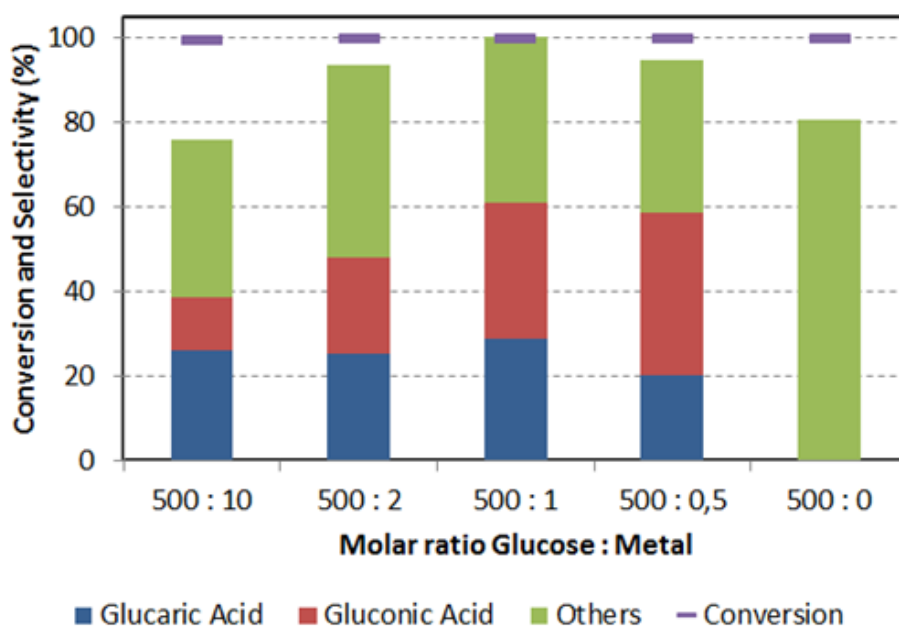

Figure 3.19. Effect of glucose:metal molar ratio on catalytic performance. Reaction conditions: glucose : metal$_{tot}$: NaOH = 4.4 : x :13.2 mmol (molar ratio 500:x:1500), T 60 ℃, O$_2$ pressure 10 bar, reaction time 3 h. Catalyst AuBi/AC.

It is known that the amount of oxygen present in the liquid phase has a great influence on catalyst activity in the selective oxidation of monosaccharides[61]. Various research groups have proposed a model for Au active sites in oxidation reactions in which the substrate is activated by the adsorption onto Au^0 sites, whereas O_2 is activated by the oxidized $Au^{\delta+}$ atoms, which in catalysts made of Au deposited on metal oxides may be those located at the boundary interface[62,63]. Since the adsorption and activation of the substrate and oxygen occur on Au sites having different charge, it may be hypothesized that the concentration of Au^0 and $Au^{\delta+}$ surface sites is affected by the liquid-phase ratio between glucose – which may act as a reducing species for oxidized Au – and O_2. In other words, a more "reducing" environment, due to either a high concentration of glucose or a low pressure of O_2, may lead to the predominance of Au^0 species and to a correspondingly lower amount of oxidized $Au^{\delta}+$ species. Under these conditions, the catalyst contribution to glucose oxidation becomes less important, and the overall performance appears to be closer to that shown in the absence of a catalyst (Figure 3.7).

An increased glucose : metal molar ratio (from 500:10 up to 500:1, Figure 3.19) led to an increased selectivity to GO+GA, whereas the selectivity to GA remained approximately unchanged. It is worth noting that in the case of low glucose : metal ratio (500:10) the C balance was poor, close to 80 %. However, in this case a considerable amount of products remained adsorbed on catalyst, and could be extracted from used catalyst with hot water, so contributing to the C balance which became close to 97 % (as shown in Figure 3.19). At very low metal concentration (glucose : metal 500:0.5), conversely, the conversion of GO into GA was less efficient and GA selectivity declined.

These experiments show that the optimal conditions for the oxidation of glucose, those leading to both the highest overall selectivity to GO+GA with a 100 % C balance, and the highest selectivity to the desired product, GA, are met (a) at moderate temperature (no higher than 60 °C), in order to limit the oxidative degradation of GO; (b) in the presence of NaOH with a NaOH : glucose molar ratio higher than 1:1, in order to accelerate the oxidation of glucose to GO and make the oxidation of GO to GA occur efficiently; (c) at a well-defined interval for the O_2 : glucose and glucose : metal ratios, which should be regulated in such a way as to keep a relatively high concentration of

surface Au atoms in the oxidized state and limit the amount of organic species which remain adsorbed on catalyst surface.

The important role of the glucose-to-oxygen ratio was confirmed by means of XPS experiments; the XP spectra of fresh AuBi/AC, and of the same catalyst after reaction under three different conditions were analyzed: (i) with 5 wt% glucose and 10 bar O_2 pressure (optimized conditions); (ii) with 20 wt% glucose and 10 bar O_2 pressure (glucose-rich conditions); and (iii) with 5 wt% glucose and 3 bar O_2 pressure (oxygen-lean conditions). Spectra are reported in Figure 6. In all cases, the surface concentration of Au was found to be much lower than the expected one (ca 0.2 wt% instead of 1 wt%); this is due to the fact that most metal was deposited inside pores of the high surface area AC. It was also found that the fresh catalyst contained ca 21 % of oxidized Au, and a very similar value was found after reaction under glucose-rich conditions. Conversely, after reaction under optimized conditions the used catalyst contained ca 11 % oxidized Au, whereas catalyst used under oxygen-lean conditions contained only traces of oxidized Au. Combining this information with results of catalytic experiments, it possible to conclude that the bad performance shown under glucose-rich conditions (Figure 3.18) was due to the saturation of surface sites by glucose and heavy compounds; under such conditions, the catalytic performance became closer to that shown in the absence of catalyst (Figure 3.7), and the oxidation state of Au sites was not affected by reaction conditions. On the other hand, under conditions at which the catalyst surface was not saturated (i.e., with 5 wt% glucose solution), the fraction of oxidized Au was a function of O_2 partial pressure.

Lastly, experiments were carried out in relation to reaction time under the optimized conditions, in order to confirm the hypothesized reaction scheme (Figure 3.20).
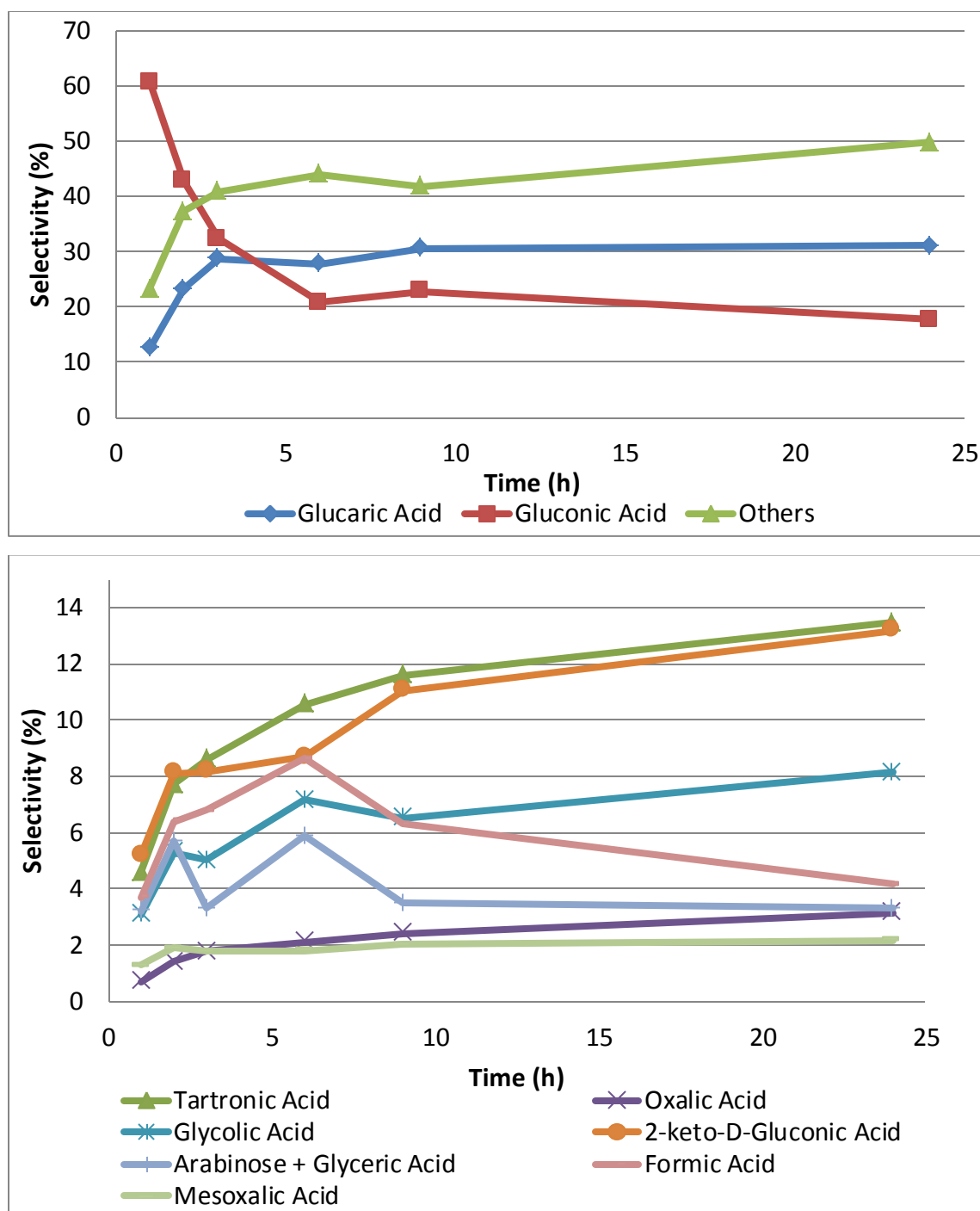
Figure 3.20. Effect of reaction time on catalytic performance. Reaction conditions: glucose : metal$_{tot}$: NaOH = 4.4 : 0.0088 : 13.2 mmol, T 60 °C, O$_2$ pressure 10 bar. Catalyst AuBi/AC. In all cases, glucose conversion was complete. Bottom figure: detail of "Others".

The results obtained confirm that under the conditions used, GO is the only primary product of the reaction; therefore, the thermal reactions leading to several by-products by glucose oxidative degradation (Figure 3.7) do not contribute to glucose

conversion in the presence of the catalyst. This is apparently due to the very high activity of the catalyst used, which leads to total glucose conversion (with 100 % C balance) already after 1 h reaction time at 60 °C. In fact, by-products form only by consecutive reactions of GO, as demonstrated by the fact that the overall selectivity to Others is nil if extrapolated to zero reaction time. It is also shown that in spite of the very high glucose conversion achieved, the extent of any GO consecutive transformation, either to GA or to Others, is relatively small and becomes significant only for prolonged reaction times; this confirms that the rate of GO formation is faster by far than its further oxidation. It is also shown that even after a 24 h reaction time there is still some residual GO (selectivity 18 %), and it seems that it is not possible to go beyond the 31 % GA yield. On the other hand, GA is a stable compound under the reaction conditions used, since it does not undergo consecutive oxidative degradations. In order to compare the catalytic performance with that of the best catalyst type reported in the literature, based on Pt/C[26], the reactivity of commercial Pt/C (3 and 5 wt% Pt) was tested, using either the optimized conditions (with and without base) of this work, or the conditions reported in ref [26]. Figure 3.21 summarizes the results obtained, compared with those obtained with our AuBi/AC catalyst the results obtained in ref[26] are also shown for the purpose of comparison. The performance of AuBi/AC appeared to be better than that of the commercial Pt/C catalysts under the optimal conditions found. Moreover, Pt/C showed moderate conversion in the absence of the base, but with high selectivity to GO. This is an important difference between Au-based and Pt-based catalysts; the former are substantially inactive in alcohol oxidation in the absence of the base (see Figure 3.15), whereas Pt catalysts show a non-negligible conversion and high selectivity to the monocarboxylic acid. When the Pt/C catalysts were used in conditions identical to those reported in ref [26] (cond. 3 in Figure 3.21), GO and GA yields were similar to those obtained with AuBi/AC, but with the latter catalyst C balance was definitely better. We were not able to reproduce results reported in ref[26] for commercial Pt/C catalyst (also shown in Figure 3.21). Our results were considerably worse than those reported in literature, despite the identical catalyst type, purchased from Aldrich, and identical reaction conditions used in our experiment.
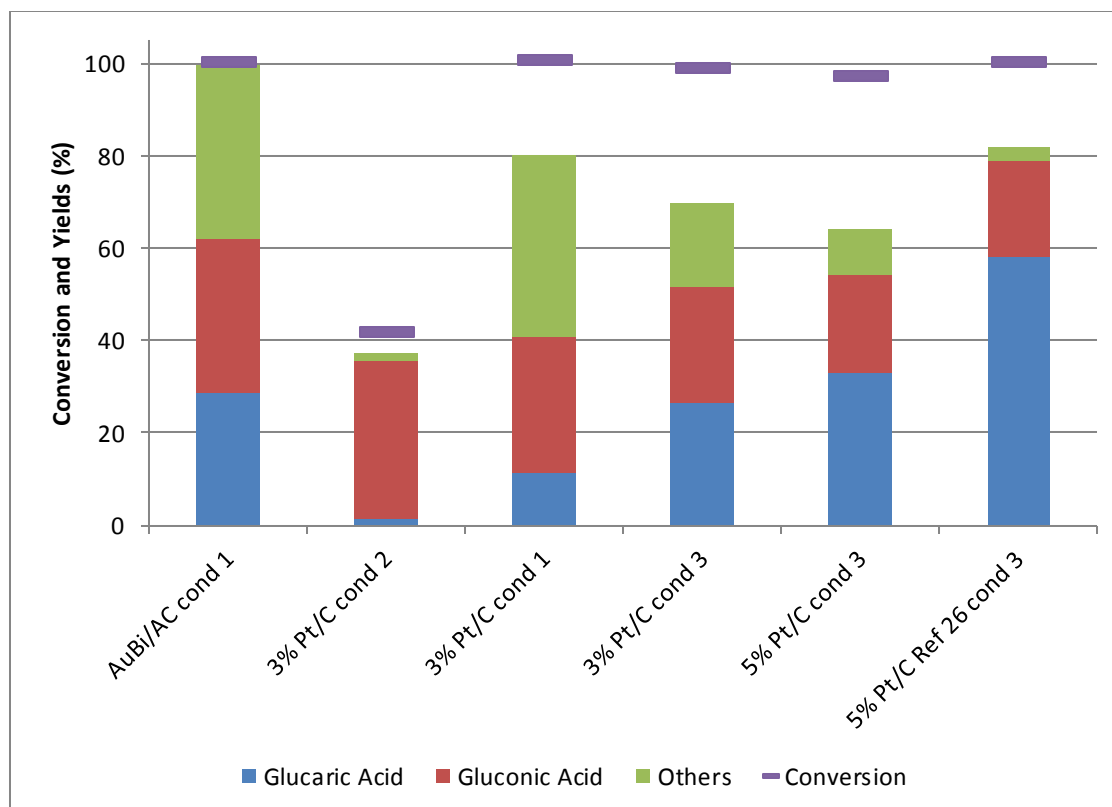
Figure 3.21. Comparison of AuBi/AC and Pt/C (commercial) catalysts (with 3 wt% and 5 wt% Pt loading) and results reported in ref[26]. Conditions 1: 5 wt% glucose in aqueous solution (15 mL water), glucose : metaltot : NaOH = 4.4 : 0.0088 : 13.2 mmol, T 60 °C, O_2 pressure 10 bar, reaction time 3h. Conditions 2: like conditions 1, but without the base. Conditions 3, as in ref [26]: 10 wt% glucose in aqueous solution (20 mL water), molar ratio Glucose:Metal:NaOH = 54:1:0 (no base), T 80 °C, O_2 pressure 13.8 bar, reaction time 3 h.

Finally the catalyst reusability was tested; the AuBi/AC sample was separated by filtration and reused, after washing with cold water. In this aim, two sets of experiments were carried out, (i) at 40 °C and 0.5 h reaction time, that is, under milder conditions than usual ones (Figure 3.22), and (ii) at optimized conditions, i.e., at 60 °C and 3 h reaction time (Figure 3.23).
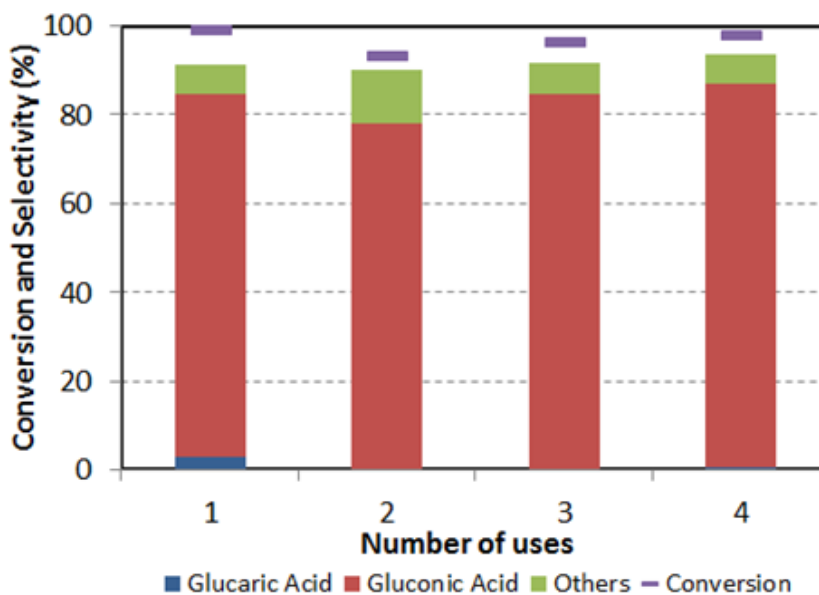
Figure 3.22. Effect of catalyst reuse. Reaction conditions: glucose : metal$_{tot}$: NaOH = 4.4 : 0.0088 : 13.2 mmol, T 40 °C, O$_2$ pressure 10 bar, reaction time 30 min. Catalyst AuBi/AC.

Figure 3.23. Effect of catalyst reuse. Reaction conditions: glucose : metal$_{tot}$: NaOH = 4.4 : 0.0088 : 13.2 mmol, T 60 °C, O$_2$ pressure 10 bar, reaction time 3 h. Catalyst AuBi/AC. After each use the catalyst was washed with cold water.

It is shown that in the former case a slight decline of conversion occurred after the 1st use; selectivity to GA, which was 3 % in the 1st test, became close to 0.5 % in successive uses. It is also important to note that the analysis with AAS of the solution after the 1st

and after the 4th use, did not detect the presence of dissolved Au; the Au content in corresponding used catalyst was analyzed too with XRF, and did not find any change in Au content. In the case of experiments carried out at 60 °C, instead, deactivation phenomena were more relevant (Figure 3.23). Even though glucose conversion was always complete, already after the 1st use a decline of yield to GA was shown, while yield to GO was affected at a minor extent only. Moreover, the formation of undetected (heavy) compounds also increased, as shown by the C loss increase. Again, the analysis of Au and Bi content in used catalysts (after 1st and 5th use) by XRF revealed that deactivation was not due to the leaching of the active phase.

The catalyst was characterized after the first use, in order to investigate on the possible formation of organic residues which might be responsible for catalyst deactivation. Figure 3.24 compares the TGA in air of the fresh and used (1st use) AuBi/AC catalyst; both samples were pre-dried at 120 °C. In the case of the fresh catalyst, combustion of the carbon started at 500 °C and was complete at 620 °C. With the used catalyst, combustion started at 250 °C, suggesting the presence of deposited organic residues; moreover, the heat released accelerated carbon combustion, which was complete at 530 °C already. It is also important to notice that these organic residues could not be extracted with hot (80 °C) water from the used catalyst; the analysis of the extractive revealed the absence of any dissolved compound. The organic residues were tried to remove by washing with an acid aqueous solution and with organic solvents as well (acetone and ethanol). However these treatments led to a worse catalytic behavior compared to washing with cold water only (Figure 3.25).
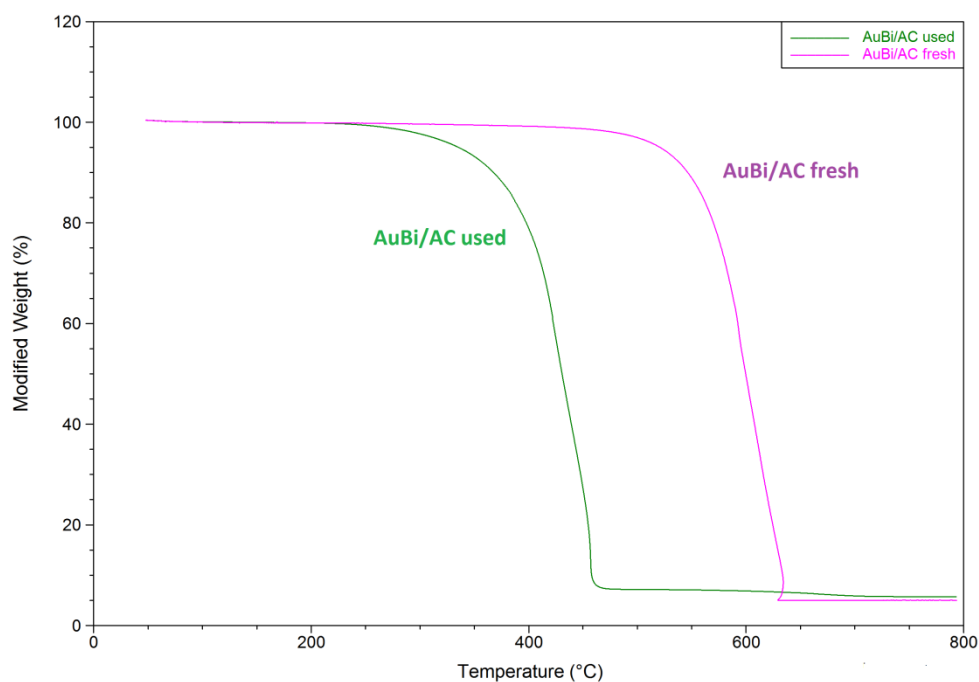
Figure 3.24. TG analysis of sample AuBi/Ac fresh and after reaction with 20 wt% glucose in water.
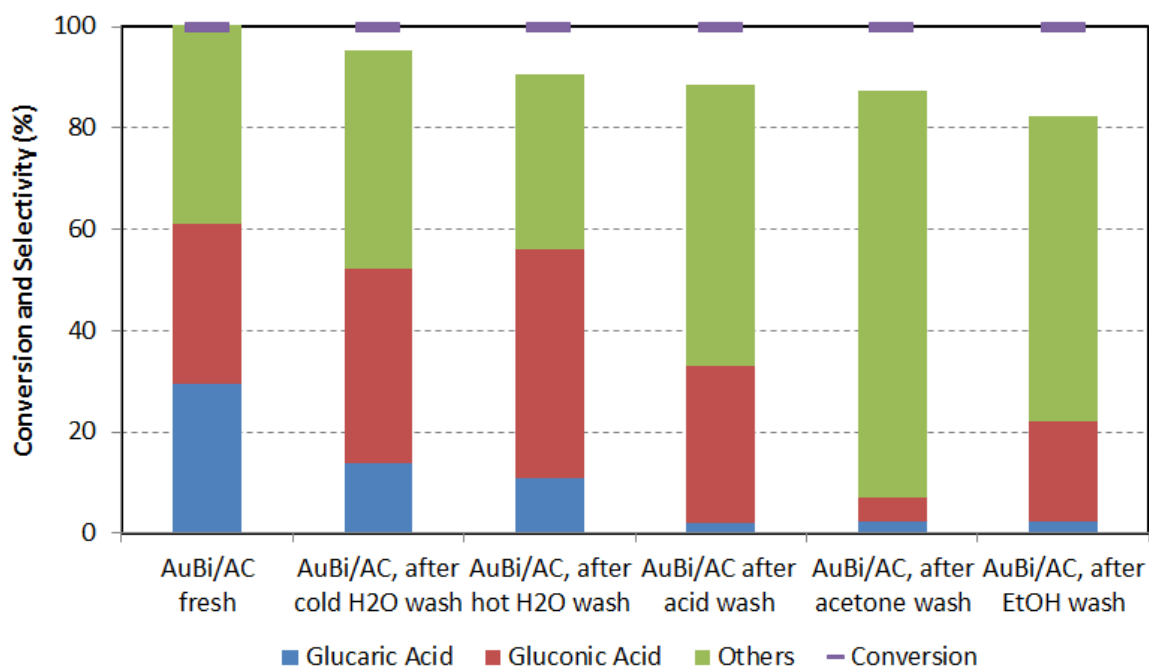
Figure 3.25. Reactivity of AuBi/AC catalyst: fresh sample, and after treatment of the used sample (1st use)

with cold water (as in Figure 3.23), hot water, acid aqueous solution (diluted H_2SO_4), acetone and ethanol.

Reaction conditions: glucose : metal$_{tot}$: NaOH = 4.4 : 0.0088 : 13.2 mmol, T 60 °C, O_2 pressure 10 bar,
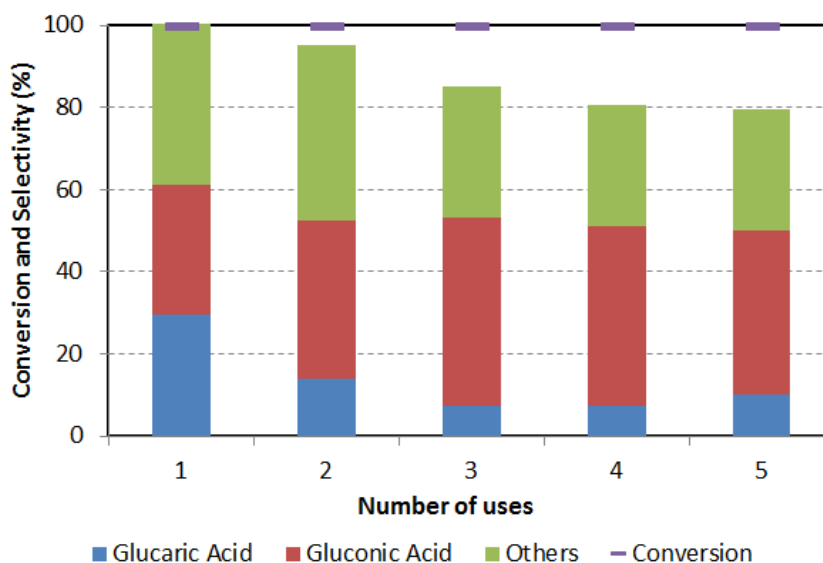
reaction time 3 h.

Characterization of the used catalyst by means of STEM (Figure 3.26) revealed another reason for catalyst deactivation. In fact, both NPs agglomeration and sintering were observed; these phenomena were likely due to both the weak interaction between support and NPs, and local overheating because of the strongly exothermal reaction.
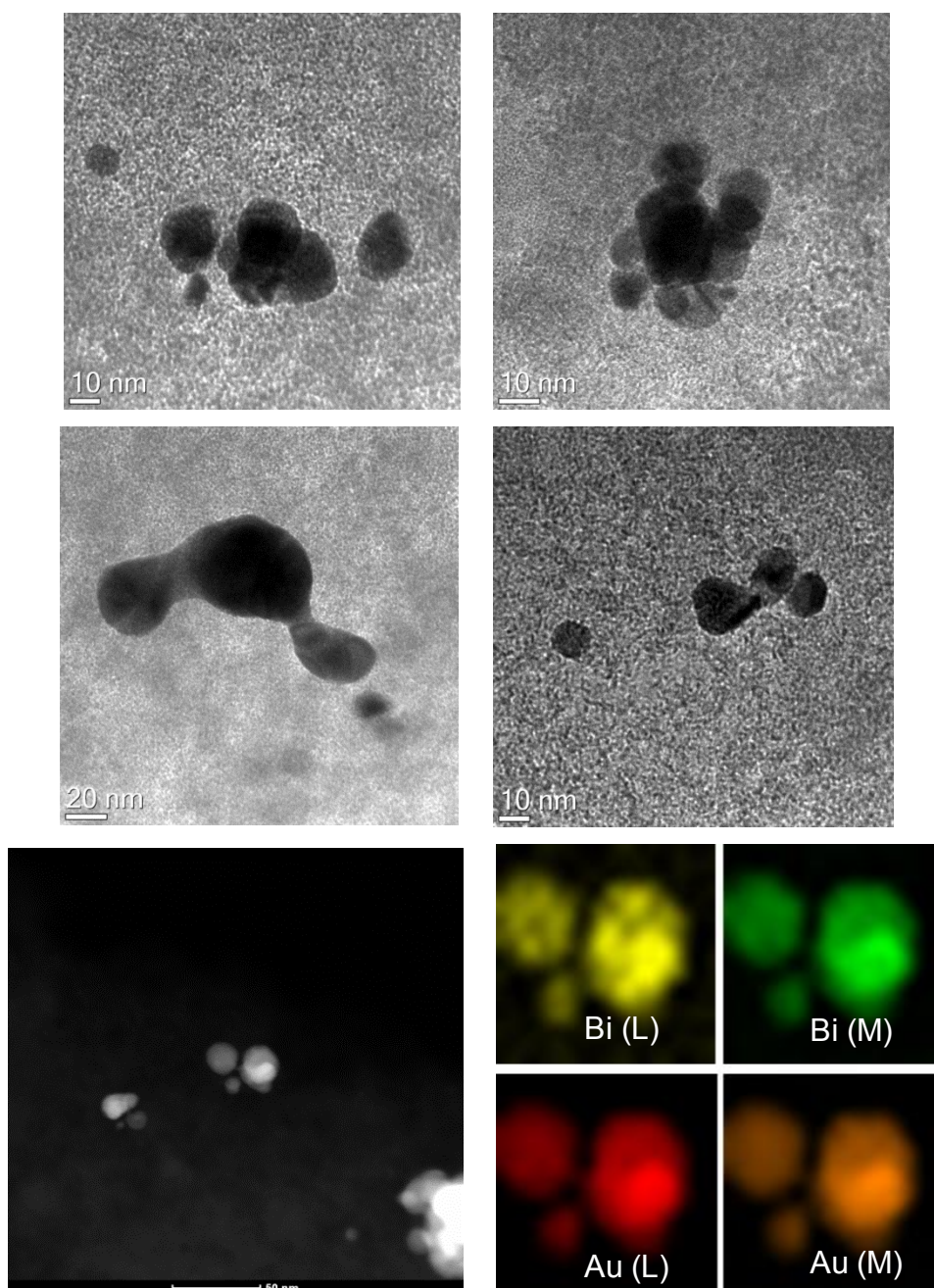
Figure 3.26. TEM image and STEM-EDX mapping (bottom figures) of AuBi/AC catalyst after 1st use (reaction conditions as in Figure 3.23). Top images: evidences for NPs agglomeration. Middle images: evidence for NPs sintering.

Results plotted in Figure 3.8 demonstrate that the smaller Au particles, those present in Au$_W$/AC (prepared with method 3), were inductive to the preferred formation of lighter acids by GO oxidative degradation. Conversely, catalysts with particle size 7.3 (Au$_{PVA}$/AC, prepared with method 2) and 12.9 (Au/AC, prepared with method 1) nm behaved more similarly. Therefore, it was decided to adopt method 1 for the preparation of several Au/M alloys to compare with AuBi/AC (see Table 3.1 for characterization).

The comparison of catalytic performance of bimetallic catalysts at 60 °C is shown in Figure 3.27, which compiles selectivity to GO, GA and "Others". In all cases glucose conversion was complete. Best overall yield to GO+GA was obtained with AuBi/AC, AuCu/AC and AuFe/AC catalysts, but AuBi/AC gave the highest yield to GA (29 % at 60 °C). Similar trend, but with a general lower selectivity to both GO and GA and a higher selectivity to Others with a worse C balance, was obtained at 90 °C (Figure 3.28). This was a further confirmation of the selectivity promoting effect of Bi for selective oxidation reactions with catalysts based on supported Au NPs.
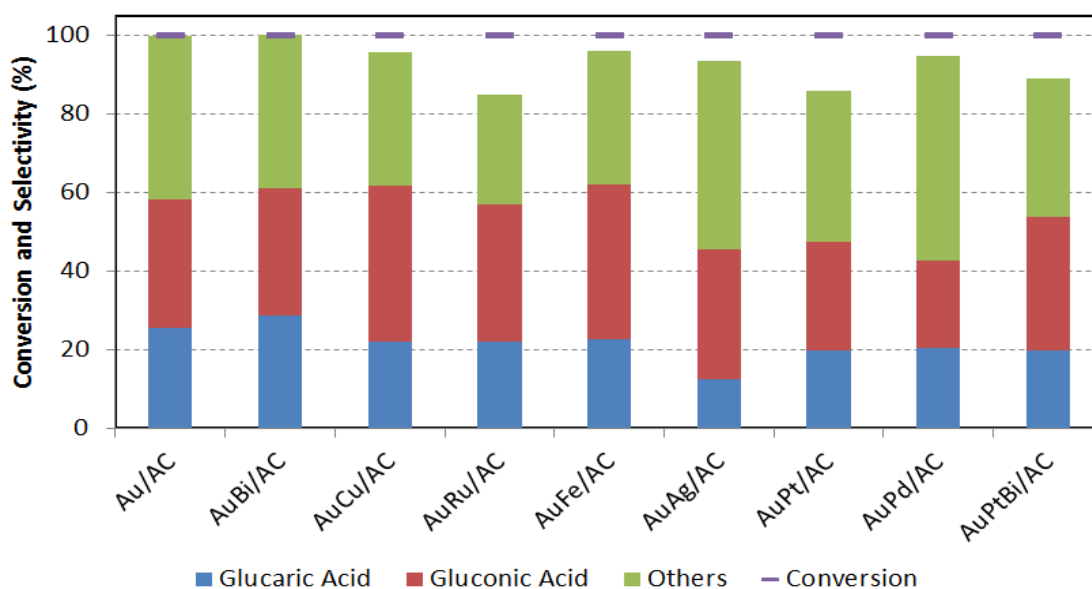
Figure 3.27. Screening of catalysts. Reaction conditions: Glucose 5 wt% in water, molar ratio Glu:Metal:NaOH = 500:1:1500, T 60 °C, oxygen pressure 10 bar, reaction time 3 h.
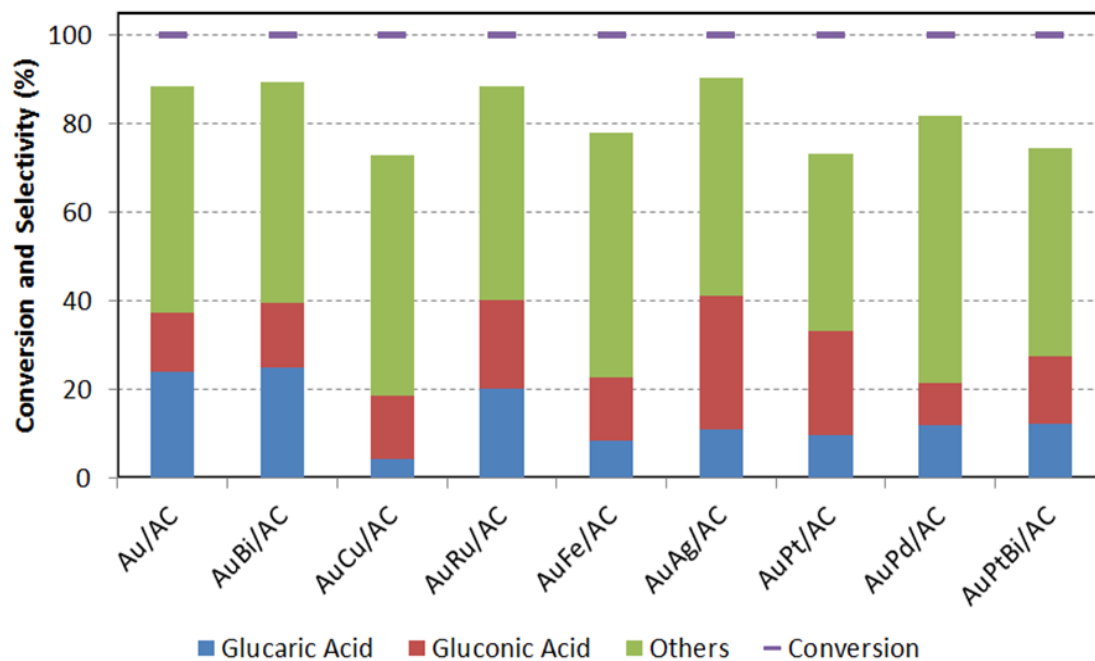
Figure 3.28. Screening of catalysts. Reaction conditions: Glucose 5 wt% in water, glucose:metaltot:NaOH 4.4:0.0088:13.2 mmol, T 90 ℃, oxygen pressure 10 bar, reaction time 3 h.

3.4 Conclusions

Catalysts based on carbon-supported Au nanoparticles were tested in the direct oxidation of glucose to glucaric acid, which is a possible intermediate for the synthesis of bio-based adipic acid. Catalysts showed to be extremely active in glucose oxidation; in fact, a glucose:Au ratio much higher than the glucose:Pt ratio reported in literature for Pt/C catalysts could be used, with both moderate reaction temperature (T 60 °C) and O_2 pressure (10 bar). Smaller Au particles led to more active but less selective catalysts, because of the enhanced formation of light carboxylic acids by oxidative degradation of the intermediately formed gluconic acid. Best yield to glucaric acid was 31 %, with 18 % to gluconic acid and 40 % to by-products. Important parameters for the control of performance were glucose concentration and glucose : metal : NaOH molar ratios, which had to be regulated in such a way as to make the oxidation of the intermediately formed gluconic acid to glucaric acid to occur efficiently, and keep a relatively high concentration of surface Au atoms in the oxidized state while limiting the formation of heavy compounds and the amount of organic species which remain adsorbed on catalyst surface. Catalyst deactivation was due to both the deposition of organic residues and to NPs agglomeration and sintering phenomena.

3.5 Acknowledgements

3.6 References

(1)   Corma, A.; Iborra, S.; Velty, A. *Chem. Rev.* **2007**, *107* (6), 2411–2502.

(2)   Delidovich, I.; Hausoul, P. J. C.; Deng, L.; Pfützenreuter, R.; Rose, M.; Palkovits, R. *Chem. Rev.* **2016**, *116* (3), 1540–1599.

(3)   Besson, M.; Gallezot, P.; Pinel, C. *Chem. Rev.* **2014**, *114* (3), 1827–1870.

(4)   Ennaert, T.; Van Aelst, J.; Dijkmans, J.; De Clercq, R.; Schutyser, W.; Dusselier, M.; Verboekend, D.; Sels, B. F. *Chem Soc Rev* **2016**, *45* (3), 584–611.

(5)   Cavani, F.; Albonetti, S.; Basile, F.; Gandini, A. *Chemicals and Fuels from Bio-based Building Blocks*; Wiley-VCH: Weinheim, Germany, 2016.

(6)   Deng, W.; Zhang, Q.; Wang, Y. *Catal. Today* **2014**, *234*, 31–41.

(7)   Lichtenthaler, F. W.; Peters, S. *Comptes Rendus Chim.* **2004**, *7* (2), 65–90.

(8)   Chheda, J. N.; Huber, G. W.; Dumesic, J. A. *Angew. Chem. Int. Ed.* **2007**, *46* (38), 7164–7183.

(9)   Gallezot, P. *Catal. Today* **2007**, *121* (1–2), 76–91.

(10)   Cavani, F. *Catal. Today* **2010**, *157* (1–4), 8–15.

(11)   Cavani, F.; Teles, J. H. *ChemSusChem* **2009**, *2* (6), 508–534.

(12)   Chieregato, A.; López Nieto, J. M.; Cavani, F. *Coord. Chem. Rev.* **2015**, *301–302*, 3–23.

(13)   Styron, S. D.; Kiely, D. E.; Ponder, G. *J. Carbohydr. Chem.* **2003**, *22* (2), 123–142.

(14)   Pohjanlehto, H.; Setälä, H.; Kammiovirta, K.; Harlin, A. *Carbohydr. Res.* **2011**.

(15)   Dijkgraaf, P. J.; Verkuylen, M. E.; van der Wiele, K. *Carbohydr. Res.* **1987**, *163* (1), 127–131.

(16)   Kiely, D. E.; Chen, L.; Lin, T.-H. *J Am Chem Soc* **1994**, *116*, 571–578.

(17)   Smith, T. N. *INFORM - International News on Fats, Oils and Related Materials 2011*; 2011; Vol. 22, 550–552.

(18)   Kiely, D. E.; Hash, K. R. Method of oxidatiousing nitric acid. US2014256983, 2014.

(19)   Smith, T. N.; Hash, K.; Davey, C.-L.; Mills, H.; Williams, H.; Kiely, D. E. *Carbohydr. Res.* **2012**, *350*, 6–13.

(20)   Thaburet, J.-F.; Merbouh, N.; Ibert, M.; Marsais, F.; Queguiner, G. *Carbohydr. Res.* **2001**, *330* (1), 21–29.

(21)   Ibert, M.; Marsais, F.; Merbouh, N.; Brückner, C. *Carbohydr. Res.* **2002**, *337* (11), 1059–1063.

(22)   Bin, D.; Wang, H.; Li, J.; Wang, H.; Yin, Z.; Kang, J.; He, B.; Li, Z. *Electrochimica Acta* **2014**, *130*, 170–178.

(23)   Ibert, M.; Fuertès, P.; Merbouh, N.; Feasson, C.; Marsais, F. *Carbohydr. Res.* **2011**, *346* (4), 512–518.

(24)   Dirkn, J. M.; van der Baan, H. S.; van den Broen, J. M. *Carbohydr. Res.* **1977**, *59* (1), 63–72.

(25)   Venema, F. R.; Peters, J. A.; van Bekkum, H. *J. Mol. Catal.* **1992**, *77* (1), 75–85.

(26)   Lee, J.; Saha, B.; Vlachos, D. G. *Green Chem* **2016**, *18* (13), 3815–3822.

(27)   Jin, X.; Zhao, M.; Vora, M.; Shen, J.; Zeng, C.; Yan, W.; Thapa, P. S.; Subramaniam, B.; Chaudhari, R. V. *Ind. Eng. Chem. Res.* **2016**, *55* (11), 2932–2945.

(28)   Jin, X.; Zhao, M.; Shen, J.; Yan, W.; He, L.; Thapa, P. S.; Ren, S.; Subramaniam, B.; Chaudhari, R. V. *J. Catal.* **2015**, *330*, 323–329.

(29)   Derrien, E.; Marion, P.; Pinel, C.; Besson, M. *Org. Process Res. Dev.* **2016**, *20* (7), 1265–1275.

(30)   Besson, M.; Fleche, G.; Fuertes, P.; Gallezot, P.; Lahmer, F. *Recl. Trav. Chim. Pays-Bas* **1996**, *115* (4), 217–221.

(31)   Boussie, T. R.; Dias, E. L.; Fresco, Z. M.; Murphy, V. J.; Shoemaker, J.; Archer, R.; Jiang, H. Production of adipic acid and derivativesfrom carbohydrate-containing materials. WO2010144862.

(32)   Murphy, V. J.; Shoemaker, J.; Zhu, G.; Archer, R.; Salem, G. F.; Dias, E. L. Oxidation Catalysts. US2011306790.

(33)   Boussie, T. R.; Diamond, G. M.; Dias, E. L.; Murphy, V. J. In *Chemicals and Fuels from Bio-Based Building Blocks*; Wiley-VCH, 2016; Vol. 1, pp 153–172.

(34)   *Sustainable industrial processes*; Cavani, F., Ed.; Wiley-VCH: Weinheim, 2009.

(35)   Ondrey, G. *Chem. Eng.* **2015**, *122* (9), 11.

(36)   Archer, R.; Diamond, G. M.; Dias, E. L.; Murphy, V. J.; Petro, M.; Super, J. D. Process for the separation of mono and di-carboxyl acid compounds. US2013345473.

(37)   Wang, Y.; Van de Vyver, S.; Sharma, K. K.; Román-Leshkov, Y. *Green Chem* **2014**, *16* (2), 719–726.

(38)   Miedziak, P. J.; Alshammari, H.; Kondrat, S. A.; Clarke, T. J.; Davies, T. E.; Morad, M.; Morgan, D. J.; Willock, D. J.; Knight, D. W.; Taylor, S. H.; Hutchings, G. J. *Green Chem* **2014**, *16* (6), 3132–3141.

(39)   Cao, Y.; Liu, X.; Iqbal, S.; Miedziak, P. J.; Edwards, J. K.; Armstrong, R. D.; Morgan, D. J.; Wang, J.; Hutchings, G. J. *Catal Sci Technol* **2016**, *6* (1), 107–117.

(40)   Rautiainen, S.; Lehtinen, P.; Vehkamäki, M.; Niemelä, K.; Kemell, M.; Heikkilä, M.; Repo, T. *Catal. Commun.* **2016**, *74*, 115–118.

(41)   Comotti, M.; Della Pina, C.; Matarrese, R.; Rossi, M. *Angew. Chem. Int. Ed.* **2004**, *43* (43), 5812–5815.

(42)   Baatz, C.; Pruse, U. *J. Catal.* **2007**, *249* (1), 34–40.

(43)   Zhang, H.; Toshima, N. *Catal Sci Technol* **2013**, *3* (2), 268–278.

(44)   Mirescu, A.; Prüße, U. *Appl. Catal. B Environ.* **2007**, *70* (1–4), 644–652.

(45)   Biella, S.; Prati, L.; Rossi, M. *J. Catal.* **2002**, *206* (2), 242–247.

(46)   Rautiainen, S.; Lehtinen, P.; Chen, J.; Vehkamäki, M.; Niemelä, K.; Leskelä, M.; Repo, T. *RSC Adv* **2015**, *5* (25), 19502–19507.

(47)   Kusema, B. T.; Campo, B. C.; Mäki-Arvela, P.; Salmi, T.; Murzin, D. Y. *Appl. Catal. Gen.* **2010**, *386* (1–2), 101–108.

(48)   Smolentseva, E.; Kusema, B. T.; Beloshapkin, S.; Estrada, M.; Vargas, E.; Murzin, D. Y.; Castillon, F.; Fuentes, S.; Simakov, A. *Appl. Catal. Gen.* **2011**, *392* (1–2), 69–79.

(49)   Kusema, B. T.; Mikkola, J.-P.; Murzin, D. Y. *Catal Sci Technol* **2012**, *2* (2), 423–431.

(50)   Kusema, B. T.; Murzin, D. Y. *Catal Sci Technol* **2013**, *3* (2), 297–307.

(51)   Kusema, B. T.; Campo, B. C.; Simakova, O. A.; Leino, A.-R.; Kordás, K.; Mäki-Arvela, P.; Salmi, T.; Murzin, D. Y. *ChemCatChem* **2011**, *3* (11), 1789–1798.

(52)   Hermans, S.; Deffernez, A.; Devillers, M. *Appl. Catal. Gen.* **2011**, *395* (1–2), 19–27.

(53)   Villa, A.; Campisi, S.; Chan-Thaw, C. E.; Motta, D.; Wang, D.; Prati, L. *Catal. Today* **2015**, *249*, 103–108.

(54)   Zhou, Y.; Wang, S.; Ding, B.; Yang, Z. *J. Sol-Gel Sci. Technol.* **2008**, *47* (2), 182–186.

(55)   Saliger, R.; Decker, N.; Prüße, U. *Appl. Catal. B Environ.* **2011**, *102* (3–4), 584–589.

(56)   Chan-Thaw, C. E.; Chinchilla, L. E.; Campisi, S.; Botton, G. A.; Prati, L.; Dimitratos, N.; Villa, A. *ChemSusChem* **2015**, *8* (24), 4189–4194.

(57)   Villa, A.; Chan-Thaw, C. E.; Campisi, S.; Bianchi, C. L.; Wang, D.; Kotula, P. G.; Kübel, C.; Prati, L. *Phys Chem Chem Phys* **2015**, *17* (42), 28171–28176.

(58)   Bergeret, G.; Gallezot, P. In *Handbook of Heterogeneous Catalysis (G. Ertl, H. Knözinger, F. Schüth, J. Weitkamp)*; Wiley-VCH Verlag GmbH & Co. KGaA, 2008; pp 738–765.

(59)   Haruta, M. *Catal. Today* **1997**, *36* (1), 153–166.

(60)   Ishida, T.; Kinoshita, N.; Okatsu, H.; Akita, T.; Takei, T.; Haruta, M. *Angew. Chem. Int. Ed.* **2008**, *47* (48), 9265–9268.

(61)   Mallat, T.; Baiker, A. *Catal. Today* **1994**, *19* (2), 247–283.

(62)   Sinha, A. K.; Seelan, S.; Tsubota, S.; Haruta, M. *Angew. Chem. Int. Ed.* **2004**, *43* (12), 1546–1548.

(63)   Davis, R. J. *Science* **2003**, *301*, 926–928.

CHAPTER 4. NIOBIUM-BASED CATALYSTS FOR THE SELECTIVE EPOXIDATION OF CYCLOHEXENE WITH HYDROGEN PEROXIDE

4.1 Introduction

4.1.1 Epoxides

Epoxides (Figure 4.1), also known as oxiranes, are an important class of chemical compounds characterized by a highly reactive group that permits their use as intermediates for the production of various industrial products including surfactants, detergents, antistatic- or corrosion-protection agents, additives to laundry detergents, lubricating oils, textiles and cosmetics[1].
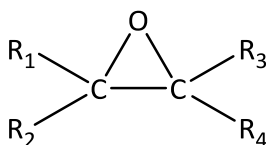
Figure 4.1. Example of an epoxide

Epoxides can be obtained by the addition of oxygen to alkenes in different ways. Industrial routes primarily employ the use of dioxygen, peroxides and peracids to introduce the epoxide oxygen. Epoxidation with percaboxylic acids can be done with in situ generation of the oxidant or with preformed molecules, but the use of peracids is not ideal because of the co-production of acid waste; moreover also the handling of this compounds involve safety problems[2]. The use of dioxygen in ethylene epoxidation, for instance, avoids the formation of undesired coproducts, as it can be performed with or without catalysts, but selectivity and yields are low: catalytic systems containing Mo, V, W, Cr or Ti are highly selective but present low activity, while Co, Ni, Mn, Cu, Ir, Rh, Pt and Ru are more active but less selective[1]. A valuable alternative is the epoxidation with hydrogen peroxide (HP): its use is cheaper compared to peracids because it does not form co-products that have to be separated with expensive separation systems, it is readily available and gives water as the only by-product. There is an abundance of

literature on catalytic systems for HP in epoxidation, and the most common catalysts , both homogeneous and heterogeneous, are based on W, Mn, Re and Ti[2]. The activation of HP was also studied in the absence of metals, for instance, using potassium peroxomonosulfate, acetonitrile and achiral ketones, carbodiimide, hydrogen carbonate ions, CO_2, perfluorinated ketones, or fluorinated alcohols. In this case results were worse compared with the ones obtained with metals systems and these processes generate large amount of waste because of the use of auxiliaries. Heterogeneous metallic catalysts are easily recovered from reaction mixture and sometimes present high selectivity, but most of these systems are characterized by low activity, instability and limited recyclability[2]. Nevertheless, the research of new heterogeneous catalytic systems stable in aqueous oxidant, with high active site accessibility, high selectivity and activity is of great interest.

4.1.2 Supported niobium oxide as a catalyst

K. Tanabe[3] and I. E. Wachs[4] were pioneers in the study of niobium oxide structure and its application as catalyst. In the last few decades many papers and reviews were published on the use of niobium in catalysis, specially by I. Nowak and M. Ziolek[5–8]. Niobium compounds can be used in catalysis as a promoter, active phase, support, solid acid or redox material[5], and are employed in wide number of reactions: alcohol dehydration, dehydrogenation, oxidative dehydrogenation, oxidation, ammoxidation, esterification, alkylation, isomerization and hydrogenation[6]. Among these, there is also a precedent in alkene epoxidations[9–13].

Niobium can be present in the catalytic system as a carbide, sulfide, nitride, oxynitride, phosphate or, as is most frequently the case, as an oxide[7]. Niobium oxides can be present in their bulk form (Nb_2O_5), as a support for other metals, as a supported active phase or as mixed oxides. Their reactivity is influenced by the surrounding niobium species and by the type of catalytic reaction[5]. The isolation of active metal sites in inorganic matrices avoids their oligo- or polymerization and aggregation to less reactive species (i.e. nanoparticles), and can give them unique activities[14]. An example is the epoxidation of propene in the liquid phase with a Ti(IV)/SiO_2 catalyst, developed by Shell in 1970s[15]. The metal sites can be immobilized in a solid matrix in different ways

(Figure 3.2): metal ions can be isomorphously substituted in framework positions of molecular sieves, metal compounds can be grafted onto the surface of the support, metal complexes can be tethered to the surface of a solid, or can be encapsulated in a solid matrix (ship-in-a-bottle concept)[14].
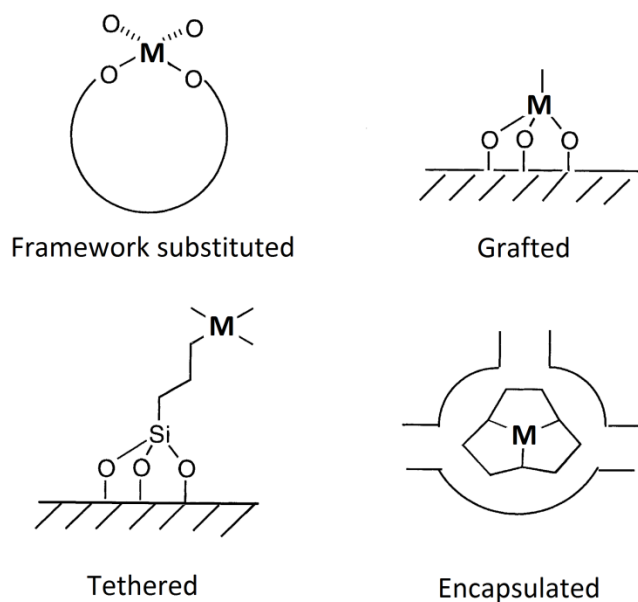
Figure 4.2. Different types of immobilization of metal sites in a solid matrix (Figure adapted from ref[14])

Single-site heterogeneous catalysts combine the advantage of homogenous catalysts with regard to the "isolation" of the active sites, with the easy separation from reactants and catalyst recyclability. They allow to for regioselective, shape-selective and enantioselective reactions to occur, permit the development of more sustainable processes with fewer hazardous solvents and reagents, they facilitate modeling with computational study, and they offer a good opportunity for the design of new catalysts and improvement of existing ones[16].

In order to have more readily available and easily prepared niobium oxide active sites, a good possibility is the use of grafted niobium oxide.

The controllable surface structure of grafted catalysts influence their catalytic reactivity[17]. A very important parameter is the coverage of the active species on the surface because it dictates the type of the two- and three-dimensional dispersion of the grafted system. Metal oxide structures can be classified as being above or below monolayer coverage, which is the maximum value of two-dimensional species on the

surface before the formation of three-dimensional nanoparticles[18]. In detail, catalysts with oxides species below the monolayer coverage can be presented as isolated monomers and oligo- or polymeric species with one or more linking oxygen between the metals atoms (Figure 4.3), referred to as two-dimensional (2D) species.
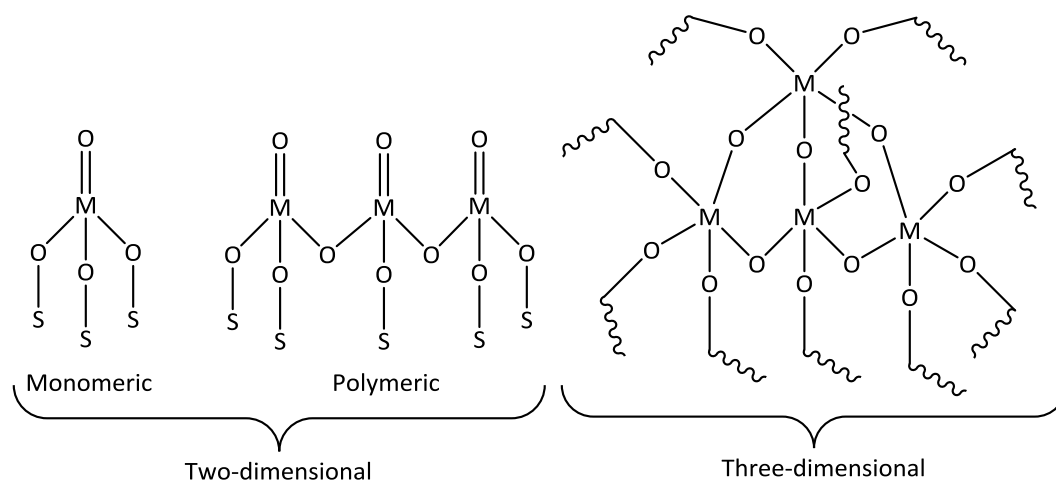
Figure 4.3. Two- and three-dimensional supported metal oxide structure (Figure adapted from ref[19])

Niobium oxide has been supported on various supports such as silica, alumina, magnesia, titania, zirconia and zeolites[7], the nature of which may influence the catalytic activity of the active site[20]. A recurring use of Nb-supported catalysts is alkene epoxidation. Ahn et al. recently published a paper about the synthesis of Nb (V) oxide supported on Zr-based metal organic framework (MOF). These catalysts have a well-defined Nb structure on the surface with high coverage and almost total participation of the Nb sites as active sites for alkene epoxidation[21]. Thornburg et al[22] grafted a wide range of Nb(V) precursors on mesoporous silica obtaining different Nb surface densities and tested it for the epoxidation of cis-cyclooctene to study the synthesis-structure-function relations. Other studies include NbO_x deposited onto MCM-41 for cyclohexene epoxidation[23], Nb supported on TS-1 for epoxidation of 1-octene[24], and deposited Nb oxide on SiO_2 for the epoxidation of methyl oleate with HP[25]. Silica is one of the most used supports: it has good thermal and mechanical resistance, it presents moderate acidity of surface hydroxyls groups and it allows for the support of a large number of different elements, it does not swell with organic solvents and it is inexpensive. The main drawback of silica is that it permits lower surface density of supported oxides

compared to other oxide supports. For example, in the case of vanadium, it is possible to obtain up to 7-9 V / nm^2 with common oxides (Al$_2$O$_3$, Nb$_2$O$_5$, TiO$_2$, CeO$_2$, ZrO$_2$) , but only 3 V /nm^2 for silica[20] (Figure 4.4). This difference is attributed to the low reactivity and greater acidic character of silica hydroxyl groups that disadvantage the deposition of vanadium[26]. From the literature, it is known that it is possible modify silica surface acidity with alkali dopants[27,28] and Grant et al. demonstrated that Na-promoted silica enhances metal oxide dispersion leading to a higher maximum two-dimensional coverage[19,29]. They studied the effect of the addition of sodium on different Group V metal oxides, and obtained an improvement from 3 to 9 atom/nm^2 for vanadium, from 1.1 to 2.5 atom/nm^2 for niobium, and from 0.8 to 2.9 atom/nm^2 for tantalum.
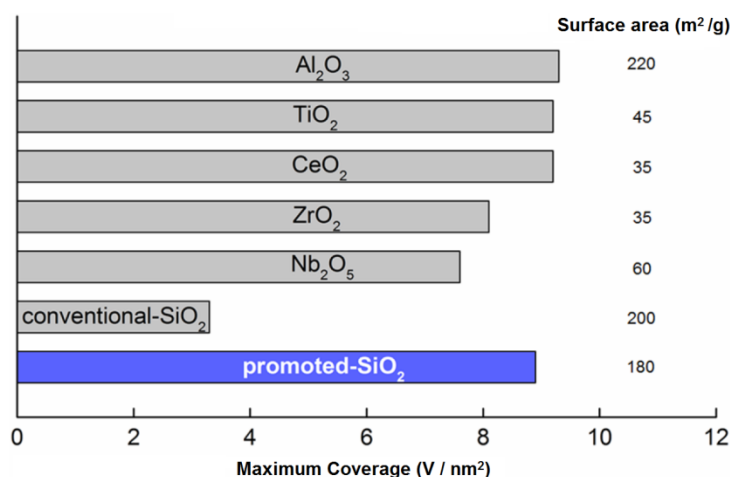
Figure 4.4. Experimental coverages of 2D V species on various oxide supports (Figure adapted from ref[19])

This fine study on catalyst design is of great importance for the development of new catalysts with improved performances, that can be gained with simple modification of the synthesis procedure.

4.1.3 Aim of the work

The Hermans group (University of Wisconsin − Madison) has previously shown that the use of Na as a promoter allows higher 2D metal oxide dispersion, leading to increased activity in the ODHP reaction using V/SiO$_2$, scaling with the metal loading[19].

In a recent paper[9], Thornburg et al. declare that with highly dispersed Group IV and V metal-based catalysts, they were able to obtain high selectivity in cyclohexene epoxidation with hydrogen peroxide and acetonitrile as solvent (see Figure 5 for proposed reaction network). In particular, these catalysts were prepared using calixarene coordination complexes as metal precursors (Figure 4.6). They claimed that using these compounds, it is possible to graft well-defined calixarene complexes of groups IV and V onto SiO_2 and create structurally uniform catalysts that can be compared each other for the cyclohexene epoxidation with HP.

Figure 4.5. Proposed reaction network for cyclohexene oxidation with hydrogen peroxide (figure adapted from ref[9])

Figure 4.6. Synthesis of silica-supported niobium oxide catalysts by Thornburg et al.(Figure adapted from ref[9])

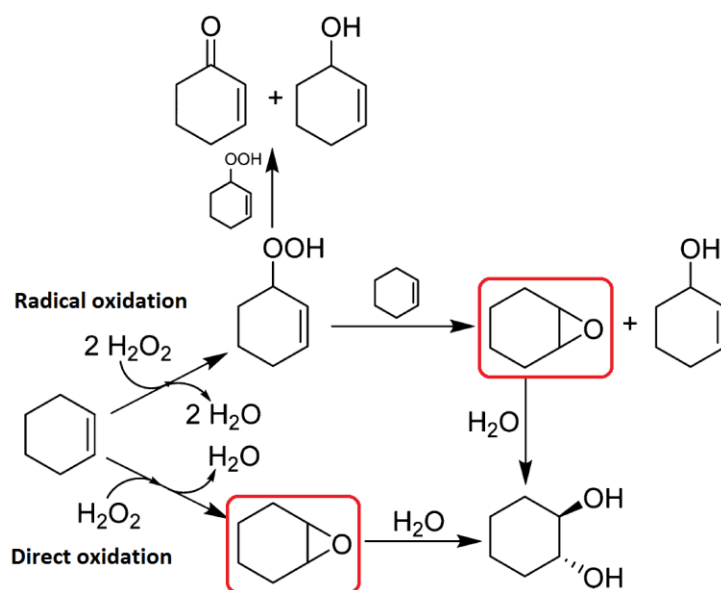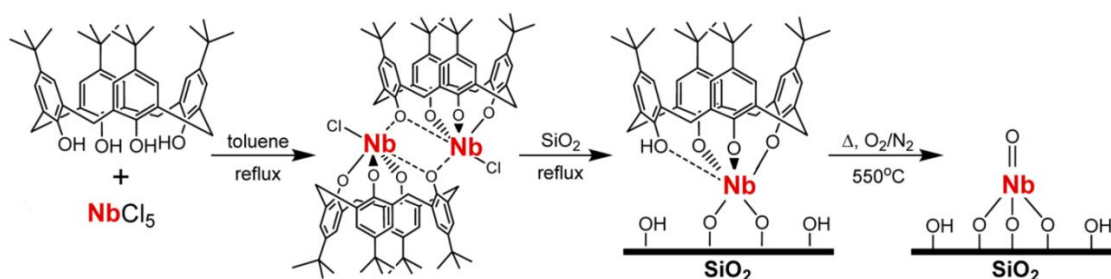Hermans research group decided to test the niobium-based catalyst prepared with the method used in propane oxidative dehydrogenation paper[19] (prepared using simple niobium ethoxide as precursor), for the selective epoxidation of cyclohexene with hydrogen peroxide, and in the present chapter is described the study of the reactivity of these catalysts. The aim is demonstrate that it is possible to obtain Nb isolated monomeric sites on SiO_2 using a simpler synthesis without the employment of long and hard procedures or complex reagents, gaining at the same time high activity for epoxidation reaction. Similarly, it is also possible to prepare Nb-based catalysts using Na-promoted silica that allow to get higher 2D surface coverage leading to higher activity, following the same trend as seen with the V-based catalyst for ODHP.

4.1.4 Previous work: catalysts synthesis and characterization

Catalysts tested in this work were prepared by Joseph T. Grant, Carlos A. Carrero and Fangying Huang before the beginning of this study following the procedure reported in the paper published on ACS Catalysis in 2015[19]. Na-promoted silica was prepared by incipient wetness impregnation of amorphous silica (Aerosil200, Evonik, surface area 200 m^2/g) with the desired amount of 1 M $NaNO_3$ solution, followed by calcination under air at 700 °C for 4 h. The supports were dried overnight at 120 °C under static conditions and then impregnated with the metal precursor inside a glovebox under dry N_2 atmosphere. The metal precursor, niobium ethoxide, was diluted with dry ethanol prior the incipient wetness impregnation. With this method catalysts with and without Na (promoted and conventional silica, respectively), and different Nb loadings were prepared. The final catalysts were vacuum-dried inside the glovebox and calcined under a flow of N_2 at 120 °C for 3 hours, then heated to 550 °C and calcined for another 3 hours under dry air.

Catalysts were characterized by N_2 physisorption for surface area and pore volume measurements. Niobium and sodium loading were measured with induced coupled plasma optical emission spectroscopy (ICP-OES) after acid digestion. Raman, IR and UV-vis spectroscopy (the last two analyses were performed on dehydrated samples inside a glovebox) were necessary to determine the type of dispersion of niobium oxide on the silica surface (2D dispersion or 3D nanoparticles) and the Nb coverage. Maximum 2D

Nb coverage obtained on conventional silica was 1.1 Nb/nm^2, while with sodium promoted silica the value arises to 2.5 Nb/nm^2.

Catalysts tested for epoxidation can be organized by Nb loading (wt% Nb), the presence or the absence of Na (wt% Na), and thus different Nb coverages and dispersions, as shown in Table 4.1. In detail, catalyst FH21X has similar metal loading of FH172, but different coverage and metal dispersion, since in the case of Nb supported on Na-promoted silica, the metal is two-dimensionally dispersed, while on FH172 it is in the form of three-dimensional nanoparticles. In fact, in the case of catalyst FH212, it was necessary increase the metal loading to 9.58 wt% in order to surpass the monolayer coverage and achieve Nb nanoparticles comparable with FH172.

Catalyst characteristics					
Type of Nb loading	Catalyst name	Nb loading (wt%)	Na loading (wt%)	Coverage (Nb/nm^2)	Nb dispersion state
Without Na					
Low	FH218	0,77	-	0,2	2D
High	FH210	2,65	-	0,8	2D
Above	FH172	4,43	-	1,6	3D Nanoparticles
With Na					
Low	FH221	0,68	0,39	0,2	2D
High	FH211	2,14	0,39	0,8	2D
Very High	FH21X	4,50	0,70	2,2	2D
Above	FH213	9,58	0,391	3,6	3D Nanoparticles

Table 4.1: Catalysts tested for the epoxidation of cyclohexene

4.2 Experimental section

Reactions were performed in sealed glass tubes and starting reaction conditions were (according to the paper of N. E. Thornburg et al[9]): molar ratio Cyclohexene (CH) : Hydrogen Peroxide (HP) : Nb = 1000 : 100 : 1, solvent CH_3CN (final reaction mixture volume 7.5 ml), T = 75 °C, stirring at 900 rpm, biphenyl as an internal standard. HP was added to initiate the reaction after 30 minutes of conditioning of the rest of the mixture at the desired reaction temperature. Sampling of the reaction mixtures were performed with a syringe at established reaction times up to 24 h, in addition to the first two samples which were collected right before (to calculate $[H_2O_2]_{blank}$) and right after the addition of HP (to calculate $[H_2O_2]_{initial}$ as difference from $[H_2O_2]_{blank}$) . Samples were analyzed by GC for qualitative and quantitative analysis of the products, and by ceric sulfate titration with ferroin indicator for the determination of HP consumption. All spent catalysts were washed three times with acetonitrile and collected for possible further investigation, as was the final reaction mixture.

Results are expressed as:

HP concentration at time t: $[H_2O_2]_t = [H_2O_2]_{from\ titration\ at\ time\ t} - [H_2O_2]_{initial}$

HP conversion at time t: $([H_2O_2]_{initial} - [H_2O_2]_t) / [H_2O_2]_{initial}$

HP-based product X selectivity at time t: $[X]_t / ([H_2O_2]_{initial} - [H_2O_2]_t)$

4.3 Results and discussion

First, a replication of Thornburg's[9] test was attempted with the most similar catalyst and similar reaction conditions: molar ratio CH : Nb : HP = 1000 : 1 : 100; 75 °C; solvent CH_3CN, the results of which are reported in Figure 7.
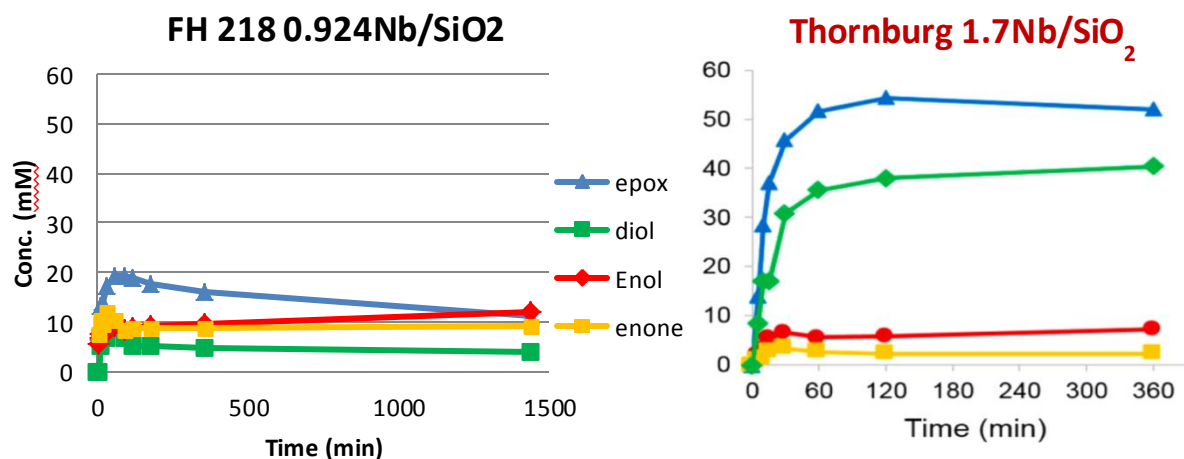
Figure 4.7. Comparison of laboratory result of the first attempt (graph on the right adapted from ref [9])

Products identified and quantified include cyclohexene epoxide (epoxide), 1,2-cyclohexanediol (diol), 2-cyclohexen-1-ol (enol) and 2-cyclohexen-2-one (enone). For simplification, only HP concentration and epox and diol results will be shown henceforth.

It was seen that product concentrations were very low and the catalyst presented significantly lower catalytic performance compared to the ones synthesized from the calixarene complexes. This indicated that the spatial distribution of the NbO_x species seemed to be very important for the epoxidation reaction and calixarene ligands are important to improve the spatial distribution of niobium.

After these results, it was decided to investigate if it could be possible to increase CH conversion towards the desired product, first by increasing the initial HP concentration from a molar ratio CH : HP = 10 : 1 to 5 : 1.

Tests were performed with catalysts FH218 and FH220 which were characterized by low Nb loading, the first prepared without and the second with Na-promoted silica (Figure 4.8 and 4.9).
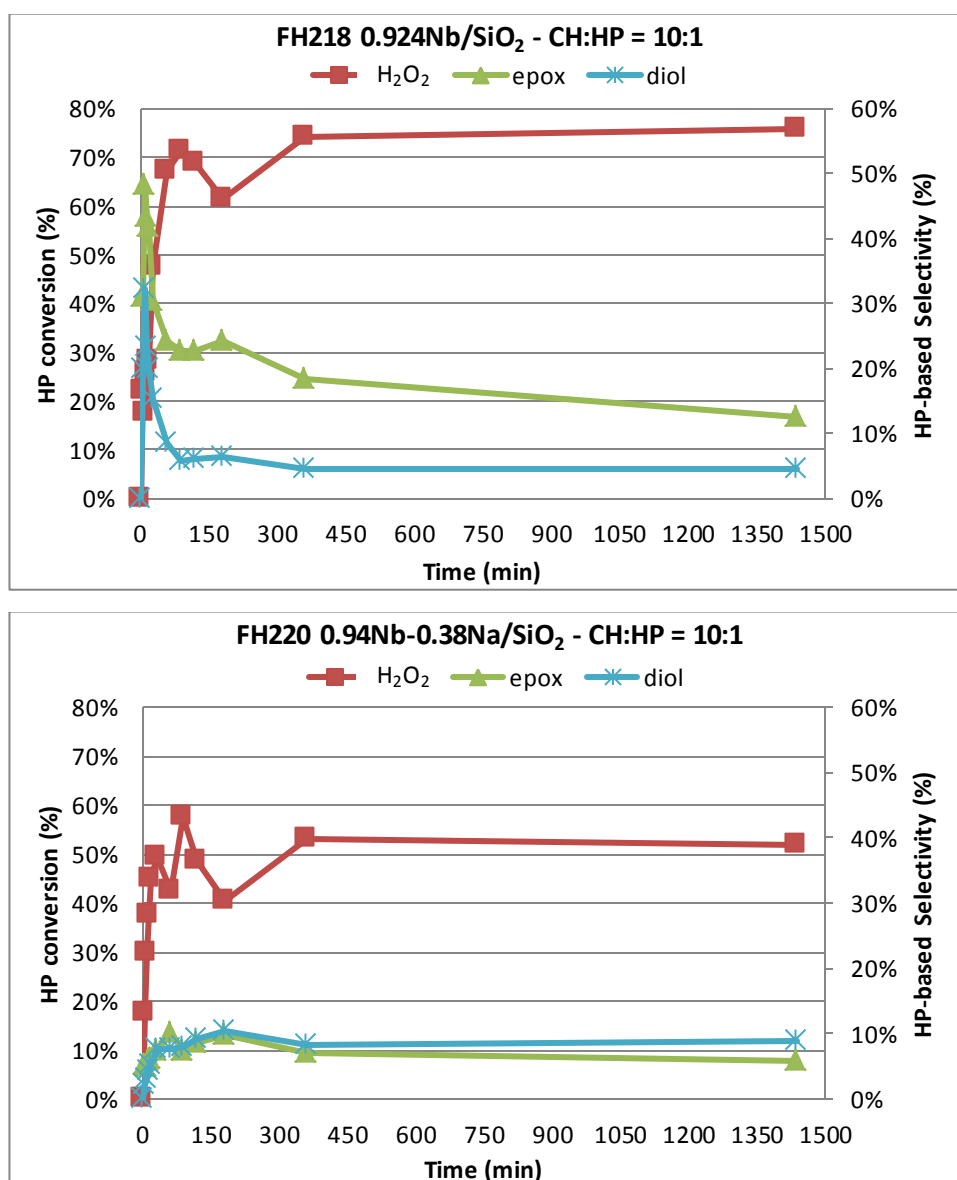
Figure 4.8. Results obtained with FH218 and FH220 and molar ratio CH : HP = 10 : 1
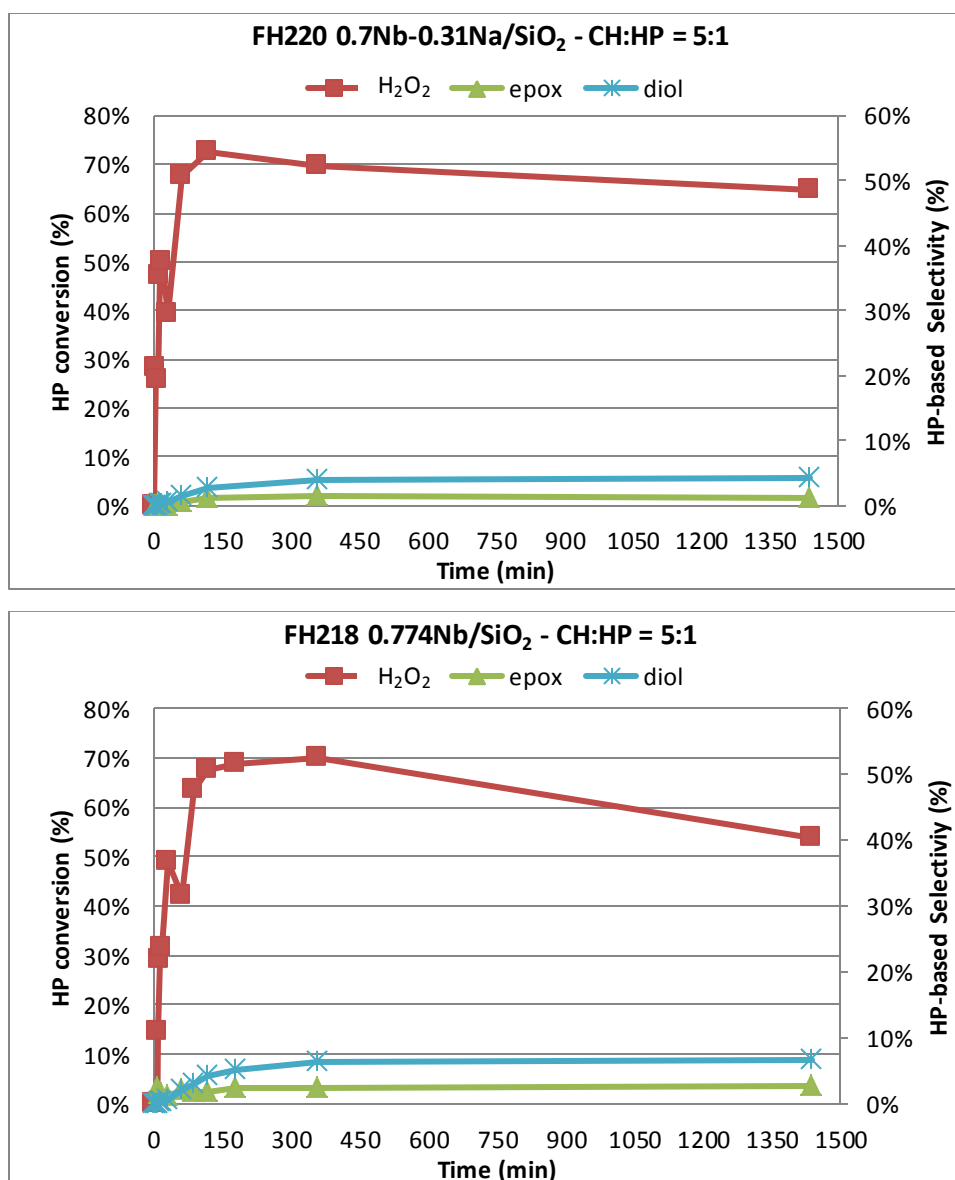
Figure 4.9. Results obtained with FH218 and FH220 and molar ratio CH : HP = 5 : 1

This variation caused problems of high pressure inside the reactor tubes and it worsened the selectivity to the "valuable products," i.e. the epoxide and the diol. Thus it was decided to use less HP, instead doubling the amount of catalyst using the following molar ratio: CH : HP : Nb = 1000 : 100 : 2.

As example, here are reported results with catalysts FH172 and FH212, which presented similar high Nb loading, without and with Na (Figure 4.10 and 4.11).
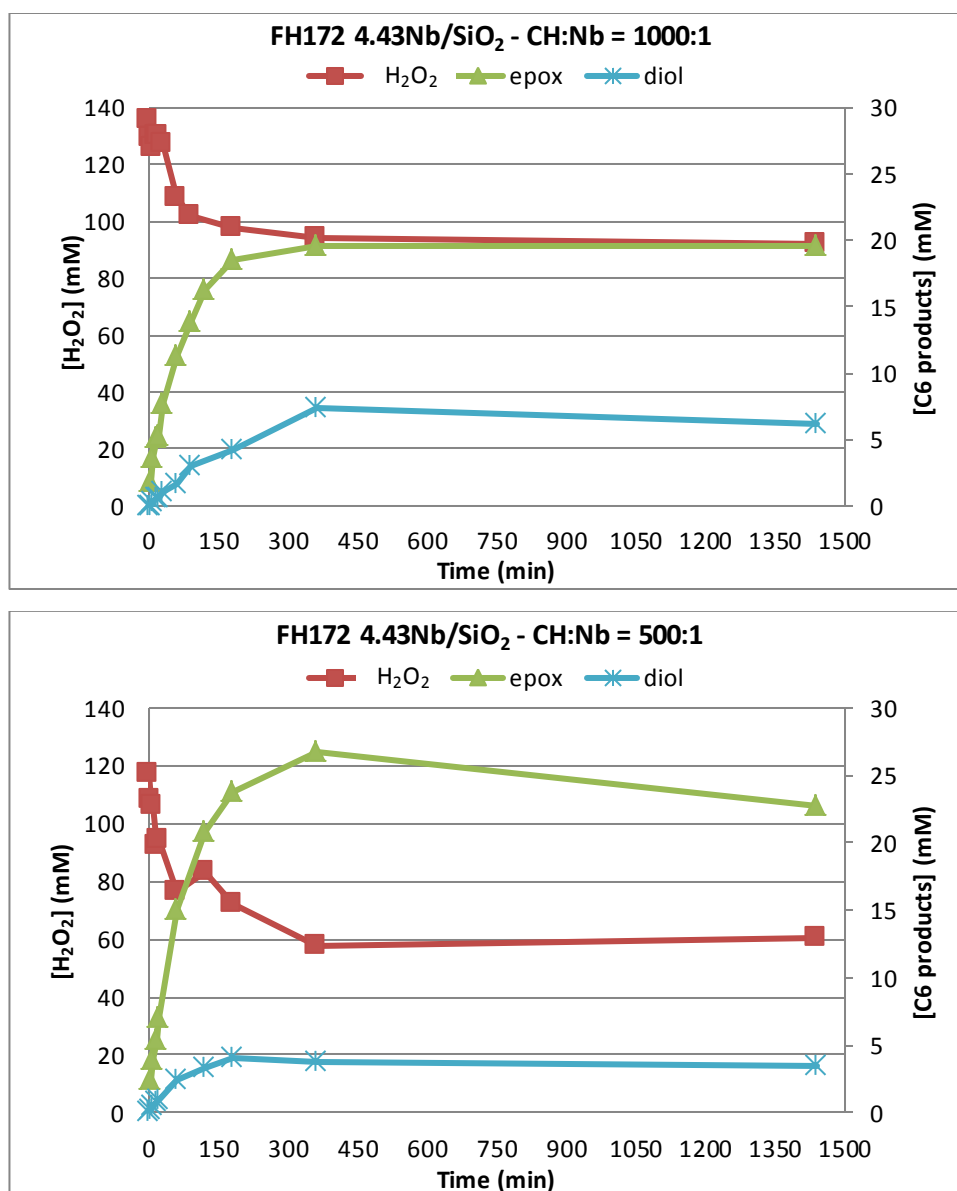
Figure 4.10. Reactions performed with FH172, comparison between different CH : Nb molar ratio

Increasing the amount of catalyst increased the concentration of the epoxide and decreased the concentration of the diol, a fact more evident in the case of the catalyst with Na-promoted silica. At the same time, more Nb also caused a major HP conversion not yielding product, lowering the HP-based selectivity of the products (HP decomposition). Nevertheless, it was decided to pursue the study with this CH : Nb ratio because of the better selectivity towards the epoxide with respect to the diol.
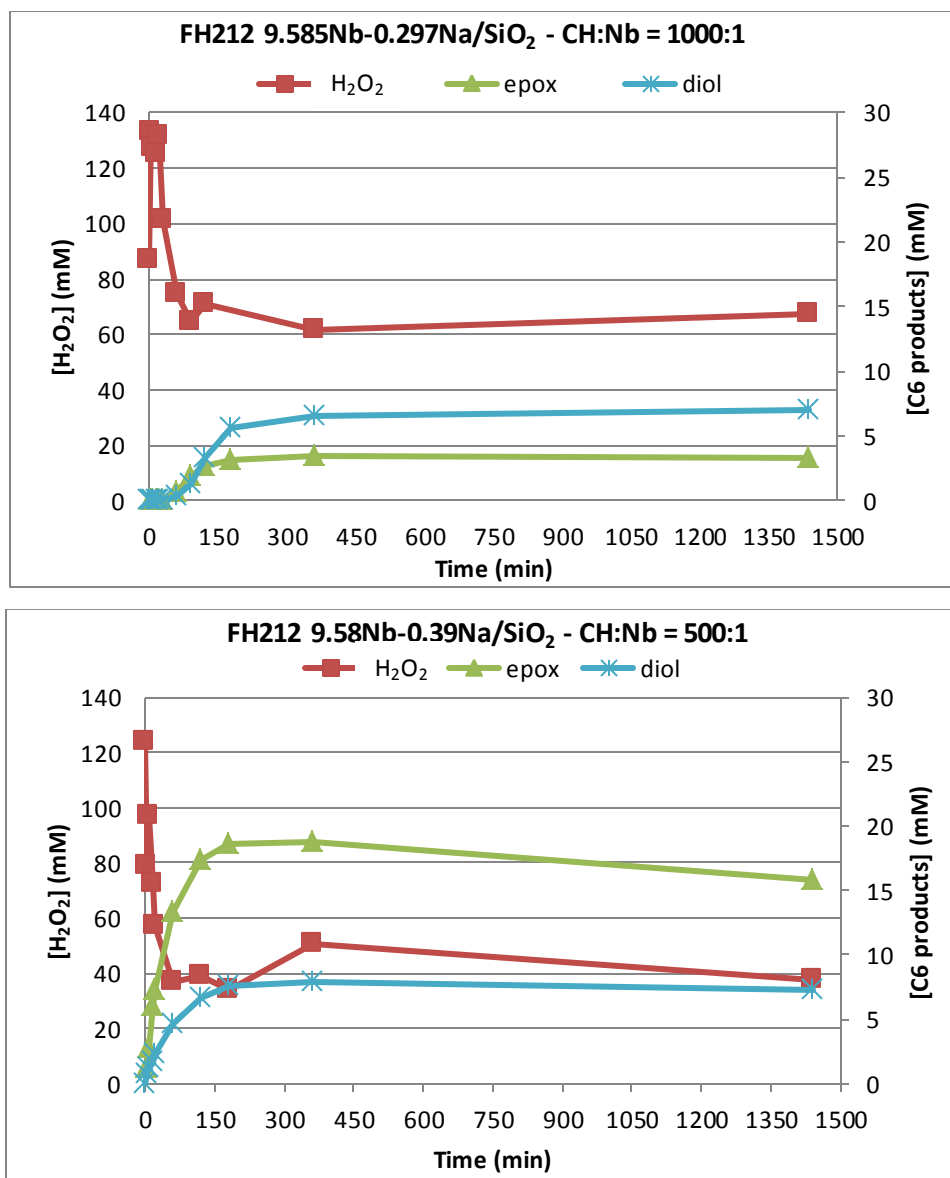
Figure 4.11. Reactions performed with FH212, comparison between different CH : Nb molar ratio

The following results show the different reactivity of catalysts without and with Na, on the basis of Nb loading (molar ratio CH : Nb : HP = 500 : 1 : 50).

Figure 4.12 presents the results of catalysts with conventional silica as the support and increasing niobium loading and different coverages.
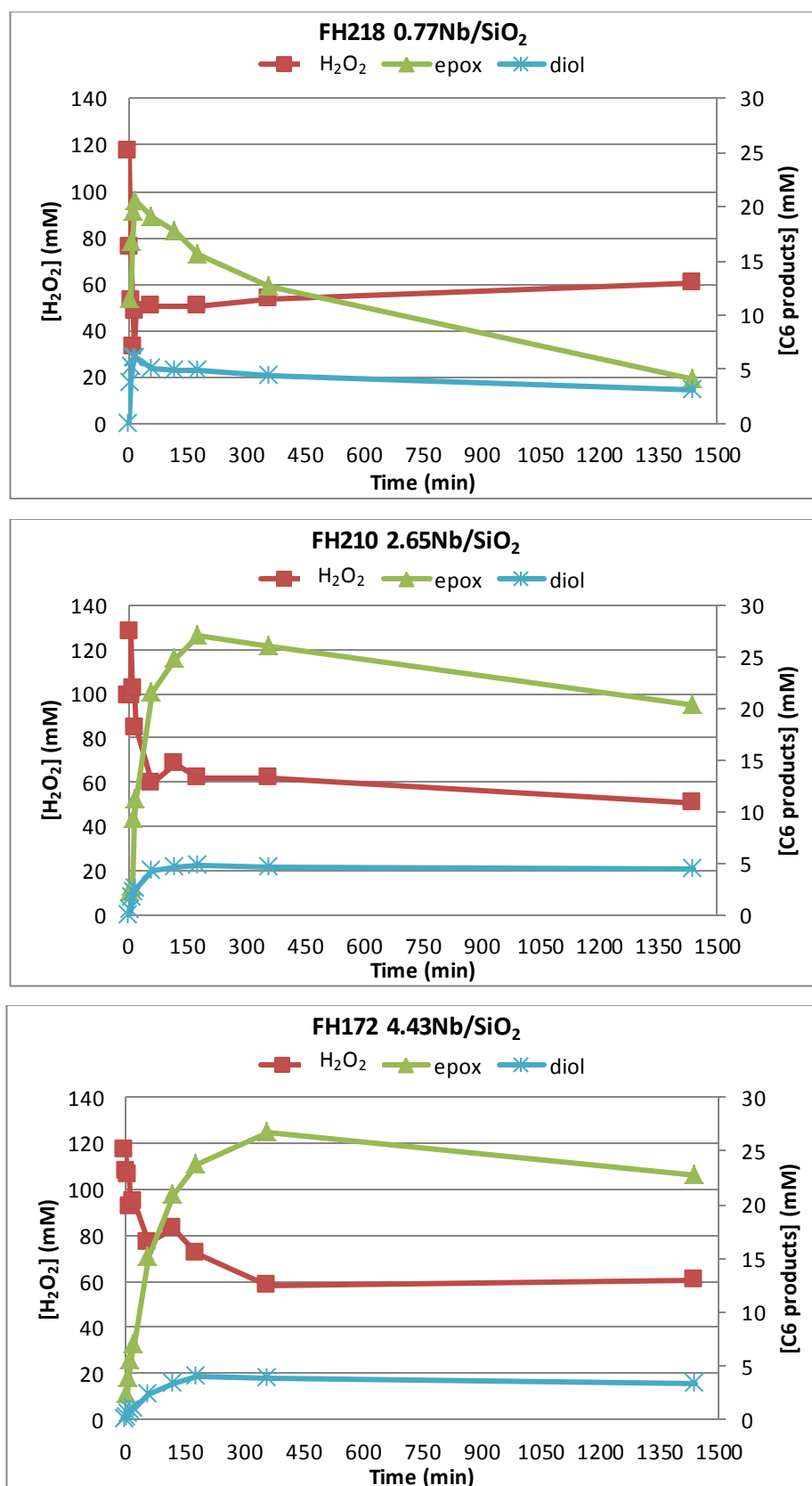
Figure 4.12. Reactions performed with catalysts supported on non-promoted silica, molar ratio CH : Nb :

HP = 500 : 1 : 50

In the case of the low loading Nb catalyst, there is a fast formation of the epoxide which then decreases during the reaction in favor of 2-cyclohexen-1-ol. Conversely, for catalysts with higher Nb loading, the epoxide formation is slower and its concentration decrease less than in the first case. HP conversion and diol concentration are almost similar in all cases. Therefore it seems that increasing Nb coverage, it is possible to improve selectivity towards the desired epoxide by hindering the degradation pathway to the alcohol.

The following graphs (Figure 4.13) illustrate the results obtained in the same reaction conditions for catalysts supported on Na-promoted silica.
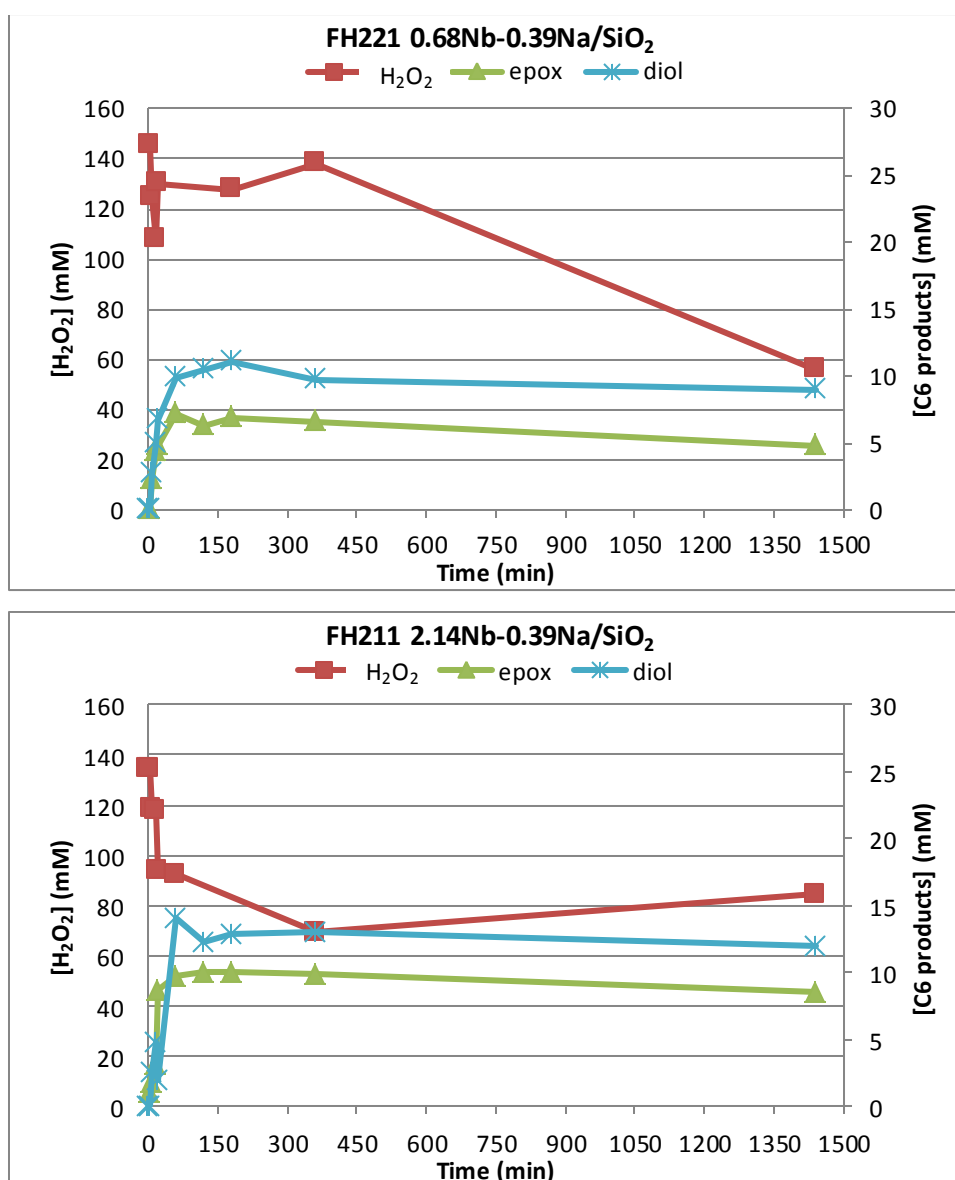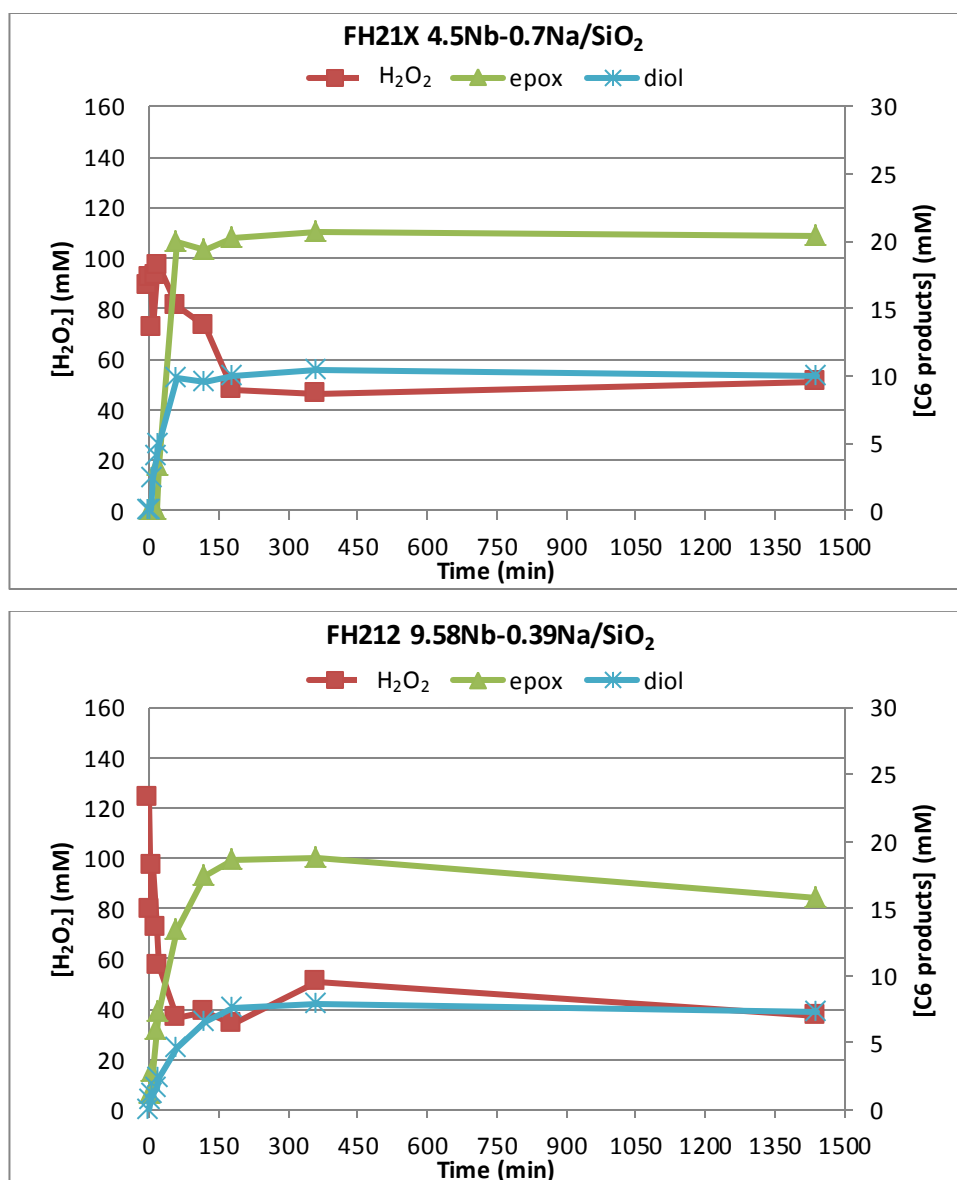
Figure 4.13. Reactions performed catalysts supported on Na-promoted silica, molar ratio CH : Nb : HP = 500 : 1 : 50

Compared with the catalysts on conventional silica of the same Nb loading (FH218 and FH210), the Na-promoted catalysts (FH 221 and FH211) produce primarily diol with less HP conversion. Additionally, the Na-promoted catalysts produce less epoxide product, but it appears to be more stable even at low loadings of Nb, in contrast to the catalysts on conventional silica. In all cases, diol and other products (2-cyclohexen-1-ol and 2-cyclohexen-1-one) concentrations are higher with Na-promoted silica.

Comparing catalysts FH21X and FH212, it seems that passing from monolayer dispersion to Nb nanoparticles, there is a slight decrease in catalyst performances for

epoxide concentrations and stabilization of this product during reaction time. Conversely, reactivity of Na-promoted catalysts changes with the increasing of Nb-loanding and surface coverage.

Thus it is possible to conclude that, in general, epoxide yields are lower for catalysts supported on Na-promoted silica when compared with the corresponding catalysts supported on conventional SiO_2, and the presence of Na promotes the diol formation.

Afterwards, it was decided to investigate the stability of the catalysts and focus the research on the effect of different reaction parameters in order to better understand what exactly happens on catalyst surface and explain the different reactivity observed in the presence of Na.

A leach test was conducted with catalysts with similar high Nb loading (Figure 4.14) to determine the stability of the supported metal oxide. The reaction was carried out in usual conditions (molar ratio CH : Nb : HP = 500 : 1 : 50, solvent CH_3CN, final reaction mixture volume 7.5 ml, T 75 °C, stirring 900 rpm, biphenyl as internal standard), but after 2 hours the reaction mixtures were hot-filtered and reloaded in the reaction tube without the catalysts for other 24 hours.

FH172 4.43Nb/SiO2

FH21X 4.5Nb-0.7Na/SiO2
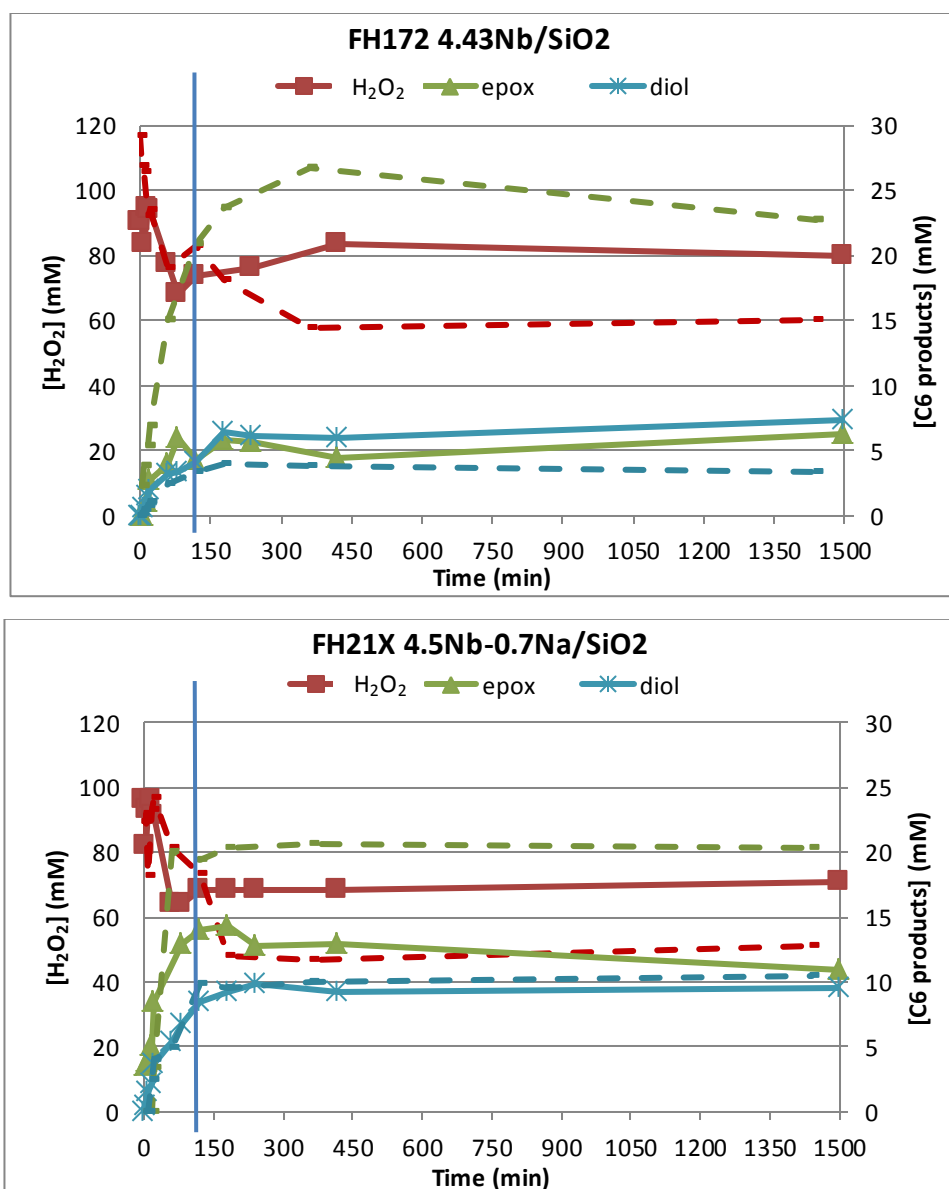
Figure 4.14. Leaching tests results (dashed lines refer to reactions without hot filtration)

HP concentration does not vary after mixture reload and product concentrations remain stable. In all cases, epoxide concentrations do not reach the ones obtained in normal conditions (dashed lines), while diol concentrations almost remain constant previously tests after 24 hours.

Therefore there is no leaching of the active phase and the catalysts are really heterogeneous.

Afterwards, reactions starting from different CH and HP concentrations were done, maintaining constant other reaction parameters and catalysts amount (Figures 4.15 and 4.16). High Nb loading catalysts, with and without Na, were tested, and the effect of

102

H_2O_2

variation of initial concentrations was studied on the basis of the initial rate of the reaction after 20 minutes (Table 4.2).

The initial rate was calculated as: ([epox] + [diol]) / time.

Catalysts characteristics						
Type of Nb loading	Catalyst name	Nb loading (wt%)	Na loading (wt%)	Coverage (Nb/nm^2)	Nb dispersion state	Initial rate (mmol product * L^{-1} * min^{-1})
Without Na						
Low	FH218	0,77		0,2	2D	2,359
High	FH210	2,65		0,8	2D	0,7148
Above	FH172	4,43		1,6	3D Nanoparticles	0,4124
With Na						
Low	FH221	0,68	0,39	0,2	2D	0,5808
High	FH211	2,14	0,39	0,8	2D	0,5079
Very High	FH21X	4,5	0,7	2,2	2D	0,345
Above	FH212	9,58	0,391	3,6	3D Nanoparticles	0,4704

Table 4.2. Initial rates of CH epoxidation after 20 minutes
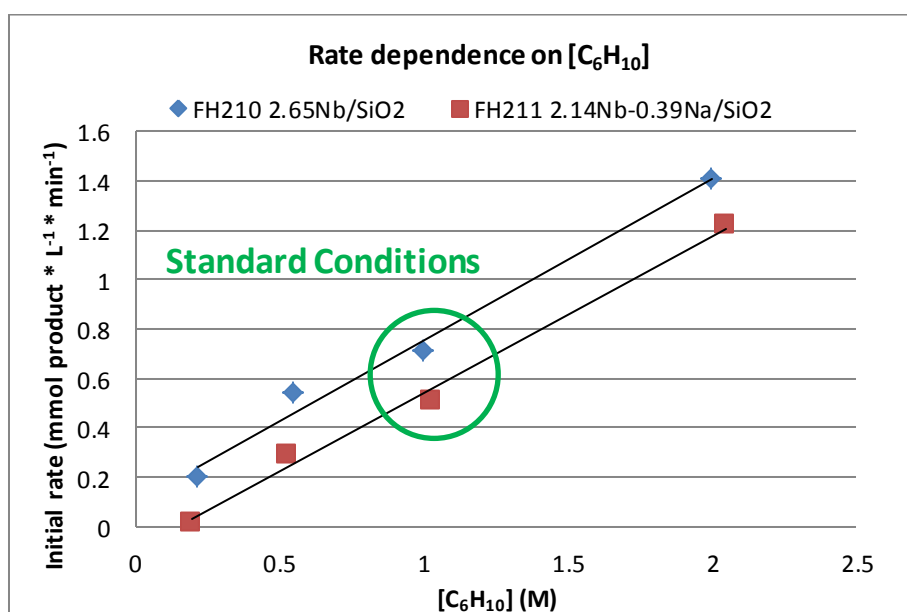
Figure 4.15. Effect of initial CH concentration on initial rate
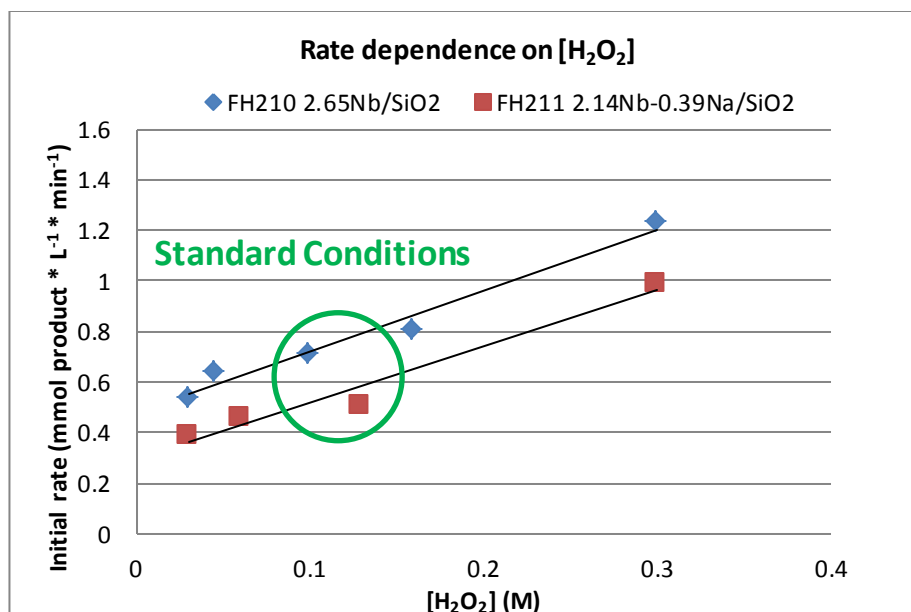
Figure 4.16. Effect of initial HP concentration on initial rate

Both for CH and HP variation, the initial rates increase with the increase of concentration, indicating a typical trend for an Adsorption-Limited Reaction in the range of concentrations investigated. Also in this case, it is clear the higher activity of Na-free catalysts respect the corresponding ones supported on Na-promoted silica.

Then the effect of Nb loading and coverage was studied, comparing the initial turn over frequencies (i-TOF) of the reactions performed in standard conditions (Table 4.3, Figures 4.17 and 4.18). The i-TOF was calculated as: $(n_{epox} + n_{diol}) / (time * n_{Nb})$

Catalyst characteristics						
Type of Nb loading	Catalyst name	Nb loanding (wt%)	Na loading (wt%)	Coverage (Nb/nm^2)	Nb dispersion state	i-TOF [mol$_{products}$ / (min*mol Nb)]
Without Na						
Low	FH218	0,77		0,2	2D	1,1515
High	FH210	2,65		0,8	2D	0,3543
Above	FH172	4,43		1,6	3D Nanoparticles	0,1995
With Na						
Low	FH221	0,68	0,39	0,2	2D	0,2855
High	FH211	2,14	0,39	0,8	2D	0,251
Very High	FH21X	4,5	0,7	2,2	2D	0,1695
Above	FH213	9,58	0,391	3,6	3D Nanoparticles	0,2329

Table 4.3. Initial Turn Over Frequencies (i-TOF) of the studied catalysts
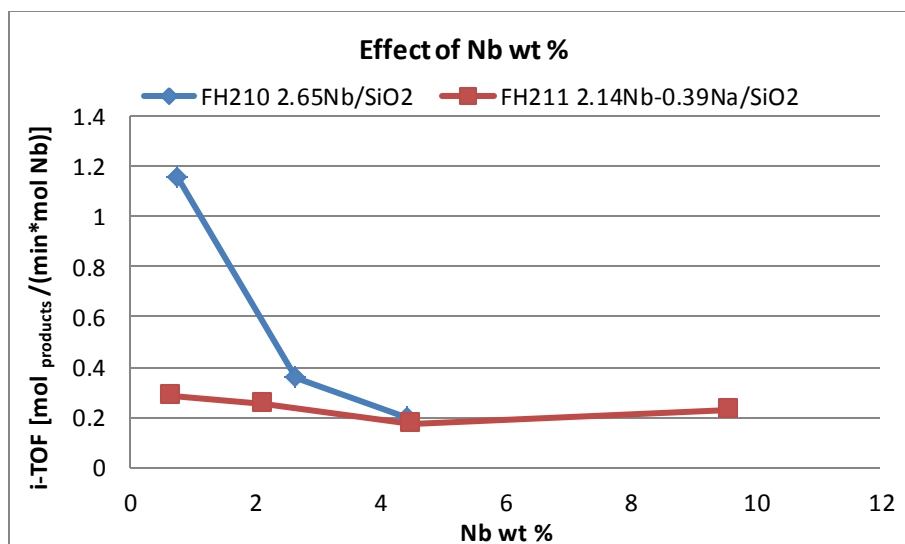
Figure 4.17. Effect of Nb wt% on i-TOF
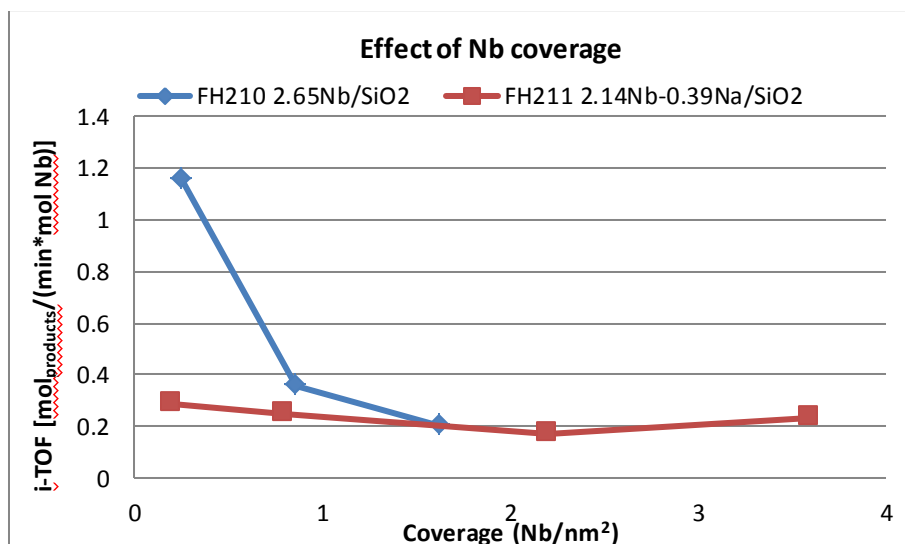
Figure 4.18. Effect of Nb coverage on i-TOF

What can be easily seen is that the presence of Na strongly affects the Nb-reactivity, drastically lowering it, regardless the Nb-loading. It is quite evident that Na has a detrimental effect on the CH epoxidation reaction.

Low loadings of 2D species are better because they are faster and more selective during short reaction times. However, the higher loading, and even nanoparticles catalysts do not degrade useful products during the course of the reaction studied.

Finally, the HP decomposition was study deeply. Reactions with conventional silica and Na-promoted silica were performed, using a mass of support equal to the corresponding mass of catalyst (Figure 4.19).
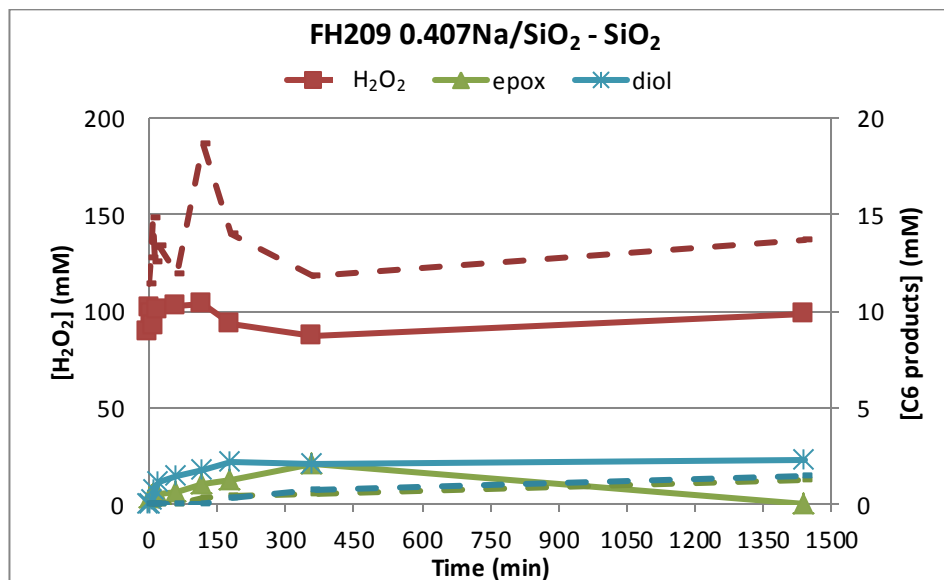
Figure 4.19. Reaction carried out with promoted silica (continue lines) and conventional silica (dashed lines)

In both cases, HP concentrations remained almost constant during the reaction, and the small amounts of epoxide and diol present in the reaction without Nb could be attributed to the oxygen from the air normally present in the reaction tube. Thus, the supports are not responsible for HP decomposition.

Afterwards, reaction without CH were done using FH218 and FH221 catalysts (without and with Na-promoted silica), under the same standard reaction conditions (Figures 4.20 and 4.21).
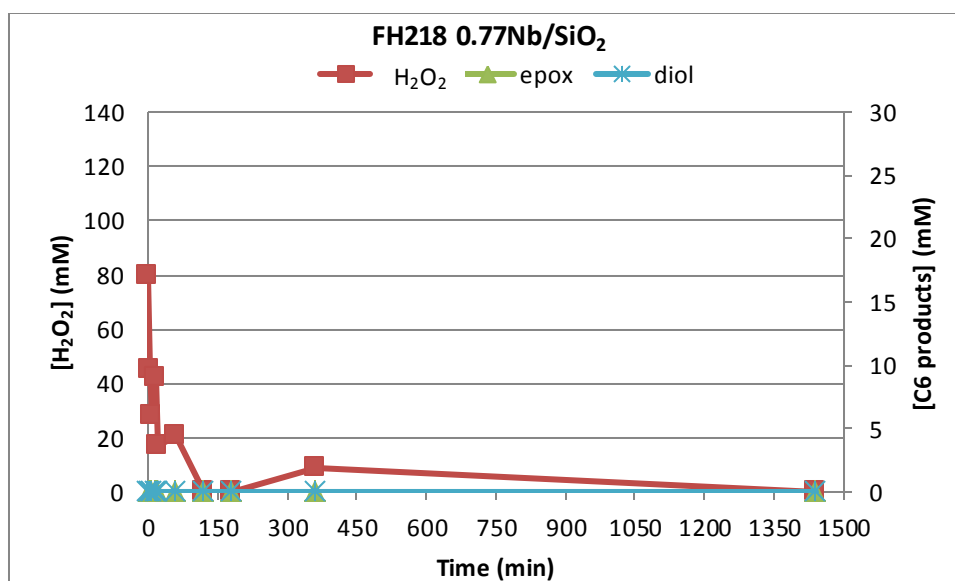
Figure 4.20. Reaction performed with catalyst supported on normal silica, without CH
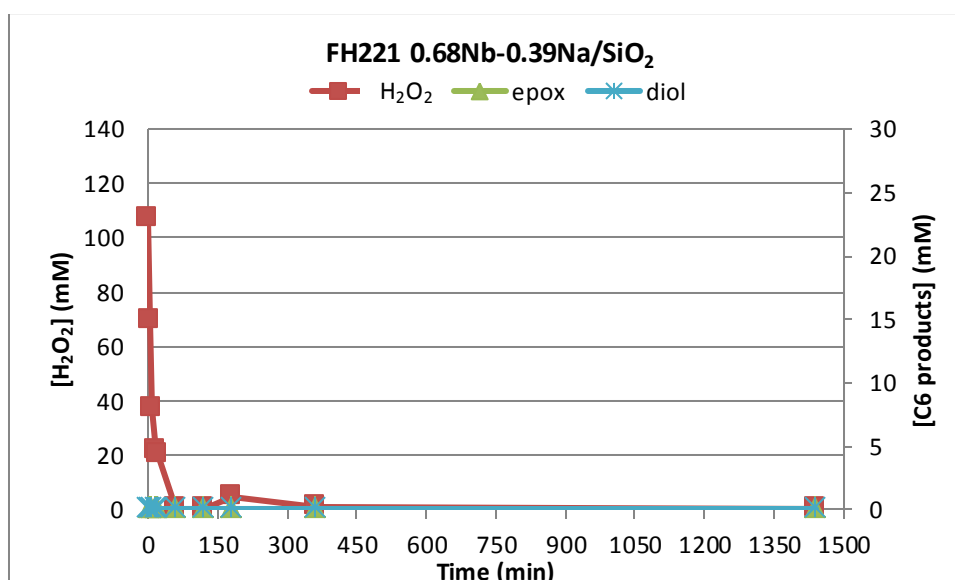
Figure 4.21. Reaction performed with catalyst supported on Na-promoted silica, without CH

These tests without CH, gave a complete HP consumption in less than 2 hours. Therefore, it is possible to speculate a fast HP decomposition by Nb species if there is not substrate to react with, but during "usual" reactions, only 60-70 % of HP conversion was observed. This could be a sign of two possible processes occuring: competition between HP and CH for the same active sites, or deactivation of the catalysts by products.

To investigate this aspect further, a reaction was carried out following the usual conditions, but after 6 hours, a second addition of HP was done using the same amount of HP added at the beginning of the reaction (Figure 4.22). The initial rates of the reactions were calculated for the first and the second addition of HP (Figure 4.23).
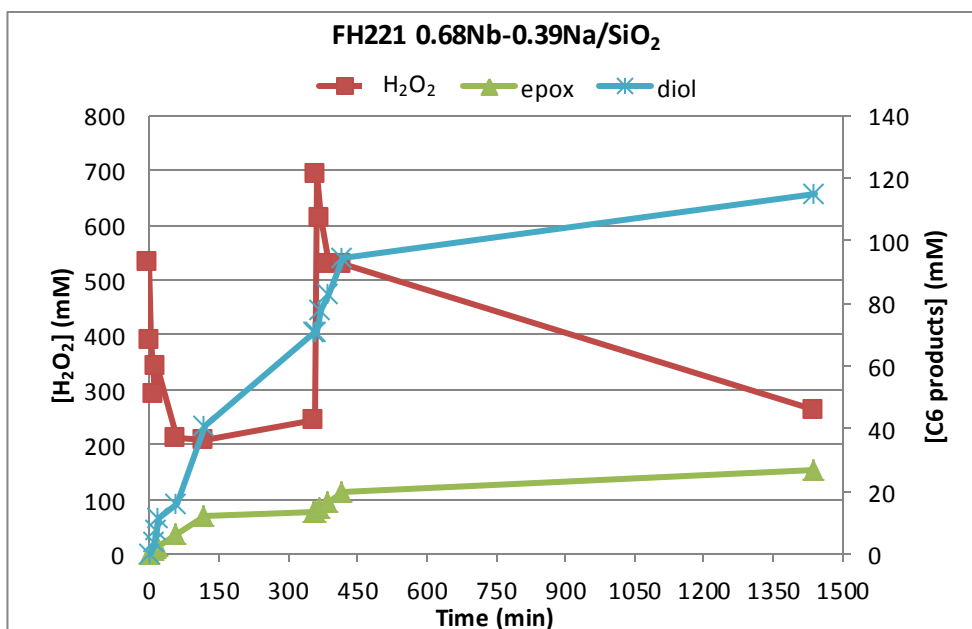
Figure 4.22. Reaction with two additions of HP
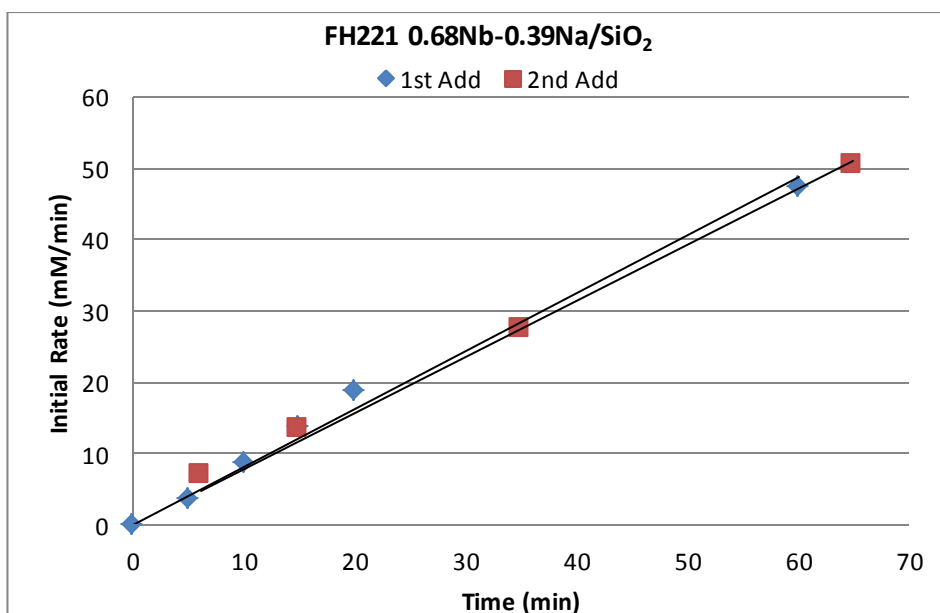
Figure 4.23. Comparison of Initial rates after the two additions of HP

After the second addition of HP, the reaction proceeded with the same initial rate reached after the first addition:

1st Initial Rate: 0.81 mM/min

2nd Initial Rate: 0.78 mM/min

Therefore, it likely that the oxidant competes with CH for the Nb active sites of the catalyst.

4.4 Conclusions and outlooks

Results show that the dispersion of niobium oxide on the silica surface is very important for catalyst performance. The impregnation of the catalyst with Na has a negative effect on the CH epoxidation reaction: it gives lower cyclohexane epoxide yields and promotes the formation of 1,2-cyclohexanediol compare to Na-free catalysts. Sodium strongly affects the Nb- reactivity, regardless the Nb-loading. In general, in Na-free catalysts, the monomeric species are much more active and selective to main reactions products (epoxide and diol) than polymeric species and particles, contrary to what previously reported in the literature for ODHP reaction[19].

The reaction seems to be rate-limited by reactant adsorption phenomena and HP likely competes with CH for Nb-active sites.
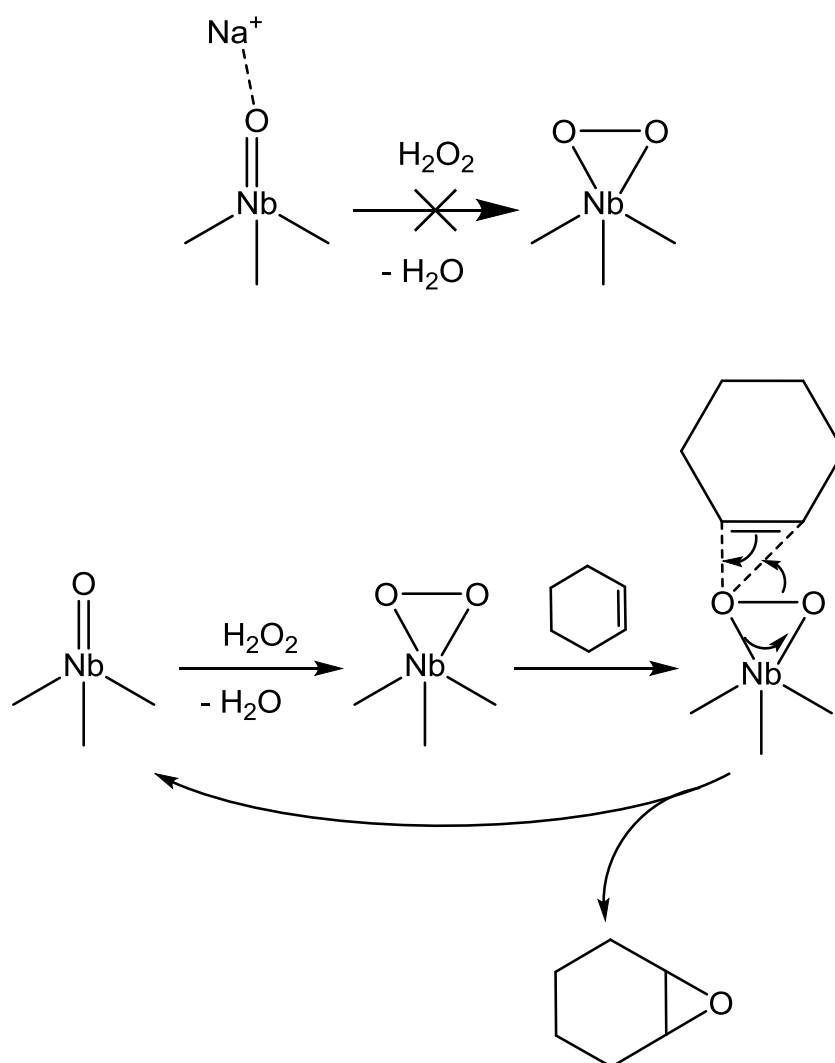
Figure 4.25. Possible reaction mechanism for Na-promoted silica catalysts and Na-free catalysts

Future work could be focused on deeper investigation of what is occurring on the catalyst surface during CH epoxidation; in Figure 4.25 are presented two possible hypotheses for catalysts with and without Na-promoted silica. It could be useful perform: diffuse reflectance IR spectroscopy (DRIFTS) experiments to study cyclohexene adsorption, and solid-state ^{93}Nb NMR to understand the specific Na effect on the catalysts performances.

4.5 Acknowledgments

I would like to thank Prof. Ive Hermans from University of Wisconsin – Madison, who allowed me to study and work in his laboratories. It was a really interesting and productive research experience.

Thank you also to Dr. Alessandro Chieregato, my personal guide in the laboratory; thank you for your important help.

Thanks to Prof. Carlos A. Carrero, Joseph T. Grant and Fangying Huang for preparing and characterizing the catalysts and explaining everything about them to me.

I would like to thank Sarah Specht, my desk neighbor and research colleague, always ready to help me and answer my questions with a smile.

And finally, thank you to all the members of the research group for making me feel at home in your beautiful workplace.

4.6 References

(1)   Sienel, G.; Rieth, R.; Rowbottom, K. T. In *Ullmann's Encyclopedia of Industrial Chemistry*; Wiley-VCH Verlag GmbH & Co. KGaA, Ed.; Wiley-VCH Verlag GmbH & Co. KGaA: Weinheim, Germany, 2000.

(2)   Grigoropoulou, G.; Clark, J. H.; Elings, J. A. *Green Chem.* **2003**, *5* (1), 1–7.

(3)   Iizuka, T.; Ogasawara, K.; Tanabe, K. *Bull Chem Soc Jpn* **1983**, *56*, 2927–2931.

(4)   Jehng, J. M.; Wachs, I. E. *Catal. Today* **1990**, *8*, 37–55.

(5)   Ziolek, M.; Decyk, P.; Sobczak, I.; Trejda, M.; Florek, J.; Klimas, H. G. W.; Wojtaszek, A. *Appl. Catal. Gen.* **2011**, *391* (1–2), 194–204.

(6)   Nowak, I.; Ziolek, M. *Chem. Rev.* **1999**, *99* (12), 3603–3624.

(7)   Ziolek, M. *Catal. Today* **2003**, *78* (1), 47–64.

(8)   Ziolek, M.; Sobczak, I.; Lewandowska, A.; Nowak, I.; Decyk, P.; Renn, M.; Jankowska, B. *Catal. Today* **2001**, *70* (1), 169–181.

(9)   Thornburg, N. E.; Thompson, A. B.; Notestein, J. M. *ACS Catal.* **2015**, *5* (9), 5077–5088.

(10)   Kilos, B.; Nowak, I.; Ziolek, M.; Tuel, A.; Volta, J. C. *Stud. Surf. Sci. Catal.* **2005**, *158*, 1461.

(11)   Trejda, M.; Tuel, A.; Kujawa, J.; Kilos, B.; Ziolek, M. *Microporous Mesoporous Mater.* **2008**, *110* (2–3), 271–278.

(12)   Tiozzo, C.; Bisio, C.; Carniato, F.; Gallo, A.; Scott, S. L.; Psaro, R.; Guidotti, M. *Phys. Chem. Chem. Phys.* **2013**, *15* (32), 13354.

(13)   Gallo, A.; Tiozzo, C.; Psaro, R.; Carniato, F.; Guidotti, M. *J. Catal.* **2013**, *298*, 77–83.

(14)   Arends, I.; Sheldon, R. A. *Appl. Catal. Gen.* **2001**, *212* (1), 175–187.

(15)   Wattimena, F.; Wulff, H. P. A process for epoxidizing olefins with organic hydroperoxides. GB1249079, 1971.

(16)   Thomas, J. M.; Raja, R.; Lewis, D. W. *Angew. Chem. Int. Ed.* **2005**, *44* (40), 6456–6482.

(17)   Tian, H.; Ross, E. I.; Wachs, I. E. *J. Phys. Chem. B* **2006**, *110* (19), 9593–9600.

(18)   Russell, A.; Stokes, J. *J Ind Eng Chem* **1946**, *38*, 1071–1074.

(19)   Grant, J. T.; Carrero, C. A.; Love, A. M.; Verel, R.; Hermans, I. *ACS Catal.* **2015**, *5* (10), 5787–5793.

(20)   Carrero, C. A.; Schloegl, R.; Wachs, I. E.; Schomaecker, R. *ACS Catal.* **2014**, *4* (10), 3357–3380.

(21)   Ahn, S.; Thornburg, N. E.; Li, Z.; Wang, T. C.; Gallington, L. C.; Chapman, K. W.; Notestein, J. M.; Hupp, J. T.; Farha, O. K. *Inorg. Chem.* **2016**, *55* (22), 11954–11961.

(22)   Thornburg, N. E.; Nauert, S. L.; Thompson, A. B.; Notestein, J. M. *ACS Catal.* **2016**, *6* (9), 6124–6134.

(23)   Nowak, I.; Misiewicz, M.; Ziolek, M.; Kubacka, A.; Cortés Corberán, V.; Sulikowski, B. *Appl. Catal. Gen.* **2007**, *325* (2), 328–335.

(24)   Prasetyoko, D.; Ramli, Z.; Endud, S.; Nur, H. *Adv. Mater. Sci. Eng.* **2008**, *2008*, 1–12.

(25)   Turco, R.; Aronne, A.; Carniti, P.; Gervasini, A.; Minieri, L.; Pernice, P.; Tesser, R.; Vitiello, R.; Di Serio, M. *Catal. Today* **2015**, *254*, 99–103.

(26)   Wachs, I. E. *Catal. Today* **1996**, *27* (3–4), 437–455.

(27)   Garcia Cortez, G.; Fierro, J. L. G.; Banares, M. A. *Catal. Today* **2003**, *78*, 219–228.

(28)   Lemonidou, A. A.; Nalbandian, L.; Vasalos, I. A. *Catal. Today* **2000**, *61* (1), 333–341.

(29)   Grant, J. T.; Love, A. M.; Carrero, C. A.; Huang, F.; Panger, J.; Verel, R.; Hermans, I. *Top. Catal.* **2016**, *59* (17–18), 1545–1553.

CHAPTER 5. OXIDATION OF MALTODEXTRINS AND STARCH

5.1 Introduction

5.1.1 Starch

Starch, $(C_6H_{10}O_5)$n, is a polymeric carbohydrate composed of glucose units linked with glycosidic bonds (Figure 5.1). In the food industry, it is mainly used as thickener/stabilizer, gelling agent, or as starting material for the production of sweeteners and polyols. It has also several nonfood industrial applications: production of paper and paperboard, textile sizing agent, production of ethanol and other products by fermentation. Native starch is composed by semicrystalline white water-insoluble aggregates called granules and its main sources are corn, cassava, potato and wheat. From the chemical point of view, starch is generally composed by two types of molecules: amylose and amylopectin. Amylose is a mostly linear (1,4)-α-D-glucan, while amylopectin has a branch-on-branch structure composed by shortly chains of (1,4)-linked α-D-glucopyranosyl units linked to other short linear chains via α-(1,6) branch points. Amylopectin is the main constituent, it is generally present as 70-75 wt% and it is composed of much larger molecules than amylose fraction. Each type of starch has its own particular molecular structure and sizes, amylose/amylopectin ratios and granular structure, that give it specific properties[1].
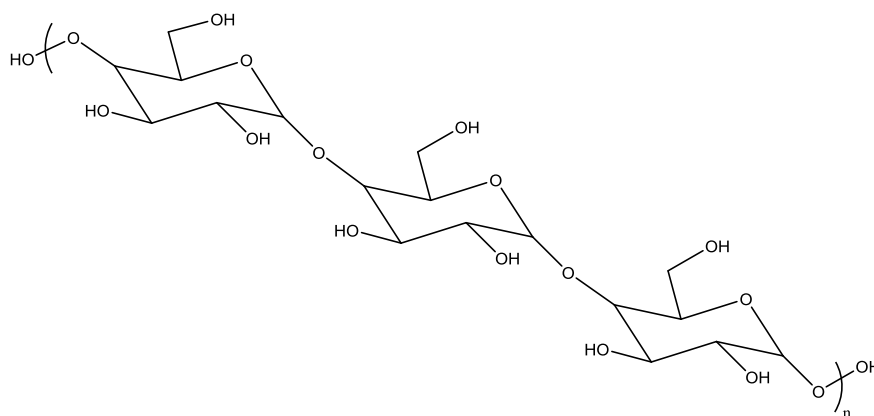
Figure 5.1. Linear segment of starch

There are different processes for starch production, for example: corn starch is obtained by wet milling that allows to separate components of the maize grains, wheat is subject to dry milling, while potato starch is separated from disintegrated potatoes after separation from juice and fiber[1].

Native starches are generally unsuitable for most application, mainly because of the formation of precipitates, microgel particles or gelation of starch paste (the irreversible loss of granular/molecular caused by thermal treatment in excess water), or because of the high viscosity of starch paste[1]. Therefore it is necessary to modify them chemically and/or physically in order to enhance some properties or minimize their defects. Physical modification are pre-gelatinization, starch granules disruption or thermal treatments. Common chemical modification are: esterification, etherification or oxidation of hydroxyl groups, chemical or enzymatic depolymerization, crosslinking of polymer chains and cationization. A particular modification can change the gelatinization temperature and pasting characteristics and stabilize the paste obtained from the cooking of a starch suspension[2].

5.1.2 Converted starch products characteristics

In starch industry, products of partial depolymerization of starch are called converted starches. These products are classified on the base of their Dextrose Equivalency (DE): it indicates the amount of reducing sugars present in the product. DE values derive from the fact that every time that the starch chain is cleaved, it generates a new aldehydic reducing end-unit, and the reducing power of converted starch can be measured. DE indicates the degree of conversion of starch to dextrose, for dextrose DE = 100, while for starch DE = 0. DE is related to the Degree of Polymerization (DP) of the product (number of D-glucosyl units of the polymer) by means of the equation: DE x DP = 100.

Converted starches can be obtain by different processes: acid attack, use of enzymes, oxidation in alkaline medium or heating treatment. The least converted starches achieved with acid treatment are called fluid starches. Extensive conversion products are maltodextrins (DP 2-20), syrup solids (DP 3-5), syrups (DP 1-3) and dextrose[1].

5.1.3 Starch oxidation

Oxidized starch is one of the most used modified starch and it is characterized by high stability, low viscosity, good fluidity, film forming and binding properties[3]. For these reasons it is used for the production of paper, building material, food, textile, founding, drilling, laundry finishing and coating industries[4,5]. In the case of pyranoside polysaccharides, the oxidation is possible at C-2, C-3 and C-6 hydroxyl position giving carbonyl and carboxyl groups; in particular, oxidation of C2 and C3 gives oxidative scission of 1,2-diols and excessive oxidation can cause undesired depolymerization of oxidized starch[6] (Figure 5.2). Therefore, important parameters used to evaluate the level of oxidation are the carboxyl and carbonyl contents and the degree of degradation[7–9].
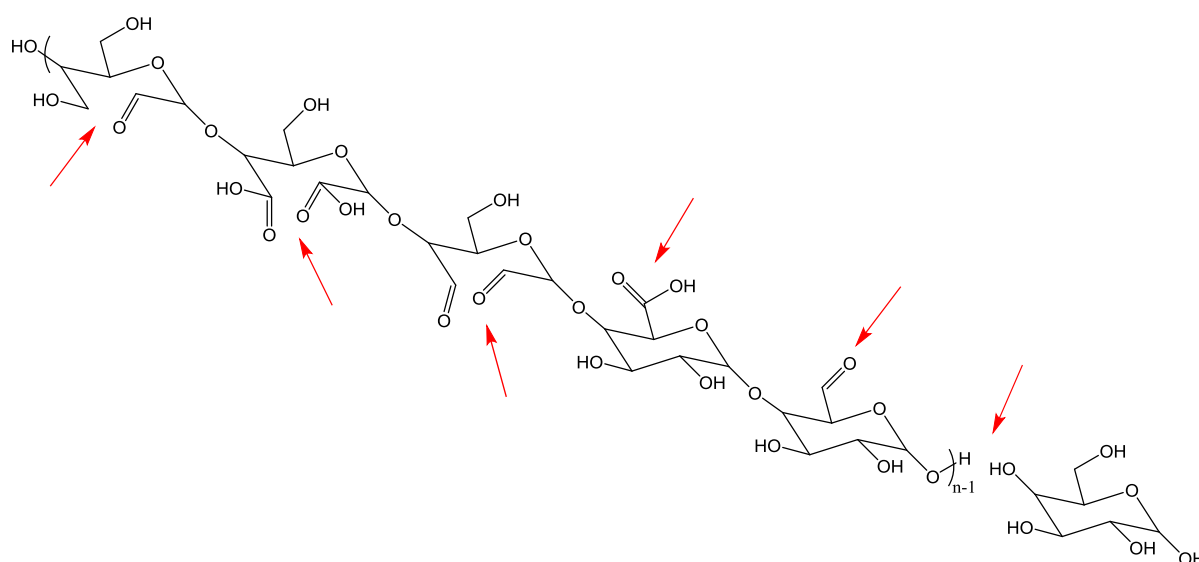
Figure 5.2. Example of starch oxidation in different chain position

The oxidation can be done with different oxidizing agents, the most used are: hydrogen peroxide[9–13], sodium hypochlorite[9,14,15], ozone[9,16–18], periodate, nitrogen dioxide or others inorganic oxidants[14,19–26] Periodates, nitrogen dioxide and other inorganic oxidants present drawbacks due to the cost of plant construction and safety (as in the case of HNO_3 as oxidant), downstream purification and gaseous effluents abatement (especially for the coproduction of NO_x). Sodium hypochlorite is one of the oldest starch oxidation agent, mainly used in paper industry to produce oxidized starch with

better mechanical and film-forming properties for paper. This method is the most used because of good availability of NaClO and well-known effect on starch properties, but during the reaction, it coproduces gaseous chlorine. Hydrogen peroxide is less used than NaClO, it does not produce dangerous by-products but it only decomposes into oxygen and water. Both NaClO and H_2O_2, generate wastewater and could leave undesired residues in food products. Ozone presents the advantage that it needs less downstream purification processes, it only releases oxygen, but its use is limited industrially because of its cost[9].

In order to obtain high degree of oxidation at the C6 carbon, limit the C2-C3 cleavage and avoid depolymerization of oxidized starch (which reduce the amount of final solid product), moderate oxidants are needed. Taking into account also the sustainability of the process from the economic and environmental point of view, air and oxygen are very desirable alternatives. In the literature there are only few examples of starch oxidation with these gaseous oxidants. Homogeneous copper[27] and vanadium[28] have been tested as catalysts for oxidation with oxygen, but in all cases the metals gave problems of separation from the oxidized product. Recently, Chen et al[29] reported the aerobic oxidation of starch with Co-V polyoxometalates providing an efficient method of separation of the soluble catalyst.

Sheng et al[30] reported the oxidation of starch without catalyst in the presence of a base, but they obtained a big amount of water soluble oxidized products.

In conclusion, it is of great interest the investigation of alternative processes involving oxygen or air as oxidant with heterogeneous catalysts or homogeneous systems that can be easily recovered from the final reaction mixture.

5.1.4 Aim of the work

The aim of the present work is to obtain an oxidized starch with high degree of oxidation and limited depolymerization. Reagents used are either hydrogen peroxide (HP) or oxygen as oxidant, water as solvent and preferably heterogeneous catalysts.

With hydrogen peroxide, homogeneous Na_2WO_4/H_3PO_4 system was tested, while with oxygen, Pt/C 3 wt%, Au/TiO$_2$ 1.5 wt%, Ru/Al$_2$O$_3$ 5 wt%, Pd/TiO$_2$ 1.5 wt%, and alumina spheres supported catalysts (Pt 4 wt%, Au 3 wt% and Ru 3 wt%) have been prepared.

These metals have been chosen because they are typical active species for alcohols oxidation[31].

Reaction results were evaluated on the base of degree of product oxidation, weight of final solid product and calcium binding properties. In particular, the feasibility of the heterogeneous oxidation of starch was initially checked using maltodextrin as model for further process optimization.

5.2 Experimental

5.2.1 Reaction feedstock

The following substrates were used:

- MD18: maltodextrin, DE 18.4

- MD15: maltodextrin, DE 13.9

- MD10: maltodextrin, DE 9.8

- Maize starch

Feedstock MD 18 was used as reference, then MD 15 and MD 10 were tested for comparison.

Finally also Maize starch was oxidized in order to obtain better product characteristics.

In all cases, the number of moles of the investigated substrate were calculated taking into account the molar weight of the anhydroglucose unit: 170 g/mol.

5.2.2 Catalysts preparation

5.2.2.1 Pt/C 3 wt%

The catalyst was prepared by Wet Impregnation of a solution of H_2PtCl_6 on the carbon support (Extruded Norit RX 1,5 EXTRA, pelletized before use, mesh 30-60).
Then it was reduced with H_2 for 3 hours at 350 °C (H_2 flow: 60 ml/min).

5.2.2.2 Au/TiO₂ 1,5 wt%

The catalysts was prepared by impregnating the support with a suspension of gold nanoparticles (for details, see Chapter 2.2.1). The support was titanium oxide Cristal Activ DT-51. The suspension was synthesized reducing $HAuCl_4$ with glucose in basic aqueous medium and using PVP (polyvinylpyrrolidone) as stabilizer at 95 °C for 2.5 minutes.

The metal was deposited on the support by Incipient Wetness Impregnation of the suspension. Finally, the catalyst was washed with boiling water for 30 minutes and calcined at 300 °C for 3 hours.

5.2.2.3 Ru/Al$_2$O$_3$ 5 wt%

Ru/Al$_2$O$_3$ 5 wt% was synthesized by Wet Impregnation of a solution of RuCl$_3$·xH$_2$O in basic aqueous medium on calcined γ-Al$_2$O$_3$ (BASF). After 24 hours of stirring, the catalyst was filtered, washed with H$_2$O and dried at 120 °C.

5.2.2.4 Pd/TiO$_2$ 1.5 wt%

The catalysts was prepared by impregnating the support (titanium oxide Cristal Activ DT-51) with a suspension of platinum nanoparticles, following the same procedure as for Au/TiO$_2$ catalyst. The suspension was synthesized reducing PdCl$_2$ with glucose in basic aqueous medium and using PVP (polyvinylpyrrolidone) as stabilizer at 95 °C for 2.5 minutes.

The metal was deposited on the support by Incipient Wetness Impregnation of the suspension. Finally, the catalyst was washed with boiling water for 30 minutes and calcined at 300 °C for 3 hours.

5.2.2.5 Catalysts with Alumina spheres support

Three different catalysts supported on alumina spheres (provided by Saint-Gobain NorPro), were synthesized:

- Pt/Al$_2$O$_3$ 4 wt%
- Au/Al$_2$O$_3$ 3 wt%
- Ru/Al$_2$O$_3$ 3 wt%

The Platinum catalyst was prepared by Wet Impregnation of a H$_2$PtCl$_6$ aqueous solution. The solid was then dried and reduced with H$_2$ for 3 hours at 350 °C (H$_2$ flow: 60 ml/min).

Au/Al$_2$O$_3$ was prepared by Deposition-Precipitation of HAuCl$_4$ at pH 7, for 3 hours at 80 °C. The catalyst was then washed with H$_2$O, dried and calcined at 400 °C for 2 hours.

The supported Ru catalyst was made following the same procedure used for Ru/Al$_2$O$_3$ 5 wt%, reported above.

5.2.3 Catalytic Measurements with Hydrogen Peroxide

Catalytic tests were first carried out using MD18 as the substrate.

It has been decided to start the research trying to replicate the same reaction conditions of experiments reported by Floor and co-workers[13] . They oxidized maltodextrins and starch with the aqueous system tungstate-hydrogen peroxide (HP).

Reactions were performed in a 100 ml three-necked flask equipped with a thermometer, a vapor condenser and a dropping funnel. Stirring and heating were provided by a magnetic stirrer and a silicon oil bath on heating plate.

Typical reaction conditions were:

- Molar ratio MD18 : **HP** : $Na_2WO_4 \cdot 2\ H_2O$: $\underline{H_3PO_4}$ = 1 : **4** : *0,034* : <u>0,02</u>

- HCl added until pH 2

- Typical amounts:

  - MD18 = 10,00 g

  - H_2O = 20 ml

  - HP = 21 ml

  - $Na_2WO_4 \cdot 2\ H_2O$ = 0,66 g

  - H_3PO_4 = 0,08 ml

  - HCl = 2-3 drops

- Reaction time 3 h

First maltodextrin was dissolved in water, then $Na_2WO_4 \cdot 2\ H_2O$, H_3PO_4 was added with HCl until pH 2. The flask was heated under stirring and when the temperature reached the desired value, HP was dropped inside (1 drop / 6 sec) and this point was taken as time zero of the reaction.

With respect to the method reported in the paper used as reference, there were some differences in the procedure:

no control of the pH during the reaction,

no check of the HP consumption,

the reaction was stopped before total HP conversion.

5.2.4 Catalytic Tests with Oxygen: Batch Reactor

Tests with oxygen as the oxidant were conducted in a batch autoclave reactor introducing in the vessel the substrate MD18 (30 wt% of the mixture), the catalyst, a base or an acid if needed and the solvent (H_2O, 30 ml). The reactor was then closed and the atmosphere of the reactor was rinsed with oxygen before filling the autoclave with the desired oxygen pressure. Stirring was provided by a rotor and the heating by a heating mantle.

The reaction time started when the desired temperature was reached.

After the reaction, the autoclave was cooled down to room temperature, then oxygen was vented and the reaction mixture was separated from the catalyst by centrifugation.

5.2.5 Catalytic Tests with Oxygen: Semibatch Reactor

In order to check whether it were possible to improve the results of the reaction by facilitating the mass transfer of oxygen, reactions using a different reactor configuration were performed, with a semibatch autoclave (volume 100 ml, heated with a silicone oil bath and provided with a vapor condenser, see Chapter 2.2.3) in which the gaseous phase flew continuously under pressure through the reaction mixture.

The concentrations of reactants in the mixture were : temperature 70 °C, oxygen flow 100 ml/min, pressure 4 bar, 3 h of reaction.

5.2.6 Treatment of the Reaction Mixture

At the end of the reaction, reaction mixtures were treated as follows:
cool the system down to room temperature,

- correct the pH to 9-10 with NaOH,
- precipitate the product as Na^+ salt slowly adding the reaction mixture to two volumes of MeOH under vigorous stirring,
- filter the precipitate,
- drying at room temperature for 2-3 days,
- store at 5 °C.

Compared to the recipe reported in the paper used as reference, there were some differences:

- the mixture was not diluted with H_2O before precipitation,

- the solid product was not freeze-dried. In other papers, the product is dried under reduced pressure at 50 °C, but this treatment caused the formation of a dense brown liquid with our products, already at 30 °C.

5.2.7 Analysis of the products

5.2.7.1 Degree of Oxidation

The easier technique to define the degree of oxidation is the acid-base titration of the carboxylic groups of the product. A method derived from different procedures described in the literature was adopted. At the end of the reaction mixture treatment, a white solid was obtained after the precipitation of the products with NaOH and MeOH. In order to determine the exact amount of –COOH groups, all the carboxylic groups must be in the same form: either protonated or de-protonated. Therefore, the solid was first solubilized in water and the aqueous solution was then passed through an H^+ ion exchange column in order to have the total free acid form of the product[32,33]. An H^+ ion exchange column was prepared in a 25 ml burette filled first with 10 cm of small glass spheres in correspondence of the restriction, then with 15 g of Amberlite IR-120H (plus) suspended in distilled water.

Before each analysis, the column has been regenerated with 100 ml of HCl 1 M (flow 4-5 ml/min) and washed with 100 ml of distilled water (checking the neutrality of the outgoing water).

0,5 g of oxidized product were dissolved in 25 ml of distilled water. Then the solution was passed through the resin with a flow rate of 4-5 ml/min and the column was washed with 100 ml of distilled water.

The oxidized product could hold the carboxylic groups in different parts of the molecule and moreover they could have different pKa, so they turn from the acidic to the salt form at different pH values. In this case it could be difficult to see a well-defined titration end-point during direct addition of NaOH. For this reason a back-titration was performed (similar to that one reported by Floor et al.[13]) adding 0,2 g of NaOH to the

solution and leaving it under stirring for 10 min. We titrated the solution with HCl 0.25 M detecting the end point with a pH-meter and phenolphthalein as indicator.

5.2.7.2 Complexing Properties

The calcium-binding capacity of the product was determined using a Ca^{2+} ion selective electrode (ISE) in combination with an Ag/AgCl reference electrode[34,35].

The electrode was calibrated with aqueous solutions of $CaCl_2$ (10^{-2} M; 10^{-3} M; 10^{-4} M; 10^{-5} M; 10^{-6} M) containing an ionic strength buffer (KCl 3 M added in order to have a final concentrations of 2 % v/v) at pH 11 (with a solution of KOH 0.1 M). Titrations were followed with a Ca^{2+} ISE and Ag/AgCl electrode: 2 g of sample were dissolved in 100 ml of distilled water and used as titrant of a 100 ml solution containing 40 mg of Ca^{2+}, 2 % v/v of ionic strength buffer (KCl 3 M) and keeping the pH constant at 11 with a solution of KOH 0.1 M.

The calcium-binding ability is defined as the number of mg of Ca^{2+} or $CaCO_3$ sequestered by 1 g of complexant, until the concentration of the free Ca^{2+} reaches 10^{-5} M (this value is considered as the upper limit in the washing process at which no incrustation occurs)[35].

5.3 Results and Discussion of Reactivity Tests with Hydrogen Peroxide

Two experiments were performed in the same conditions as those reported in the reference paper of Floor and van Bekkum[13]. In table 5.1 are reported the results obtained in comparison to those published.

MD18 : HP molar ratio	T (°C)	Product weight (g)	mmol –COOH / g product	Results from reference paper
1 : 4	90	5.4	2.0	4.2-5.7 g 2.0-2.3 mmol/g
1 : 4	70	7.4	2.2	5.5 g 1.9 mmol/g

Table 5.1. Results obtained from experiments replicated from the reference paper.

Results obtained were consistent with the reference ones, therefore it is possible to replicate the reaction; however, in the reference paper nothing about the Ca^{2+} sequestering properties was reported.

Afterwards tests were performed in order to investigate the effect of various reaction parameters. Results are reported in the following table and figures.

Table 5.2 summarizes the results of all the catalytic tests with HP.

Substrate	HP : sub*	Na₂WO₄ : sub*	H₃PO₄ : sub*	HCl (drops)	H₂O (ml)	T (°C)	t (h)	Solid weight (g)	mmol COOH / g product	SC mg Ca / g product	Note
MD18	4	0.034	0.02	2	0	70	3	7.4	1.75	9.3	
MD18	4	0.034	0.02	2	0	50	3	7.0	1.15	10.9	
MD18	2	0.034	0.02	2	10.5	90	3	8.5	1.81	5.3	
MD18	3	0.034	0.02	2	5.2	90	3	6.9	2.02	4.7	
MD18	3	0.034	0.02	3	5	70	3	8.4	1.87	5.6	
MD18	4	0.034	0.02	2	0	90	7	8.5	2.96	7.6	
MD18	4	0.034	0.02	0	0	30	24	7.4	1.34	7.5	
MD18	4	0.034	0.02	3	20	90	3	7.3	2.14	11.6	
MD18	4	0	-	0	20	90	3	3.8	0.19	2.4	
MD18	4	0	-	4	20	90	3	5.7	0.32	2.7	
MD18	4	-	-	KOH until pH 10	20	90	3	4.5	0.30	2.2	
MD18	4	-	-	KOH until pH 10	20	90	3	4.4	0.19	2.7	pH control every 30 min
MD10	4	0.034	0.02	6	20	90	3	9.0	1.52	8.7	
MD15	4	0.034	0.02	6	20	90	3	6.1	1.60	7.7	

*Table 5.2. Results of catalytic tests with HP (yellow and orange boxes highlight the best results). *: molar ratio*

The influence of the pH was investigated in the oxidation of MD18 with HP and without catalyst (Figure 5.3). The increase of the basicity of the mixture caused a slight decrease of Ca^{2+} SC while it had not a strong influence on the number of –COOH groups. An exception was the reaction conducted at pH 10 with a continuous control of the pH, which was maintained constant with dropping of a NaOH solution, while in previous cases the pH decreased during the reaction.
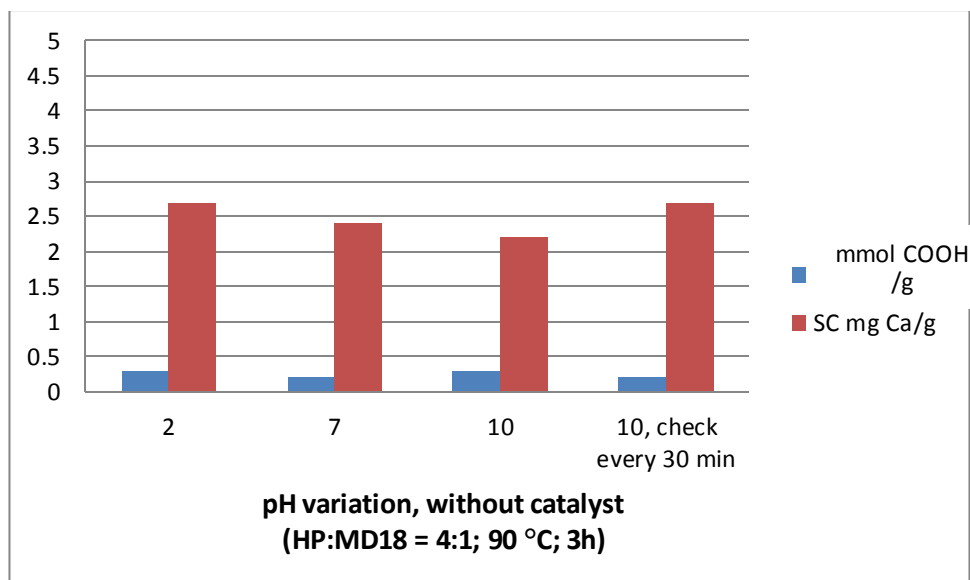
Figure 5.3. Tests with MD18 and HP without catalyst at different pH.

Subsequently, tests with different HP : MD18 molar ratios were carried out (Figure 5.4). The decrease of the HP seemed not to affect the number of carboxylic groups, but the influence was important on the Ca^{2+} SC. This could be due to the formation of slight depolymerization products which could be able to better coordinate the Ca^{2+} ions. Thus the best HP : MD18 molar ratio was 4 : 1.
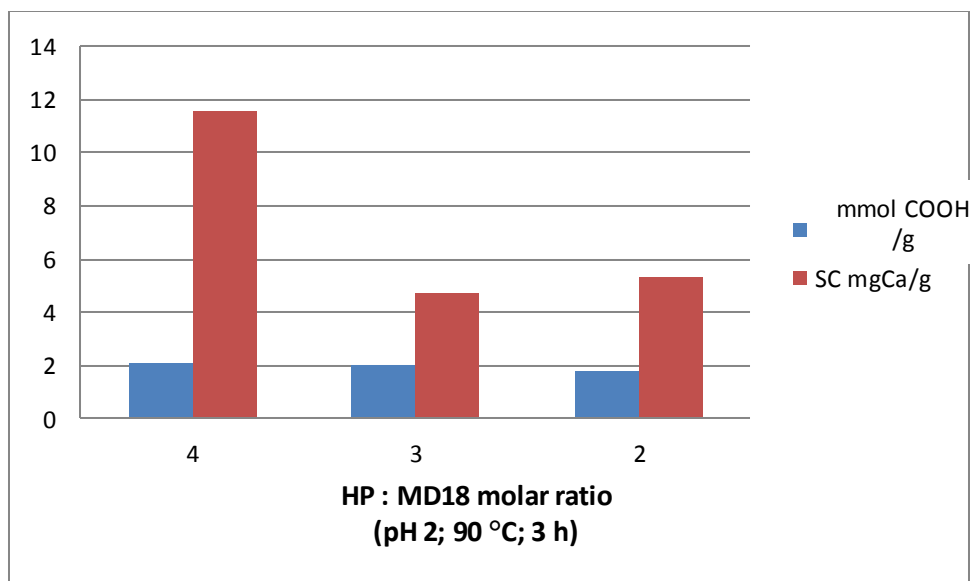
Figure 5.4. Tests with MD18 and HP with different HP:MD18 molar ratio.

The role of temperature was then investigated (Figure 5.5): a decrease of the number of carboxylic groups was shown along with a decrease of the temperature, but the Ca^{2+} SC was not affected so much by this parameter.
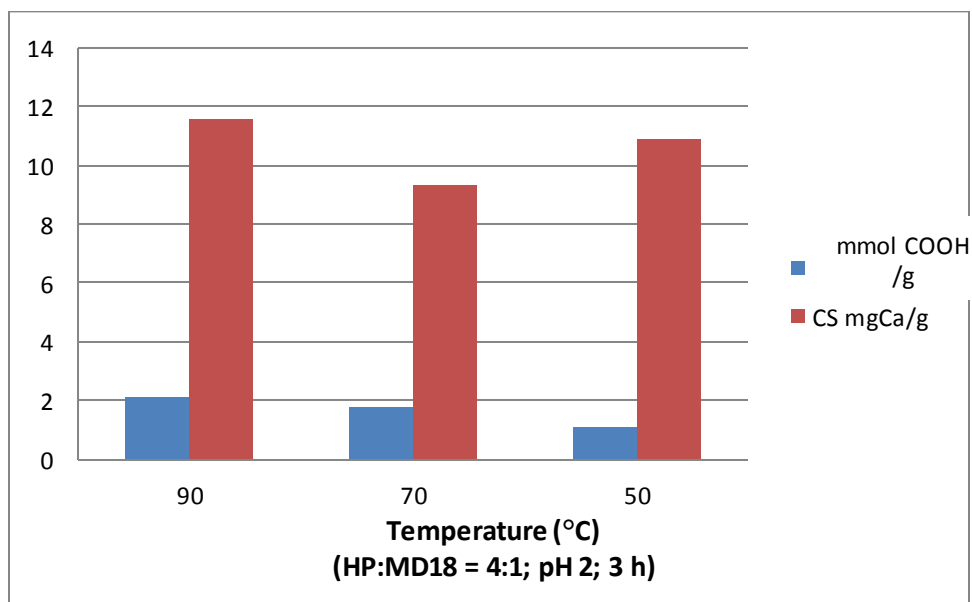
Figure 5.5. Tests with MD18 and HP at different temperatures.

The characteristics of the products were studied in function of the reaction time (Figure 5.6) and a worsening of the number of carboxylic groups was observed for prolonged

reaction times (24 h), and a decrease of and Ca^{2+} SC was shown as well after 3 h, probably due to the progressive break and/or overoxidation of maltodextrins chains.

Figure 5.6. Tests with MD18 and HP at different reaction time.

Finally the reaction was repeated using the best reaction conditions with the other two samples of maltodextrins having different chain length, MD10 and MD15; results were compared with those obtained with MD18 (Figure 5.7).

The best product characteristics were obtained with the shorter-chain substrate, probably because of the easier oxidation of smaller molecules.
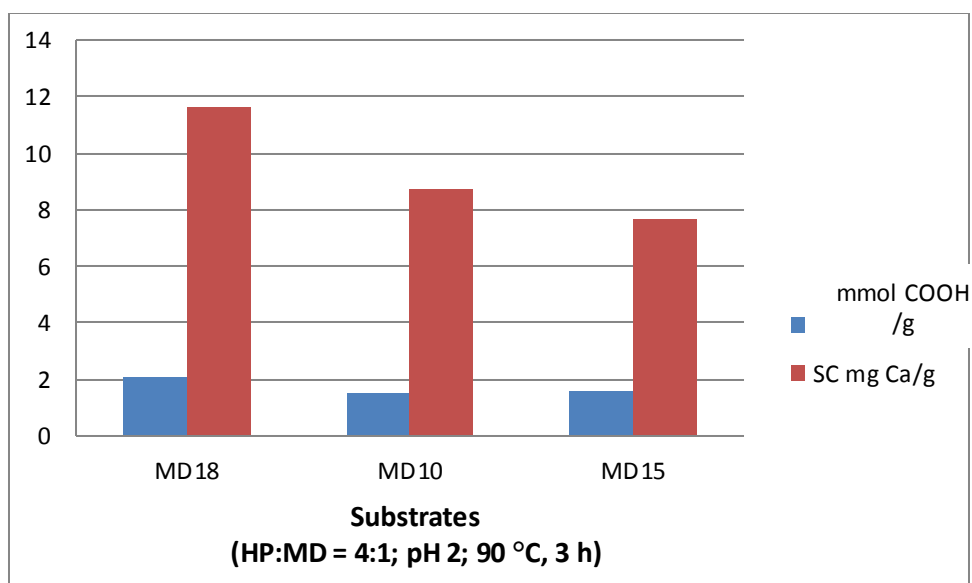
Figure 5.7. Tests with HP and different feedstock.

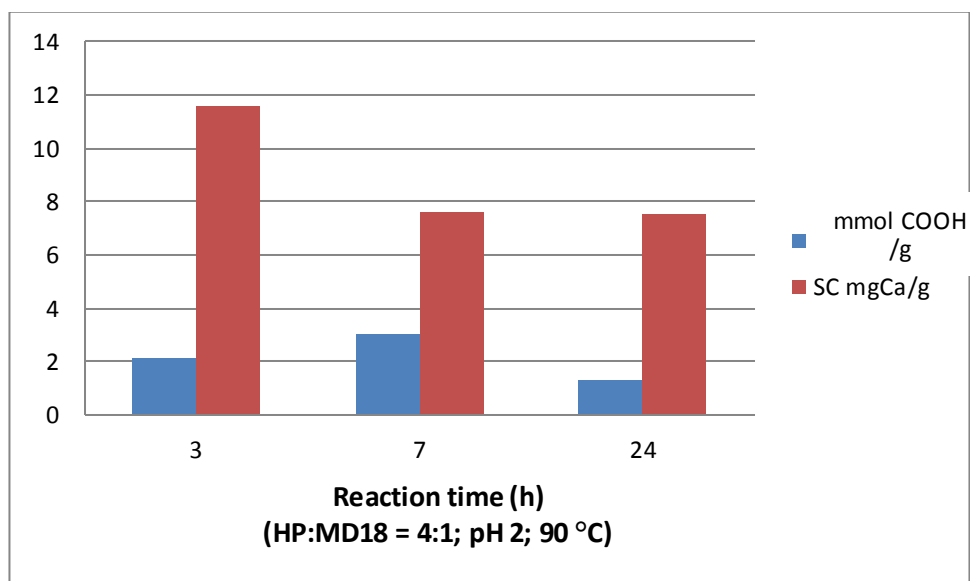In conclusion, it is possible to compare our results with those reported by Thaburet et al[34] . They oxidized different glucose syrups, maltodextrins and starch with NaOCl-NaBr-TEMPO (2,2,6,6-tetramethylpiperidine-1-oxyl) and measured the carboxylate content and the calcium complexing ability of their oxidized products. In general, in maltodextrins oxidation, they obtained a number of carboxylic groups between 5.9 and 6.5 mmol COOH/g product and a Ca^{2+} SC of 8-32 mg Ca/g product. In some cases, their results were slightly better than those obtained by us.

The substrate more similar to MD18 (DE 18.4, DP 5.4) used in ref 34 was Glucidex 17 (DP 5.9, DE 16.9). In the paper the authors reported the following product characteristics: 5.9 mn COOH/g and Ca^{2+} SC equal to 14 mg Ca/g. Under the optimised reaction conditions, our best results were obtained with MD18: 2.1 mmol COOH/g and 11.6 mg Ca/g. The number of carboxylic acids groups was lower, but the calcium binding capacity was similar.

5.4 Results and Discussion of reactivity tests with Oxygen

The reactivity of different catalysts was tested using oxygen as the oxidant: Au/TiO_2, Pt/C, Ru/Al_2O_3 and Pd/TiO_2.

Results obtained are reported in Table 5.3.

Catalyst	Me : MD18*	Base : MD18*	H_2O (ml)	$P\ O_2$ (bar)	T (°C)	t (h)	Solid Weight (g)	mmol COOH/ g product	SC mg Ca / g product
Pt/C 3 wt%	0,001	0	30	4	70	3	7.9	0.34	2,3
Pt/C 3 wt%	0,001	0	30	4	90	3	7.9	0.52	2,2
Pt/C 3 wt%	0,001	0	30	10	70	3	8.1	0.57	1,9
Pt/C 3 wt%	0,001	0,5	30	10	70	3	7.2	0.72	4,6
Pt/C 3 wt%	0,001	0	30	10	90	3	8.6	0.15	2,4
Pt/C 3 wt%	0,001	1	30	10	70	3	8.6	1.42	5,2
Au/TiO$_2$ 1,5 wt%	0,0005	0	30	4	70	3	7.9	0.41	2,8
Au/TiO$_2$ 1,5 wt%	0,0005	0	30	4	90	3	8.5	0.71	7,9
Au/TiO$_2$ 1,5 wt%	0,0005	0	30	10	70	3	5.8	0.43	4
Au/TiO$_2$ 1,5 wt%	0,0005	0,5	30	10	70	3	7.5	0.86	9,2
Au/TiO$_2$ 1,5 wt%	0,0005	0	30	10	90	3	6.1	0.05	5,5
Au/TiO$_2$ 1,5 wt%	0,0005	1	30	10	90	3	6.1	1.61	6,4
Au/TiO$_2$ 1,5 wt%	0,0005	1	25	4, flow 100ml/min	70	3	9.4	1.47	7

Catalyst	Me : MD18*	Base : MD18*	H₂O (ml)	P O₂ (bar)	T (°C)	t (h)	Solid Weight (g)	mmol COOH/ g product	SC mg Ca/g product
No	0	0	30	10	70	3	9.2	0.7	6,5
No	0	0,5	30	10	70	3	8.4	1,04	7,9
No	0	1	30	10	70	3	7	1.49	6,9
No	0	1	25	4, flow 100 ml/min	70	3	8.5	1.41	6,1
Ru/Al₂O₃ 5 wt%	0,0005	0	30	10	70	3	10.3	0.09	2,9
Ru/Al₂O₃ 5 wt%	0,0005	0,5	30	10	70	3	8.9	0.83	4,8
Ru/Al₂O₃ 5 wt%	0,001	0	30	10	70	3	9.8	0.08	1,9
Ru/Al₂O₃ 5 wt%	0,002	1	30	10	70	3	5.5	1.01	5,9
Pd/TiO₂ 1,5 wt%	0,001	1	30	10	70	3	9.6	1.51	6,6
Pd/TiO₂ 1,5 wt%	0,001	0	30	10	70	3	10.1	0.14	3

Table 5.3. Results of catalytic tests with Oxygen (yellow and orange boxes highlight the best results) *:

molar ratio

We first tested the reactivity of Pt- and Au-based catalysts, at two different temperatures and oxygen pressures, at neutral pH (Figures 5.8 and 5.9).
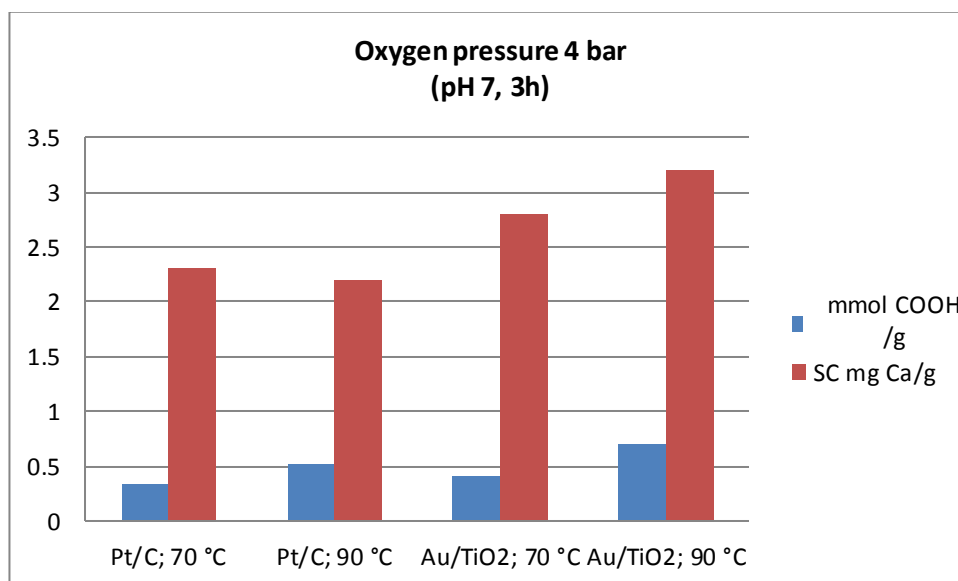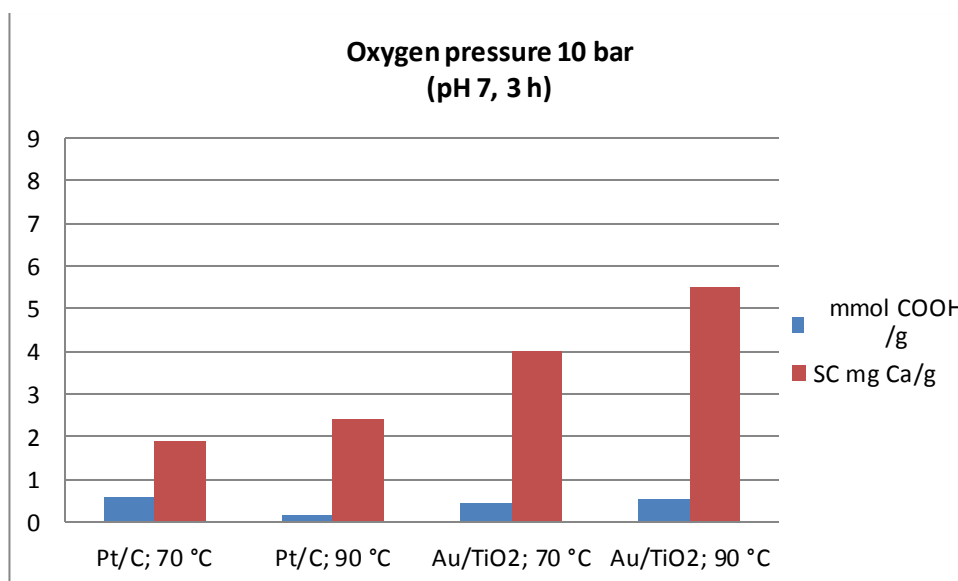

Figure 5.8. Tests with MD18 and Oxygen at 4 bar.

Figure 5.9. Tests with MD18 and Oxygen at 10 bar.

In the case of platinum (Pt/C 3 wt%), a small effect of temperature in the reaction conducted under 4 bar oxygen pressure was shown, while slightly better results were obtained at 10 bar oxygen pressure and 90 °C. However, in overall the O_2 pressure did

not show an important effect on reactivity, which implies that O_2 is not involved in the rate-determining step of the process. In the case of gold (Au/TiO$_2$ 1.5 wt%), an improvement of the characteristics of the product was shown when the reaction was carried out at higher temperatures and higher pressure. The Au catalyst was clearly better than the Pt one.

Thereafter, reactions were carried out in the presence of the base.

First, reactions were performed without catalyst and different amounts of the base (Figure 5.10): upon increasing the pH of the reaction mixture, an increase of the number of carboxylic groups of the product was shown, but the best Ca^{2+} SC was obtained with an intermediate base amount. Furthermore, comparing the result at neutral pH (NaOH/MD = 0) without catalyst with results reported in Figure 5.9, under the same experimental conditions but in the presence of the catalyst, it is shown that indeed in the latter case the conversion was decreased compared with the case without catalyst. This means that the catalyst needs basic conditions in order to be active.
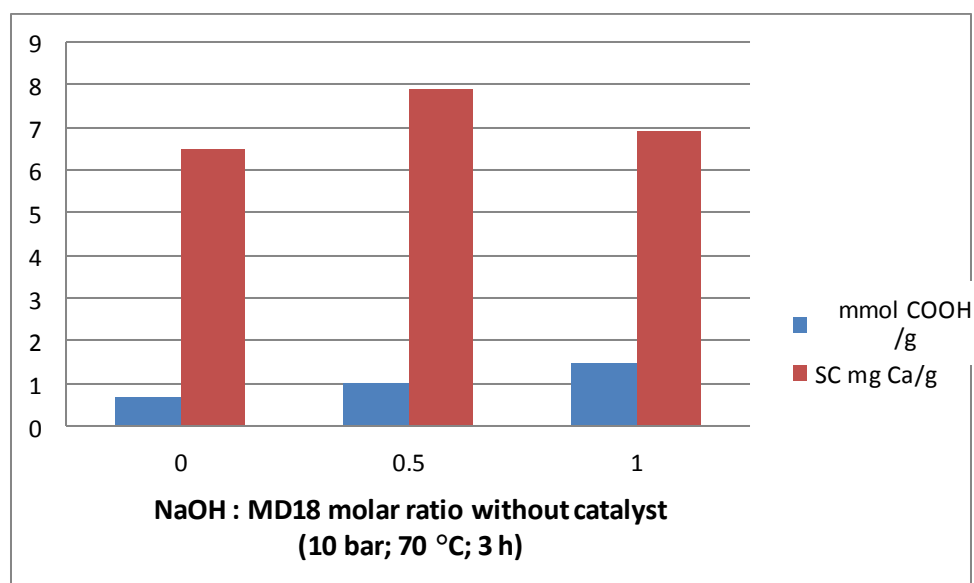
Figure 5.10. Tests with MD18 and Oxygen with different NaOH : MD 01915 molar ratio.

The reactivity of the following catalysts was tested with different MD18 : NaOH molar ratios:

- Pt/C 3 wt%
- Au/TiO$_2$ 1.5 wt%

- Ru/Al$_2$O$_3$ 5 wt%
- Pd/TiO$_2$ 1.5 wt%

Other reaction conditions were: oxygen pressure 10 bar, T 70 °C, reaction time 3 h.

Results are shown in Figures 5.11-5.14.

Figure 5.11. Tests with MD18 and Oxygen with Pt/C catalyst at different NaOH : MD18 molar ratio.
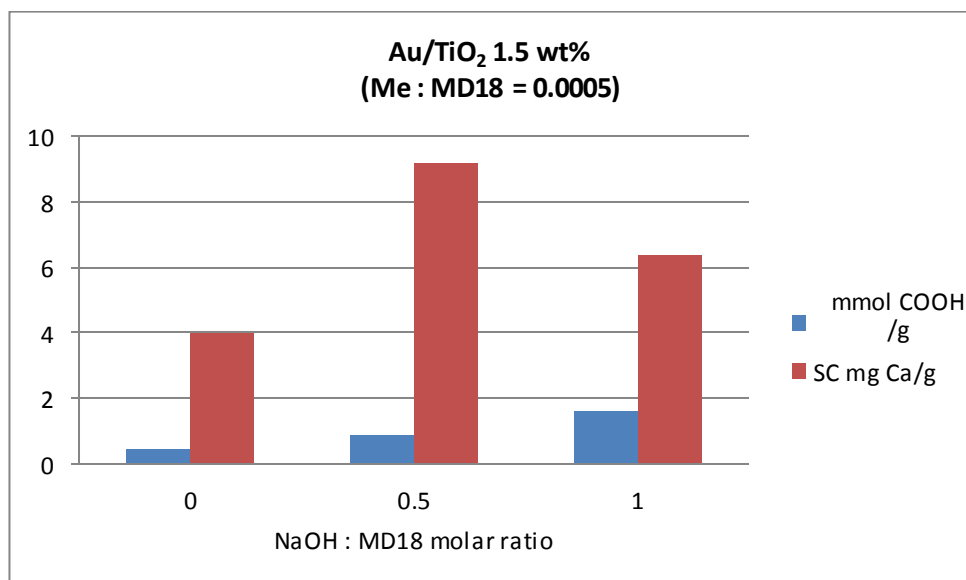
Figure 5.12. Tests with MD18 and Oxygen with Au/TiO$_2$ catalyst at different NaOH : MD18 molar ratio.
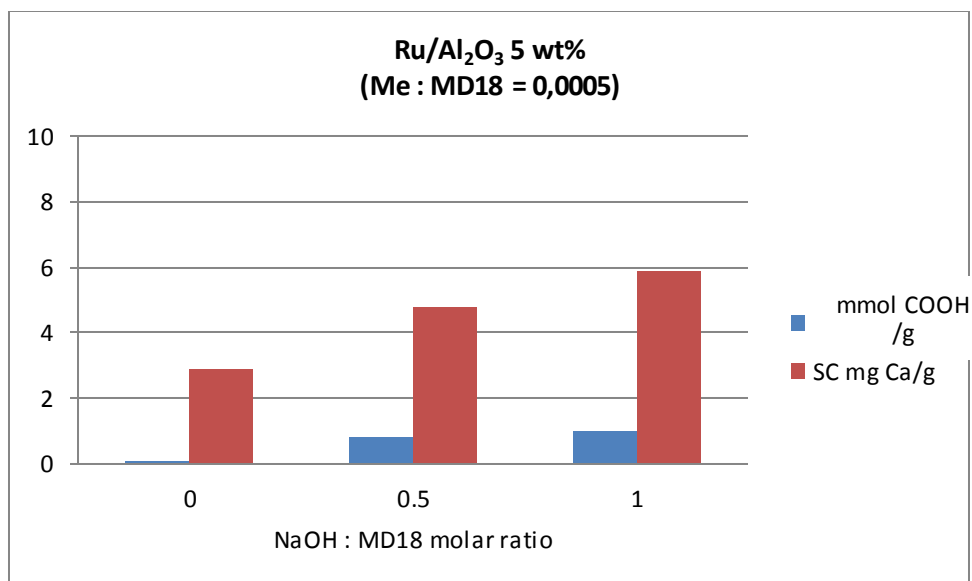
Figure 5.13. Tests with MD18 and Oxygen with Ru/Al$_2$O$_3$ catalyst at different NaOH : MD18 molar ratio.
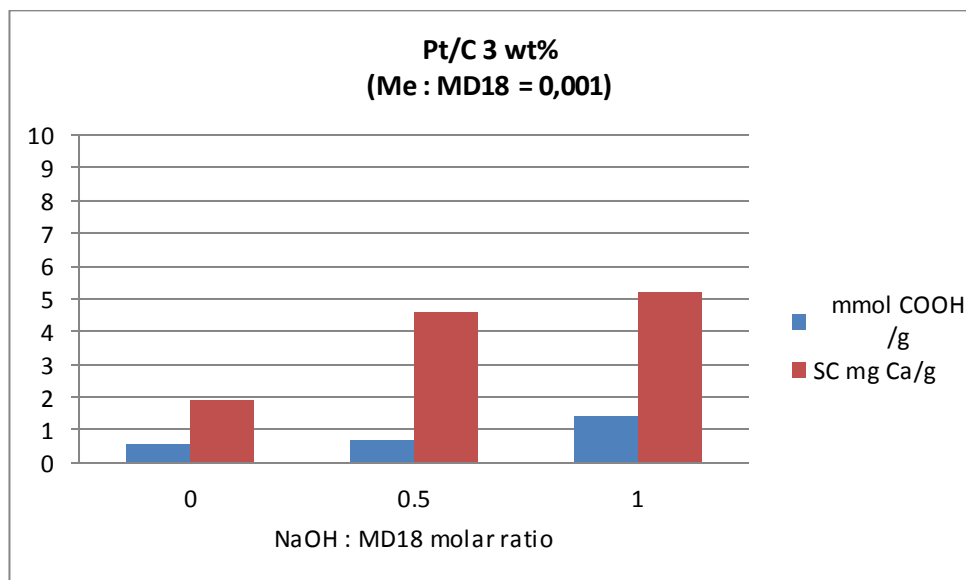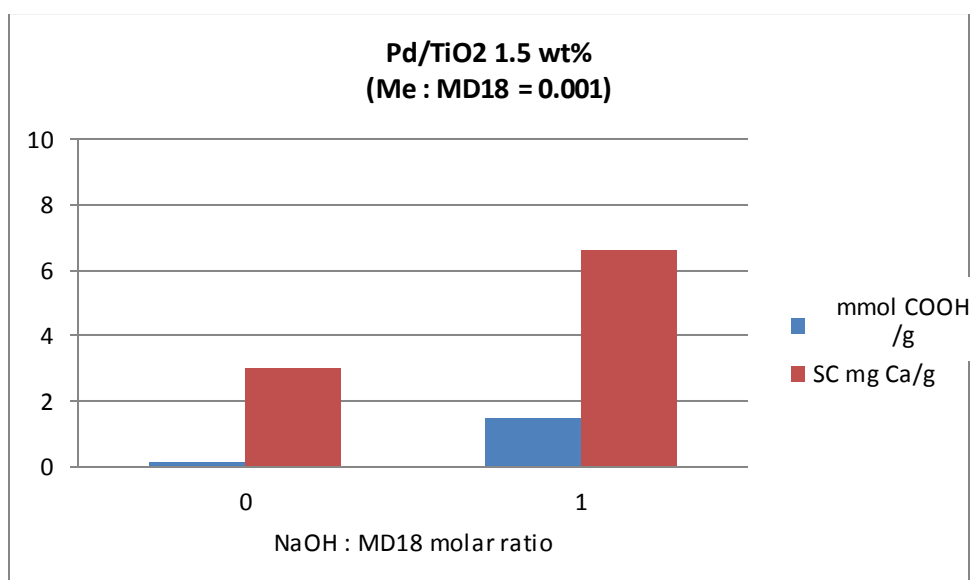

Figure 5.14. Tests with MD18 and Oxygen with Pd/TiO$_2$ catalyst at different NaOH : MD18 molar ratio.

In all cases, except for the Ca^{2+} SC for Au/TiO$_2$ catalyst, the increase of the base amount led to an increase of both the number of carboxylic groups and the Ca^{2+} SC. Best results were achieved with the Au/TiO$_2$ catalyst, which can provide better product characteristics with a lower Metal : MD18 molar ratio than with the other catalysts. However, in all cases results obtained were similar to those achieved under the same experimental conditions but without catalyst (Figure 5.8).

In order to check whether it were possible to improve the results by improving the the mass transfer of the oxidant, two reactions were repeated using a different reactor: a semibatch autoclave (volume 100 ml, heated with a silicone oil bath and provided with a vapor condenser) in which the gaseous phase in flown continuously under pressure and is bubbling through the reaction mixture.

Reactions were performed with molar ratio NaOH : MD18 = 1:1 without catalyst and with Au/TiO$_2$ (molar ratio Au : MD18 = 0.0005) (Figure 15). The concentrations of reactants in the mixture were the same already used for previous tests, temperature was 70 °C, oxygen flow 100 ml/min, pressure 4 bar, and reaction time was 3 h.
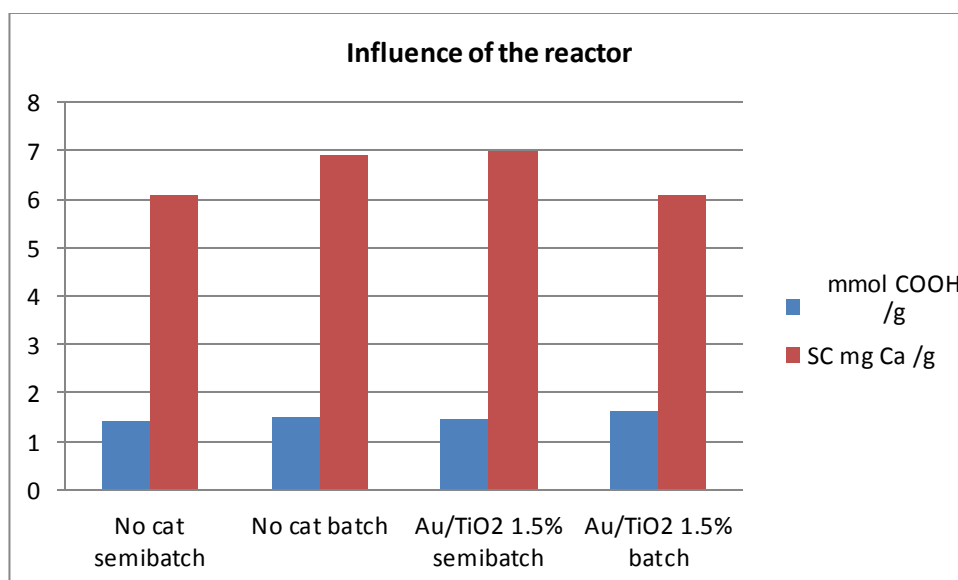
Figure 5.15. Tests with MD18 and Oxygen without catalyst and with Au/TiO$_2$ catalyst in different reactor.

In the case of the reaction without catalyst, no improvement of the product characteristics were obtained compared to the experiment carried out in the batch reactor under similar conditions, indeed the Ca^{2+} SC decreased a little. The opposite was shown for the oxidation with Au/TiO$_2$ carried out in the semibatch reactor. In overall, it seems that the reactor type did not lead to any important difference in products characteristics. Moreover, it was confirmed that unfortunately the presence of the catalyst did not lead to noticeable improvements compared to the case without catalyst; indeed, the presence of the base had a more important effect.

In conclusion, a comparison with results reported by Thaburet et al[34] (Glucidex 17 = 5.9 mn COOH/g and Ca^{2+} SC equal to 14 mg Ca/g) for oxidation with NaOCl and TEMPO, shows that with oxygen a lower number of carboxylic groups and a lower calcium binding capacity was obtained. This difference could be attributed to several reasons, such as the lower reactivity of O_2, and problems related to mass transfer between the gas and the liquid phase and from the latter to the catalyst surface.

5.5 Starch oxidation

With this feedstock, it was necessary to change the analytical method because starch is not soluble in the reaction mixture under the chosen conditions (30-40 wt% of solid feedstock in the reaction mixture, T max 60 °C).

At the end of the reaction two phases were obtained: a solid one composed of non-reacted starch and oxidized product, and a liquid one composed of water and soluble oxidation products. Moreover it was also important to take into account the nature of the catalyst used.

About the liquid mixture, it was possible to proceed as in the case of MD18: precipitation of sodium salt products with NaOH and MeOH and usual determination of the concentration of –COOH groups and of Ca^{2+} SC. About the solid, it was decided to wash it with water in order to remove all the residual base or acid. Then a back-titration was performed, adding a known excess of NaOH and titrating with HCl in order to calculate the number of carboxylic groups.

First, starch was oxidized with HP and tungstate, starting from a 40 wt% suspension and using the same reaction system with the three necked flask used for MD18. Other conditions were:

- Molar ratio starch : **HP** : $Na_2WO_4 \cdot 2\ H_2O$: $\underline{H_3PO_4}$ = 1 : **4** : *0,034* : $\underline{0,02}$

- HCl added until pH 2

- Typical amounts:

    - starch = 13.30 g

    - H_2O = 30 ml

    - HP = 24.5 ml

    - $Na_2WO_4 \cdot 2\ H_2O$ = 0,87 g

    - H_3PO_4 = 0,10 ml

    - HCl = 2-3 drops

- Temperature 55 °C

- Reaction time 3 h

HP was added dropwise in 2 h, but after 30 min the mixture thickened and became almost solid.

The same happened also during a second test at 50 °C with 30 wt% only of solid feedstock. So it was decided to carry out a reaction with a lower amount of HP, i.e., with molar ratio starch : HP = 1:2.

In this case the mixture did not solidify but the number of carboxylic groups was very low: 0.14 mmol COOH/g product.

Then a reaction with starch, NaOH and water in the batch autoclave was performed before testing other catalysts. Reaction conditions were: starch 40 wt% in 30 ml H_2O, molar ratio starch : NaOH = 1:1, temperature 45 °C, oxygen pressure 10 bar. We noted the formation of a solid paste while NaOH was dissolving, thus tests were carried out in order to understand under which conditions the mixture could be stable.

Solutions with 30 and 40 wt% of starch were prepared and they were all stable until 50 °C. Then we added NaOH (molar ratio starch : NaOH = 2) but the solid formation was again observed in both cases. Conversely, adding the base until pH 8 only (NaOH 0.1 M), the mixture did not solidify.

It was decided to carry out a reaction in the absence of catalyst under these conditions: starch 30 wt% in 30 ml H_2O, NaOH 0.1 M until pH 8, temperature 50 °C, oxygen pressure 10 bar, time 3h. Carboxylic functionality determination showed no formation of oxidised groups.

Therefore following tests were conducted in the presence of catalysts.

Heterogeneous catalysts used for MD18 oxidation were in the form of powder and they could not be easily separated from the product of starch oxidation since the latter was a powder too. Therefore, since a heterogeneous catalytic system had to be used, a solid catalyst with very different particle dimensions was necessary, in order to allow an easy recovery. Different catalysts were prepared supporting the metal active phase on alumina spheres with a diameter between 3-4 mm. In this way, it was possible to separate the catalyst passing the mixture through a metallic grid.

The following catalytic system were prepared:

- Pt/Al_2O_3 4 wt% by wet impregnation of H_2PtCl_6 solution
- Au/Al_2O_3 3 wt% by deposition precipitation of $HAuCl_4$
- Ru/Al_2O_3 3 wt% by wet impregnation of $RuCl_3$ solution

All catalysts were tested in the batch autoclave with 30 wt% of starch, 30 ml of H_2O, oxygen pressure 10 bar, temperature 50 °C, reaction time 3 h. Results are reported in Table 5.4.

Catalyst	Carboxylic groups (mmol –COOH/ g product)
Au/Al_2O_3	0.03
Pt/Al_2O_3	0.02
Ru/Al_2O_3	0

Table 5.4. Results of tests with starch and catalysts supported on alumina spheres

The number of carboxylic groups was very low with all catalysts; no product formation was found with Ru-based system.

Compared with the previous results of MD18 oxidation and data reported in the paper of Thaburet et al.[34], the number of carboxylic groups found after our reactivity tests is by far lower. As mentioned above, the lower reactivity of O_2 compared to HP may be the reason for such a large difference of performance; moreover, in the case of starch the insolubility of the reactant makes the contact between the reactant and O_2 even more problematic.

The same reactions were repeated in the presence of the base (NaOH 0.1 M until pH 8). Results are reported in Table 5.5.

Catalyst	Carboxylic groups at pH 8 (mmol –COOH/ g product)
Au/Al_2O_3	0.04
Pt/Al_2O_3	0.02
Ru/Al_2O_3	0.01

Table 5.5. Results of tests with starch and alumina spheres supported catalysts in alkaline medium

As it is possible to see, there were no differences between the two series of results, thus the addition of a base until pH 8 did not improve the performance in starch oxidation.

5.6 Considerations on the determination of calcium sequestering capacity of commercial products

Literature data about Ca^{2+} SC of the major additives for the inhibition of incrustation in detergents are reported below, in comparison with results obtained with the analytical method adopted for this work (ISE determination):

- Sodium tripolyphosphate $Na_5P_3O_{10}$

  Theory: 104 mg Ca/g product = 260 mg $CaCO_3$/g (from the literature[35])

  ISE determination: 120 mg Ca/g = 300 mg $CaCO_3$/g

- Sokalan CP5

  Theory: 116 mg Ca/g = 290 mg $CaCO_3$/g (from the technical brochure[36])

  ISE determination: 80 mg Ca/g = 200 mg $CaCO_3$/g

- Sokalan CP7

  Theory: 144 mg Ca/g = 360 mg $CaCO_3$/g (from the technical brochure[36])

  ISE determination: 75 mg Ca/g = 188 mg $CaCO_3$/g

Results obtained were different from the expected ones, this is probably due in part to the fact that the determination of Ca^{2+}SC of Sokalan commercial products is carried out with a turbidity method suitable for soluble compounds.

This latter method, derived from the Hampshire text, consists in the titration of a solution of dispersing agent against calcium acetate in the presence of an excess of carbonate ions, until the solution becomes cloudy[36,37].

We tried to replicate the same procedure on commercial products, but quite different results were obtained:

- Sodium tripolyphosphate $Na_5P_3O_{10}$

  Theory[35]: 104 mg Ca/g product = 260 mg $CaCO_3$/g

  Turbidimetry: 55 mg Ca/g = 137 mg $CaCO_3$/g

- Sokalan CP5

  Theory[36]: 116 mg Ca/g = 290 mg $CaCO_3$/g

  Turbidimetry: 78 mg Ca/g = 195 mg $CaCO_3$/g

- Sokalan CP7

  Theory[36]: 144 mg Ca/g = 360 mg $CaCO_3$/g

Turbidimetry: 80 mg Ca/g = 200 mg $CaCO_3$/g

Indeed, it is shown that the ISE method and the turbidimetry method gave similar results with Sokalan CP5 and CP7, while the results obtained with Na tripolyphosphate were different in the two cases. The difference between the expected value and experimental results could be attributed to the difficulty of the determination of the titration end point , since the formation of the "clouding" is not very clear. An attempt to replicate the method was done using a spectrophotometer with an optical fiber probe, but the difference of transmittance at the end point was very low.

Considering these difficulties, it was decided to carry out the determination by means of the Ca^{2+} ISE and Ag/AgCl reference electrode.

5.7 Conclusions

Maltodextrins and starch were oxidized with different oxidants and catalytic systems.

With HP as the oxidant and MD18 as substrate, the number of carboxylic groups achieved in the product was similar to those reported in the paper of Floor and van Bekkum [13], but in the case of O_2 as the oxidant the result was lower than that reported by Thaburet et al[34], who used NaOCl and TEMPO as oxidants.

The Ca^{2+} SC characteristics gained were similar with both HP and oxygen, but results were lower than those reported by Thaburet et al.[34] and also lower compared to commercial products taken as the reference.

Moreover, in O_2 oxidations, it was not possible to obtain an improvement of the characteristics of the products compared to the experiment carried out without any catalyst. It seemed that the best effect was achieved by the addition of the base in the reaction mixture.

The low reactivity of the reaction systems tested can be attributed to different reasons. First, in their paper, Thaburet et al.[34] reported better oxidation results with glucose syrup and better sequestering properties starting from longer chain maltodextrins. So it is possible to speculate that the bigger is the maltodextrin chain length, the harder is the oxidation reaction, but the better is the calcium binding capacity.

About reaction with heterogeneous catalysts, it is probable that the worse results are due to the different phases present in the reaction system (reactant in solution, solid catalyst and gaseous oxidant). The mass transfer between the various species in the reaction mixture could be the limiting factor of the process.

The same reason could be the cause of the almost null conversion of starch, because the substrate is not solubilized in H_2O under the reaction conditions used.

During oxidation reactions also substrate depolymerization can occur, as also reported by Thaburet et al.[34] which reduces the sequestering capacity of the final product.

Finally, also the spatial conformation of maltodextrins and starch have to be taken into account, which can prevent the availability of the hydroxyl groups of the glucose units during the reaction. Some papers reported the oxidation of water soluble starches (i.e. Thaburet et al[34], Wing et al.[38], …), but reactivity tests were performed in diluted solutions, with homogeneous catalysts, high temperatures, and long reaction time.

From results obtained below, it can be inferred that the oxidation of maltodextrins and short and medium-length polysaccharides shows problems, especially when oxygen is used as the reactant. Indeed, it is not surprising that the literature on this topic is so scarce.

Quite different is the case for the oxidation of monosaccharides; about this topic there is a large amount of literature showing that it is possible to oxidize monosaccharides and obtain several different products in function of the oxidant used, of catalyst type and reaction conditions. One important example is the oxidation of glucose, which can afford either gluconic or glucaric acid (see Chapter 3).

5.8 Acknowledgments

5.9 References

(1)   BeMiller, J. N.; Huber, K. C. In *Ullmann's Encyclopedia of Industrial Chemistry*; Wiley-VCH Verlag GmbH & Co. KGaA, Ed.; Wiley-VCH Verlag GmbH & Co. KGaA: Weinheim, Germany, 2011.

(2)   Chiu, C.-W.; Solarek, D. In *Starch: Chemistry and Technology*; Elsevier Inc., 2009.

(3)   Chattopadhyaya, S.; Singhal, R. S.; Kulkarni, P. R. *Carbohydr. Polym.* **1998**, *37* (2), 143–144.

(4)   Scaller, B. L.; Sowell, R. L. In *Starch: Chemistry and Technology*; Academic Press, 1967; Vol. Volume II, pp 237–251.

(5)   El-Sheikh, M. A.; Ramadan, M. A.; El-Shafie, A. *Carbohydr. Polym.* **2010**, *80* (1), 266–269.

(6)   Finch, C. A. *Br. Polym. J.* **1986**, *21* (1).

(7)   Kuakpetoon, D.; Wang, Y.-J. *Carbohydr. Res.* **2006**, *341* (11), 1896–1915.

(8)   Halal, S. L. M. E.; Colussi, R.; Pinto, V. Z.; Bartz, J.; Radunz, M.; Carreño, N. L. V.; Dias, A. R. G.; Zavareze, E. da R. *Food Chem.* **2015**, *168*, 247–256.

(9)   Vanier, N. L.; El Halal, S. L. M.; Dias, A. R. G.; da Rosa Zavareze, E. *Food Chem.* **2017**, *221*, 1546–1559.

(10)   Pietrzyk, S.; Juszczak, L.; Fortuna, T.; Łabanowska, M.; Bidzińska, E.; Błoniarczyk, K. *Starch - Stärke* **2012**, *64* (4), 272–280.

(11)   Zhang, Y.-R.; Wang, X.-L.; Zhao, G.-M.; Wang, Y.-Z. *Carbohydr. Polym.* **2012**, *87* (4), 2554–2562.

(12)   Zhang, S.-D.; Zhang, Y.-R.; Wang, X.-L.; Wang, Y.-Z. *Starch - Stärke* **2009**, *61* (11), 646–655.

(13)   Floor, M.; Schenk, K. M.; Kieboom, A. P. G.; Van Bekkum, H. *Starch-Stärke* **1989**, *41* (8), 303–309.

(14)   Nieuwenhuizen, M. S.; Kieboom, A. P. G.; Van Bekkum, H. *Starch-Stärke* **1985**, *37* (6), 192–200.

(15)   Forssell, P.; Hamunen, A.; Autio, K.; Suortti, P.; Poutanen, K. *Starch-Stärke* **1995**, *47* (10), 371–377.

(16)   Kesselmans, R. P. W.; Bleeker, I. P. Catalyst-free ozone oxidation of starch. WO97/35890.

(17)   Chan, H. T.; Bhat, R.; Karim, A. A. *J. Agric. Food Chem.* **2009**, *57* (13), 5965–5970.

(18)   Castanha, N.; Matta Junior, M. D. da; Augusto, P. E. D. *Food Hydrocoll.* **2017**, *66*, 343–356.

(19)   Veelaert, S.; De Wit, D.; Tournois, H. *Polymer* **1994**, *35* (23), 5091–5097.

(20)   Fiedorowicz, M.; Para, A. *Carbohydr. Polym.* **2006**, *63* (3), 360–366.

(21)   Bragd, P. L.; Van Bekkum, H.; Besemer, A. C. *Top. Catal.* **2004**, *27* (1–4), 49–66.

(22)   Kato, Y.; Matsuo, R.; Isogai, A. *Carbohydr. Polym.* **2003**, *51* (1), 69–75.

(23)   deNooy, A. E. J.; Besemer, A. C.; H. Van Bekkum. *Carbohydr. Res.* **1995**, *269*, 89–98.

(24)   Ponedel'kina, I. Y.; Araslanova, D. I.; Tyumkina, T. V.; Lukina, E. S.; Odinokov, V. N. *Starch - Stärke* **2014**, *66* (5–6), 444–449.

(25)   Kochkar, H.; Morawietz, M.; Hölderich, W. F. *Appl. Catal. Gen.* **2001**, *210* (1), 325–328.

(26)   Painter, T. J.; Cesàro, A.; Delben, F.; Paoletti, S. *Carbohydr. Res.* **1985**, *140* (1), 61–68.

(27)   Achremowicz, B.; Gumul, D.; Bala-Piasek, A.; Tomasik, P.; Haberko, K. *Carbohydr. Polym.* **2000**, *42* (1), 45–50.

(28)   Bala-Piasek, A.; Tomasik, P. *Carbohydr. Polym.* **1999**, *38* (1), 41–45.

(29)   Chen, X.; Yan, S.; Wang, H.; Hu, Z.; Wang, X.; Huo, M. *Carbohydr. Polym.* **2015**, *117*, 673–680.

(30)   Ye, S.; Qiu-hua, W.; Xue-Chun, X.; Wen-yong, J.; Shu-Cai, G.; Hai-Feng, Z. *LWT - Food Sci. Technol.* **2011**, *44* (1), 139–144.

(31)   Mallat, T.; Baiker, A. *Chem. Rev.* **2004**, *104* (6), 3037–3058.

(32)   Marconi, M. *Chimica* **1951**, *6*, 384–385.

(33)   Klingenberg, J. J.; Kim, H. Z. **1966**.

(34)   Thaburet, J.-F.; Merbouh, N.; Ibert, M.; Marsais, F.; Queguiner, G. *Carbohydr. Res.* **2001**, *330* (1), 21–29.

(35)   Besemer, A. C.; Jetten, J. M.; Slaghek, T. M. *Starch - Stärke* **2003**, *55* (10), 443–449.

(36)   Sokalan CP types, Technical Information, BASF .

(37)   Richter, F.; Winkler, E. W. *Tenside Deterg.* **1987**, *24* (4), 213–216.

(38)   Wing, R. E.; Willett, J. L. *Ind. Crops Prod.* **1997**, *7* (1), 45–52.

Appendix A

Permission for journal article use

Dear Stefania Solmi,

We hereby grant permission for the requested use expected that due credit is given to the original source.

If material appears within our work with credit to another source, authorisation from that source must be obtained.

Credit must include the following components:

- Journals: Author(s) Name(s): Title of the Article. Name of the Journal. Publication year. Volume. Page(s). Copyright Wiley-VCH Verlag GmbH & Co. KGaA. Reproduced with permission.

If you also wish to publish your thesis in electronic format, you may use the article according to the Copyright transfer agreement:

3. Final Published Version.

Wiley-VCH hereby licenses back to the Contributor the following rights with respect to the final published version of the Contribution:

a. […]

b. Re-use in other publications. The right to re-use the final Contribution or parts thereof for any publication authored or edited by the Contributor (excluding journal articles) where such re-used material constitutes less than half of the total material in such publication. In such case, any modifications should be accurately noted.

Wiley authors

If you are a Wiley author wishing to republish extracts of your own published work, include your article in your thesis or use copies for your internal teaching purposes, please refer to the gratis reuse rights that you retain when you signed your copyright transfer agreement. Alternatively, if you still require a formal permission license please

locate you work on Wiley Online Library, click 'request permission', select 'Author of this Wiley work' and your appropriate reuse rights to download your permissions license.

For details on how to self-archive your work visit here and our author compliance tool here. For article sharing policies, including information on sharing articles on Scholarly Collaboration Networks (SCNs), such as ResearchGate please view our handy infographic here . Please note that ResearchGate has not yet signed the STM sharing principles.

Kind regards

Bettina Loycke

Senior Rights Manager

Rights & Licenses

Wiley-VCH Verlag GmbH & Co. KGaA

Boschstraße 12

69469 Weinheim

Germany

www.wiley-vch.de

T +(49) 6201 606-280

F +(49) 6201 606-332

rightsDE@wiley.com

I have not failed. I've just found 10 000 ways that won't work.

Thomas A. Edison

This is not the end.

It is not even the beginning of the end.

But it is, perhaps, the end of the beginning.

Winston Churchill, November 10, 1942

Final Acknowledgments

La pagina dei ringraziamenti può sembrare la fiera delle ovvietà, ma sinceramente penso che sia giusto citare tutte le persone che hanno fatto qualcosa per me in questi tre anni di lavoro, per quanto banale possa essere.

Prima di tutto, vorrei ringraziare colui che non è mai stato nominato in nessuno dei ringraziamenti a fine capitolo, ma che ovviamente ha avuto un ruolo fondamentale. Senza di lui non avrei mai avuto questa speciale opportunità formativa, sia dal punto di vista scientifico che personale. Un sincero grazie al Prof. Fabrizio Cavani.

Ringrazio la mia famiglia, i miei genitori Cristina e Roberto, mio fratello Alessandro e mia nonna Bruna che mi sono sempre stati vicini e che mi hanno dato un aiuto fondamentale nel portare a termine questo lungo percorso di studi.

Grazie anche a tutti i miei amici sia di Modena che di Bologna: quelli del Venerdì Volley (AHU!), le ragazze "delle elementari", Vale, Sabri e Fede, le ex coinquiline di Via Galliera Claudia e Isabella, Lorenzo (Boro), gli ex compagni della magistrale, i nuovi amici della Panca e dell'arrampicata, e gli speciali compagni di laboratorio di catalisi. Il lavoro è la nostra attività quotidiana principale ma, per fortuna, non è tutto nella vita.

Un grazie poi a Wikipedia e Sci-Hub: il sapere deve essere libero, gratuito e alla portata di tutti.

Infine un importantissimo grazie a colui che da due anni mi è accanto ogni giorno, sia che lo si passi insieme che a 7500 Km di distanza. Grazie perché non sarebbe stato assolutamente lo stesso e altrettanto speciale senza di te. Grazie Marci.